



The Ocean Engineering Committee

Final Report and Recommendations to the 27th ITTC

1. GENERAL

1.1 Membership and Meetings

The members of the Ocean Engineering Committee of the 27th International Towing Tank Conference were as follows:

- Prof. Wei Qiu (Chairman), Memorial University of Newfoundland, Canada
- Mr. Halvor Lie (Secretary), MARINTEK, Norway
- Dr. Jean-Marc Rousset, Ecole Centrale de Nantes, France
- Dr. Dong-Yeon Lee, Samsung Ship Model Basin, Korea
- Prof. Sergio H. Sphaier, Federal University of Rio de Janeiro, Brazil
- Prof. Longbin Tao, University of Newcastle upon Tyne, United Kingdom
- Prof. Xuefeng Wang, Shanghai Jiao Tong University, China
- Dr. Takashi Mikami, Akishima Laboratory (MITSUI ZOSEN) Inc., Japan
- Dr. Viacheslav Magarovskii, Krylov Shipbuilding Research Institute, Russia

Four Committee meetings were held respectively at:

- Samsung Heavy Industries, Geoje Shipyard, Korea, December 2011.
- MARINTEK, Trondheim, Norway, September 2012.
- Ecole Centrale de Nantes, France, June 2013.

- Shanghai Jiao Tong University, China, February 2014.

1.2 Tasks Based on the Recommendation of 26th ITTC

- Update the state-of-the-art for predicting the behavior of bottom founded or stationary floating structures including moored and dynamically positioned ships emphasizing developments since the 2011 ITTC Conference. The committee report should include sections on:
 - The potential impact of new technological developments on the ITTC
 - New experimental techniques and extrapolation methods
 - New benchmark data
 - The practical applications of computational methods to prediction and scaling
 - The need for R&D for improving methods of model experiments, numerical modeling and full scale measurements.
- Review ITTC Recommended Procedures relevant to ocean engineering
 - Identify any requirements for changes in the light of current practice, and, if approved by the Advisory Council.
 - Identify the need for new procedures and outline the purpose and content of these.
- Complete the VIV and VIM guidelines and benchmark study initialized by the



Specialist Committee in Vortex Induced Vibrations of the 26th ITTC. The report on the benchmark test shall include clear definition of all the test parameters.

- Complete and report on the wave run-up benchmark study for a single cylinder.
- Carry out a wave run-up benchmark study for cases of four columns using the experimental data from MARINTEK.
- Investigate and report on the thruster-thruster interaction, ventilation and their scaling for DP systems.
- Investigate and report on physical and numerical modeling of vessels in side-by-side operations with an emphasis on wave elevation in the gap.
- Investigate and report on motions of large vessels and floating structures in shallow water.
- Jointly organize and participate in the joint ISSC/ITTC workshop on uncertainty in measurement and prediction of wave loads and responses.

1.3 Structure of the Report

The work carried out by the Committee is presented as follows:

2. State of the Art Reviews

- Section 2.1: Predicting the Behaviour of Stationary Floating Structures and Ships
- Section 2.2: Predicting the Behaviour of Dynamically Positioned Structures
- Section 2.3: Highly Nonlinear Effects on Ocean Structures
- Section 2.4: Predicting Vortex Induced Vibrations and Vortex Induced Motions
- Section 2.5: New Experimental Techniques
- Section 2.6: New Extrapolation Methods

- Section 2.7: Practical Applications of Computational Methods to Prediction and Scaling
- Section 2.8: Improving Method of Model Experiments, Numerical Methods and Full-Scale Measurements

3. Review of Existing Procedures

Section 3 reviews the procedures, 7.5-02-07-03.1 Floating Offshore Platform Experiments, 7.5-02-07-03.2 Analysis Procedure for Model Tests in Regular Waves and 7.5-02-07-03.3 Model Tests on Tanker-Turret Systems, and addresses the need for new procedures.

New Documentation

- Section 4 discusses the development of guideline for VIV and VIM model tests.
- Section 5 presents numerical benchmark studies of VIV.
- Section 6 presents benchmark studies of wave run-up for cases of single and four columns.
- Section 7 discusses the investigation of thruster-thruster interaction, ventilation and their scaling effect for dynamic positioning (DP) systems.
- Section 8 presents the study of physical and numerical modeling of vessels in side-by-side operations.
- Section 9 discusses the motions of large ships and floating structures in shallow water.
- Section 10 summarizes the outcome of the first joint ISSC/ITTC workshop on uncertainties in measurement and prediction of wave loads and responses.

Conclusions and Recommendations

Sections 11 and 12 present the conclusions and recommendations, respectively.

2. STATE OF THE ART REVIEWS

2.1 Stationary Floating Structures and Ships

2.1.1 Spar Platforms

Majority of the new field developments using spar platforms have been in deepwater offshore regions. There are many technical challenges with deployment and operation in deep or ultra-deep water, typically including the design and construction of drilling and production facilities to withstand the harsh deepwater environment and regulatory issues that arise from operations at these depths.

Research has been carried out particularly to address the global motions of spar hulls in waves, current and wind including vortex induced motion (VIM). The wave and current interaction is also an important issue for the spar platform.

VIM of spars has been studied by many researchers using numerical and experimental methods. Gonçalves et al. (2012) applied the Hilbert-Huang Transform Method to analyze VIM of a mono-column platform and showed a good agreement compared to that from the traditional analysis. Gonçalves et al. (2012a) presented an overview of relevant aspects on VIM of spars and mono-column platforms and showed that the loading condition had the largest impact on VIM responses because the low aspect ratio leads large 3D effects on the vortex shedding.

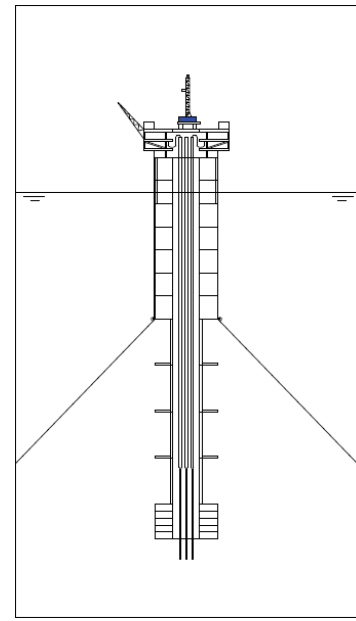


Figure 2.1.1.1 Sketch of S-Spar (Sun and Huang, 2012)

Lefevre et al. (2013) presented CFD studies on the VIM of a spar using STAR-CCM+. The numerical solutions were compared with model test results. Good agreement was found. Recommendations on computing spar motions, including the use of turbulence models, mesh resolutions and the choice of time step, were given for CFD simulations of spar VIM. Constantinides and Oakley (2013) simulated the VIM of a truss spar using AcuSolve. A cylindrical domain and a specialized boundary condition were used to avoid the creation of separate setups for each heading in the spar design phase.

A JIP has recently been set up to specifically address VIM. The project started in the summer of 2013 and will be completed in the summer of 2016. MARIN and USP will carry out model tests as well as CFD computations. Comprehensive benchmark data will be produced from model tests for the validation of numerical simulations.

Efforts have been made to investigate the responses of spars in waves and current.

Murray et al. (2012) conducted a model test campaign on a 1:50 Radial Wellbay Spar (RAW Spar) at the OTRC, Texas A&M University. The model test results were compared with numerical simulations by an ABAQUS-based time-domain semi-empirical model by Muehlner et al. (2012b). Kurian et al. (2013) conducted experimental and numerical studies on a truss spar subjected to long and short crested waves. The numerical solutions agreed well with the experimental results. Lower responses were also observed for short crested waves. Zhang et al. (2012) conducted model tests and investigated the added mass coefficients of a truss spar. In the model tests, the truss spar was subjected to uniform current. It was found that the added mass coefficients decrease as the reduced velocity was increased. Hong et al. (2013) presented an experimental study on the motion of a 1/100 scaled model of a spar-type floating platform. The effect of test conditions, e.g., the center of gravity, mooring stiffness and the fairlead location, were investigated. Rodriguez and Neves (2012) studied the nonlinear instabilities of spar platforms in waves with a focus on the parametric resonance phenomenon. Parametric Amplification Domains (PADs) were computed, showing the boundaries of the instability regions and the maximum roll amplitudes.

New design concepts have also been developed. For example, Sun and Huang (2012) developed a new spar concept called "S-Spar" (Figure 2.1.1.1). The "S-Spar" combined the features of classic spars and truss spars. Numerical predictions were performed using the panel method. The new concept led to smaller wave forces and motions than those of the classic spars.

2.1.2 TLPs

In the past three years, research has been carried out on TLPs using experimental and numerical methods focusing on motions and

loads on tethers due to air-gap and wave impact on deck.

Some of the results of the Cooperative Research on Extreme Seas and their impact (CresT) JIP were presented and discussed in the work of Hagen (2011), Bitner-Gregersen (2011), Hennig et al. (2011), Forristal (2011), and Forristal and Aubult (2013) in the 30th and 32nd OMAE Conferences. Figure 2.1.2.1 shows the TLP model used in the CresT JIP.



Figure 2.1.2.1 The TLP Model Used in CresT (Hennig et al., 2011)

Hagen (2011) discussed the wave nonlinearities that might lead to unrealistically low estimates of the extreme tether tension for the TLP, especially those related to wave-in-deck events. The 100-year return period value was shown to increase considerably if the nonlinearities beyond the second order were included.

Bitner-Gregersen (2011) presented the reliability assessment of the air-gap of a generic TLP for a given extreme wave condition. The study demonstrated the effects of wave nonlinearity beyond the second order, diffraction and radiation by the TLP, spatial variations of crest statistics, deck heights and sea water level variations. Based on a stochastic model, sensitivity studies were carried out to identify the importance of parameters on the probability of failure.



Uncertainties related to the analyses were identified and ranked.

Hennig et al. (2011) reported some results of extreme wave loads and responses observed in the model tests of the TLP. It was concluded that the wetted deck area, depending on the type of wave impact, wave-in-deck event and design variation, affects significantly the actual responses of TLP. The effect of the wave short-crestedness on extreme loadings was also assessed.

Based on the JIP experimental results, Forristal (2011) showed that the maximum crest heights in an area are greater than those at a single point. It was also stated that Piterbarg's theory (Piterbarg, 1996) can accurately predict this behaviour. Model tests showed that the short-term statistics of the diffracted waves under a TLP have the same form as that of the incident waves. Based on these evidences, the author proposed a method for the calculation of air-gap.

More recently, also in the context of the CresT JIP, Forristal and Aubult (2013) analyzed the effect of wave diffraction on the measured wave heights under the deck of the TLP. The results demonstrated that the first-order diffraction theory can be used to find the wave heights under the deck of the TLP, and it should also be used to correct the wave measurements for a TLP. The second-order theory gave marginal improvements and is therefore not recommended.

Based on extensive model tests, Gaidai et al. (2012) proposed another method for estimating the extreme value statistics of air-gap for a TLP subjected to random events. The method used only the area extreme value at each point to obtain a robust identification of the crossing rate function that determines the extreme value distribution. It was shown that this method can lead to an accurate prediction by using much

less data in comparison with the conventional statistical procedure.

Johannessen (2011) investigated the high-frequency loading and the response of a TLP in irregular steep waves. By comparing the model test results of tether loadings, it was concluded that the weakly nonlinear methods seem to be incapable of estimating the excitation at very high frequencies, while a much simpler impulse formulation gave a better estimate of horizontal excitations at these high frequencies.

Muehlner et al. (2012a) investigated the effect of high-frequency oscillations of a TLP on the fatigue of its tendons by direct calculations in time domain. The coupled analysis of the TLP with tendons and risers was carried out by considering several nonlinearities, including large displacements, finite wave height, viscous drag, higher-order wave effects, and variable added mass of the TLP columns. The analysis results showed that the fatigue damage due to high-frequency oscillations in the tendons was significant.

Mansour et al. (2013) investigated the design aspects of TLP tendon and tendon foundation systems. The studies involved the numerical simulation of progressive failure of tendons in cyclonic events. The TLP responses during the transition from the restrained condition (TLP with all tendons) to the free-floating condition have been numerically simulated and validated against model test results.

Relatively new TLP concepts have also been proposed and studied. Chandrasekaran et al. (2011) investigated a relatively new platform concept for ultra deepwater offshore exploration using an experimental method. The platform, Triceratops, combines the characteristics of TLP and spar, and consists of deck structure supported by three buoyant leg structures (BLS) connected through ball joints. Model tests in regular waves showed that the

compliance of the ball joints significantly affects the motion responses and the tether tensions. Only surge motions are transferred from the BLS to the deck. Figure 2.1.2.2 shows a typical triceratops.

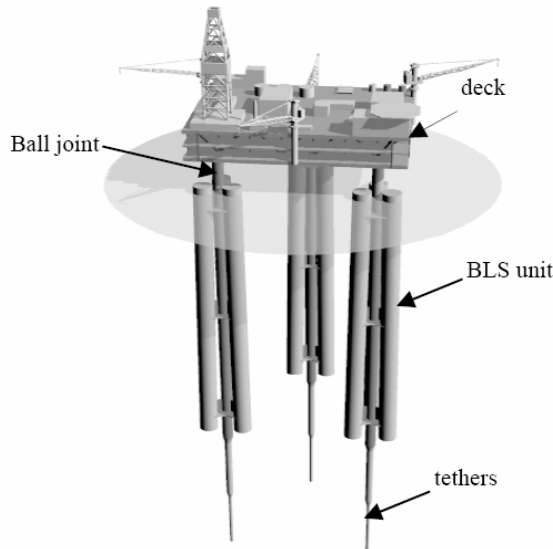


Figure 2.1.2.2 The Triceratops Concept (Chandrasekaran et al., 2011)

Rao et al. (2012) carried out hydrodynamic analyses of a relatively new concept of a TLP, namely Tension Based Tension Leg Platform (TBTLP) (see Figure 2.1.2.3), which was proposed for greater water depth than that for the conventional TLPs. Time series of free vibrations and the response amplitude operators (RAOs) were obtained and compared for three different cases of TLPs with and without tension base in various water depths. The efficacy of the provision of a tension base has been proved by comparing the RAOs.

More recently, Srinath and Chandrasekaran (2013) investigated the effect of perforated members on the dynamic response of TLPs through model testing. Experiments in regular unidirectional waves showed that surge and pitch response amplitudes decrease in the presence of retrofitting perforated cylindrical members. Depending on the wave period, the reduction may vary from 4% to 25%.

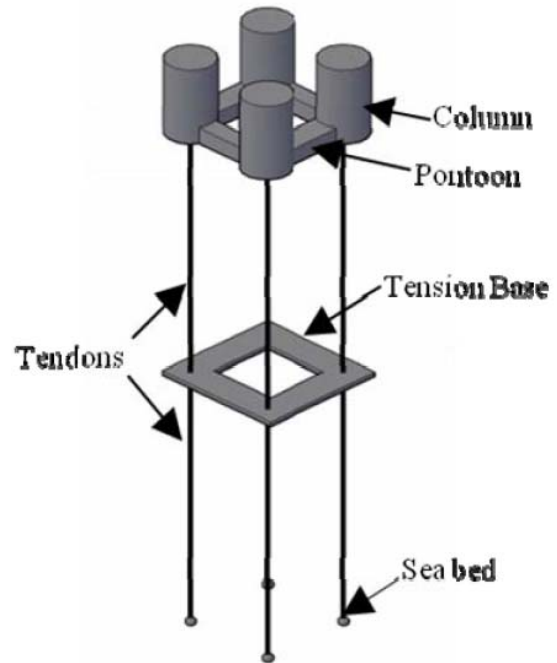


Figure 2.1.2.3 The TBTLP Concept (Rao et al., 2012)

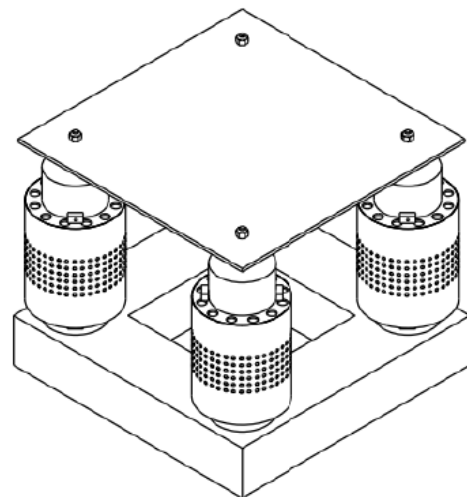


Figure 2.1.2.4 The TLP with Perforated Members (Srinath and Chandrasekaran, 2013)

New installation methodologies regarding TLP and its tendons have also been proposed. For tendon installation, Li et al. (2012) proposed an innovative approach, which involved the horizontal assembly of TLP tendon segments on a construction barge, instead of the typical vertical installation using



expensive heavy lift vessels. The partially assembled tendon was then incrementally pulled out through a stinger at the barge stern and secured with a holdback clamp so that the next tendon joint can be connected. The process repeated itself until the whole tendon was assembled and deployed. The tendon was then upended to a vertical configuration and connected to a TLP or a foundation pile.

Rijken (2013) provided two engineering solutions for the installation of TLPs under swell conditions. These methods aim to reduce heave motions either by installing heave plates or by temporarily decreasing the waterplane area. Both methods reduce the heave RAOs when the wave period is greater than 12 s. They may be applicable to situations where the installation window may contain prolonged periods of persistent swell.

In terms of hydrodynamic behavior of TLPs, some interesting work has been published. Cruz et al. (2012) reported the parametric yaw motions of a TLP in close proximity to a moored FPSO. It was also observed in the experiments that as the TLP yaw motion amplifies, the TLP sway amplitudes reduce, revealing a strongly non-linear coupling between these modes. A nonlinear mathematical model that takes hydrodynamic interactions of two bodies and nonlinear restoring into account was also proposed to investigate the occurrence of parametric instabilities of this type of system. Rudman and Cleary (2013) applied the Smoothed Particle Hydrodynamics (SPH) method to the fully-coupled simulation of the impact of a highly non-linear breaking rogue wave on a moored semi-submersible tension leg platform. They showed the detailed effect of wave impact angle on the subsequent platform motions and determined how the cable tension varied with wave impact angle and the time after impact. The application of the method and the presented results highlighted how the simulations could be used for practical design

purposes and in the assessment of operating conditions, especially in extreme wave conditions.

TLPs with direct and indirect applications as offshore wind energy devices have also been investigated. Bachynski and Moan (2012) studied four TLP wind turbine (TLPWT) concepts using a fully-coupled nonlinear time-domain method and a linear frequency-domain method. The designs included a wide range of displacements. The wind-induced responses were found to be significant and dependent on the TLPWT hull according to the nonlinear simulations. The nonlinear time-domain results for coupled wind and wave simulations indicated that wind loads were important for both operational and survival cases. In the operational cases, the operating turbines provided low-frequency excitations and some pitch damping. The wave-induced motions tended to become more important in more severe sea states. In the parked condition, the aerodynamic torque was found to be quite strong, and it was proved to be a critical force component for the smallest TLPWT design.

The Tension-Leg-Buoy (TLB), a concept developed based on the TLP for offshore wind turbine applications, was investigated by Myhr and Nygaard (2012). They addressed the effects of the Excess Buoyancy (EB) and mooring lines layout. Other offshore wind energy applications related to TLPs can be found in Copple and Capanoglu (2012), Ren et al. (2012) and Stewart et. al (2012).

Bae and Kim (2013) presented an analysis method for a mono-column TLP-type floating offshore wind turbine (FOWT) designed for 200m water depth. In the proposed method, rotor dynamics and control, aero-dynamics, tower elasticity, floater dynamics, and mooring line dynamics were considered. The full dynamic coupling among them was investigated in time domain along with the effects of sum-frequency wave-excitations. The



sum-frequency wave loading effects can be significant in the coupled analysis when blades are fixed (not rotating) at a minimal angle like in the survival condition. Therefore, there are significant differences between uncoupled and coupled analyses, and care needs to be taken when applying the conventional dynamic analysis methods, which are typically used for floating offshore oil and gas platforms, to the design of FOWTs. There exist complicated coupling effects among blade rotation, tower flexibility, blade-control mechanism, platform and mooring dynamic characteristics, and they should be fully considered for effective and robust design of future FOWTs.

2.1.3 Semi-Submersibles

Semi-submersibles are subjects of continuing interest and have been studied by a number of authors using a variety of methods.

DaSilva and Knecht (2011) introduced the practical implementation of a stochastic approach involving known aspects that affect the air gap for semi-submersibles. These effects include the first-order vessel motions under an undisturbed wave field, diffracted wave elevation under the platform, slow drift quadratic transfer function (QTF), vessel set-down, and the heel effects due to mooring stiffness. The results showed good correlation between the model test results and the analytical methods.

VIM of semisubmersibles has been addressed in various degrees. For example, Xu (2011) introduced a new semisubmersible design (NexGen) as a wet-tree floater by maintaining the simplicity of a conventional semisubmersible design. Its improved heave motion and VIM performance was demonstrated through hull-form optimization studies. The difference between the NexGen semi-submersible design and a conventional semi-submersible design lies in the blisters attached to the columns, the distribution of

pontoon volume, and the pontoon cross-section shape. In the NexGen design, the pontoon volume was re-distributed to minimize heave loading while maintaining sufficient structural rigidity, a long heave natural period and adequate quayside buoyancy. The blisters attached to the columns effectively break the vortex shedding coherence along the column length and therefore suppress VIM.

Kyoung et al. (2013) conducted model tests and numerical simulations to validate the global performance of a Heave and VIM Suppressed (HVS) semisubmersible. Xu et al. (2012) validated the VIM responses of a HVS semisubmersible by model tests and CFD computations. Both the model test and the CFD analysis showed better performance of the HVS design than an equivalent conventional semisubmersible. Gonçalves et al. (2012) presented new experimental results on VIM of a large volume semisubmersible platform. The wave effects were the main focus. According to the results, regular and irregular waves led to considerable differences in responses. Bai et al. (2013) conducted model tests in a towing tank to study the VIM response of a Deep Draft Semisubmersible (DDS) with four rectangular columns and four pontoons. CFD computations based on the RANS model were also carried out. The experimental results showed that the VIM responses of the DDS mainly include horizontal motions (surge, sway and yaw), among which sway is dominant. It was demonstrated in the numerical simulations that the CFD method could be used for the prediction of VIM.

Gonçalves et al. (2012) experimentally studied the Vortex Induced Yaw (VIY) motion on a large volume semisubmersible platform. It was shown that a resonant behavior occurred in yaw motions with considerable amplitudes.

Mansour and Kumar (2013) presented the numerical results for the motion response of a

Free Hanging Solid Ballast (FHSB) Semisubmersible in extreme hurricane. The new feature was proved to improve the performance of a conventional semisubmersible.

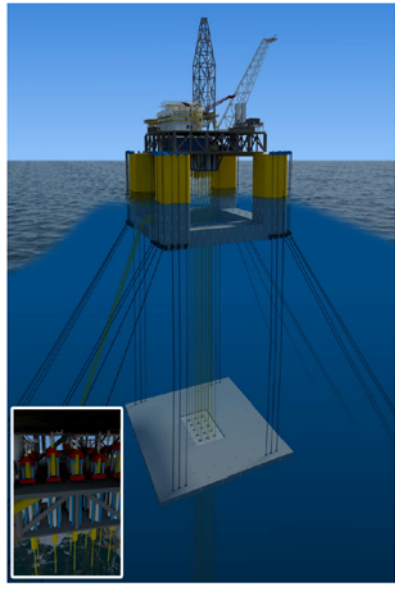


Figure 2.1.3.1 The Free Hanging Solid Ballast (FHSB) Semi-submersible (Mansour and Kumar, 2013)

Kurian et al. (2012) conducted model tests on a moored semisubmersible with one failure mooring line. Results showed that the platform migrated to a new mean position with a considerable transient response after the line failure.

Shan et al. (2012) conducted model tests and studied the wave run-up phenomenon of column arrays. The leg spacing was found to be a factor that affects the wave run-ups.

2.1.4 FPSO Vessels

FPSO vessels have been operated in a variety of water depths due to their flexibility, reliability, and low cost. Efforts have been made to investigate the responses of FPSO vessels in waves. Studies have been addressing

low frequency motion, the effect of internal liquid cargo, the hydrodynamic interaction when operated in a close proximity, the shallow water effect, and fully nonlinear analysis.

Minnebo et al. (2012) investigated the response of FPSO systems subjected to squalls and developed a robust approach to estimate the design value. It was shown that the governing squall parameter concerning FPSO offset is the peak wind speed, both for spread moored and turret moored vessels. It was shown that the dynamic amplification limitation method has great potential for use as a Design Value Estimating method, as it combines the physical correctness of the squalls and the response characteristics of the FPSO system.

A procedure for selecting the optimum heading for a FPSO with spread mooring operating in Santos basin considering the wave induced motions was presented by Oliveira (2012). A search algorithm has been implemented to allow the comparison of a large number of statistical results and to determine an adequate heading for the FPSO. It was found that the optimum ranges concerning the roll motion, the vertical displacement and the vertical acceleration at the riser connection point don't occur at the same heading. An approximation of the best range can be selected by considering the restraints.

Zhang et al. (2012) studied a SPM mooring system for two side-by-side vessels. A new side-by-side mooring bay designed by Keppel Offshore & Marine Technology Centre was investigated, and its global performance and dynamic stability were compared against those of the traditional SPM-mooring system. The multi-body systems include a SPM buoy with a turntable mooring system, a VLCC FPSO, oil tanker, and the hawsers/fenders and yokes between them. The work clearly showed that the newly-designed SPM mooring system

experienced smaller relative motions between vessels and was more stable in the same environment compared to the traditional SPM mooring system.

In the work of van't Veer et al. (2012), a validated methodology was introduced to calculate the oscillatory loads on bilge keels of ships operating at zero forward speed in irregular sea states. To calculate these loads, the local relative fluid velocities acting normal to the bilge keel were combined with a KC dependent drag coefficient. The local relative velocity to the bilge keel was obtained from 3D potential-flow computations. The KC dependent drag coefficient of the bilge keel geometry was calculated by 2D CFD simulations in harmonic flow oscillations utilizing a rectangular fluid domain. With the proposed approach, it was possible to quantify the ultimate load on the bilge keel in extreme design conditions and to obtain the long term load distribution necessary for fatigue analysis. Model tests for several FPSO vessels have been used to validate the methodology.

Kaminski and Bogaert (2010) presented the recent progress made in the full-scale tests of real membrane containment systems subjected to the action of breaking waves, which were used to model the sloshing impacts in LNG tanks of LNG carriers or Floating LNG terminals (FLNGs). The waves were generated in a water flume using a wave focusing method. The tests were carried out through the Sloshef project. Necessary steps were taken to improve the test repeatability, and to collect data for the analysis of scaling laws, hydro-structural interaction, and effects of membrane corrugations.

The motions and mooring loads of a turret moored Floating Storage and Regasification Unit (FSRU) and a Liquefied Natural Gas Carrier (LNGC) including sloshing were studied by Cho et al. (2011). The turret moored FSRU weathervanes on a turret, and the side-by-side LNGC moves and interacts with FSRU. It was concluded that the longitudinal sloshing considerably affects the surge motion and mooring tensions. It was shown in their work that sloshing needs to be considered simultaneously in the analysis of side-by-side moored FSRU and LNGC.

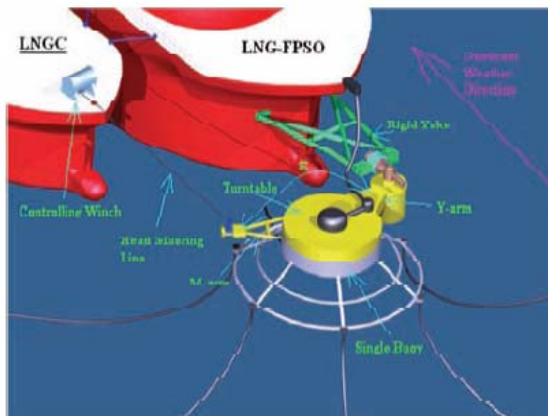


Figure 2.1.4.1 Bow Connection Details of New Concept SPM Mooring System (Zhang et al., 2012)

2.1.5 Floating LNG Production Storage and Offloading Vessels

Kim et al. (2012) introduced improved methods for offloading operability of side-by-side moored FLNGs. The operational envelop of loading arm is a function of relative motions between two vessels and the wave drift forces. In the proposed methods, one concept (Concept 1) involved an articulated type of reduction device with oil and spring as a damper in the cylinder with a stroke of 0.15m (9.0m in real scale). This motion device can be installed at the bow and the stern of a FLNG and a LNGC to reduce the relative motions. The waves in the gap lead to drift forces in head seas. For reduced waves in the gap between the FLNG and the LNG carrier, the wave absorber type of device, Concept 2, was introduced. This device can lead to a reduction of the second-order drift forces. It can be installed between fenders on a



side of FLNG. From the experimental studies, it was found that the proposed motion reduction devices significantly reduced the relative motions between two vessels, and eventually, improved the offloading operability.

2.2 Dynamically Positioned (DP) Structures

Xu et al. (2013) presented a new control strategy considering roll-pitch motion control. Traditionally, DP systems only deal with horizontal motions without considering vertical ones including roll and pitch. However, large roll and pitch motions may be induced by thruster actions, which obviously should be avoided. The main idea in the new control strategy was to consider roll-pitch velocity and acceleration feedback in the horizontal control law in order to avoid large roll-pitch motions. The time-domain simulation results showed that the new control strategy can suppress roll and pitch motions. However, it will reduce the positioning accuracy in the horizontal-plane in some degree. Moreover, the energy consumption with the new control strategy was lower than that with the conventional one.

Smit et al. (2011) investigated to what extent the current feed forward control would improve the positioning performance of dynamically positioned FPSO vessels in varying currents, for example, tidal current reversals and so called ‘internal soliton’ currents. The DpSim software developed by MARIN was extended with a module containing the current feed forward control. When the current feed forward control was applied to dynamic positioning in varying currents, the mean and the standard deviation of the control point excursion were reduced. The heading performance and the power usage did not change significantly while achieving this reduction.

For dynamically positioned crane barges operating in a close proximity to FPSO vessels during lifting operations, the hydrodynamic interactions are important and must be considered in the analysis. Tannuri et al. (2012) presented a large set of experimental tests considering a DP Barge in a close proximity to a FPSO. Results include the hydrodynamic interactions and their effect on the DP performance in terms of station-keeping and thrust demand.

van Daalen et al. (2011) presented a generic optimization algorithm for the allocation of dynamic positioning actuators, such as azimuthing thrusters and fixed thrusters. The algorithm is based on the well-known Lagrange multipliers method. In their work, the Lagrangian represents not only the cost function (the total power delivered by all actuators), but also all constraints related to thruster saturation and forbidden zones for azimuthing thrusters. The Newton-Raphson method was recommended to solve the thruster allocation problem. Depending on the configuration, it may lead to significant power (energy) savings. An iterative process has also been studied by taking the limitations of actuators into account.

2.3 Highly Nonlinear Effects on Ocean Structures

2.3.1 Slamming

Slamming is a complex nonlinear problem. It has been continuously studied by many researchers using experimental and numerical methods. In the numerical simulations, methods based on the potential-flow theory and CFD methods such as SPH, VOF and CIP have been employed.

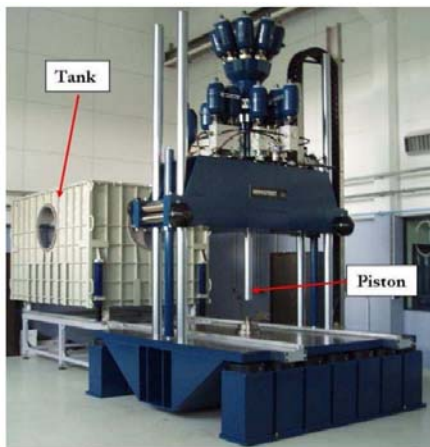


Figure 2.3.1.1 High-Speed Shock Apparatus
(Alaoui and Nême, 2012)

Various model tests have been carried out to further investigate the fluid-structure interactions during the water entry. Alaoui and Nême (2012) carried out an experiment to study fluid-structure interactions during the slamming impacts. The vertical impact velocities were maintained constant by using a specially designed high-speed shock machine. Three rigid structures, including a cone, a square pyramid and a wedge-cone, were tested. Good repeatability of impact velocities and slamming loads was observed, and empirical formulas for non-dimensional slamming coefficients were obtained. The predicted slamming coefficients of the cone by the ABAQUS/Explicit code are in good agreement with the experimental results.

Constantinescu et al. (2011) carried out experiments for cones with varying deadrise angles using a hydraulic shock machine. In their work, three numerical methods were employed to study 2D slamming of wedges and pseudo-3D slamming of cones. The first method, Impact++ABAQUS, was based on Wagner's theory and the displacement potential formulation. The second one combined the Arbitrary Lagrangian-Eulerian (ALE) analysis and a commercial finite element software program, ABAQUS/Explicit. The third method was based on the Coupled Eulerian-Lagrangian

(CEL) approach and the VOF method. Experiments were also conducted to validate the numerical results. The third method was proved to be potentially suitable for 3D slamming studies.

Damblans et al. (2012) carried out model tests to investigate the process of lowering a large scale mud mat (plate with shirts) with different porosities into calm water, regular wave, and irregular wave. Constant velocities were kept by using an electric jack. Impact loads were measured during the tests. Effects of porosity, impact velocity, and inclination angles of the plate on the impact coefficient were studied. Furthermore, a numerical method based on RANS with VOF for free surface capturing was applied to simulate the slamming phenomena and to predict the impact loads.

Huera-Huarte et al. (2011) conducted a series of experiments to study slamming forces on a rigid flat plate. A novel test apparatus, named Slingshot Impact Testing System (SITS), was developed. The tests were conducted with high impact velocities up to 5 m/s and a wide range of deadrise angles from 0.3° to 25° . The cushion effect due to trapped air with small deadrise angles ($<4^\circ$) was confirmed from the tests. An empirical formula for non-dimensional impact coefficients was proposed in their work.

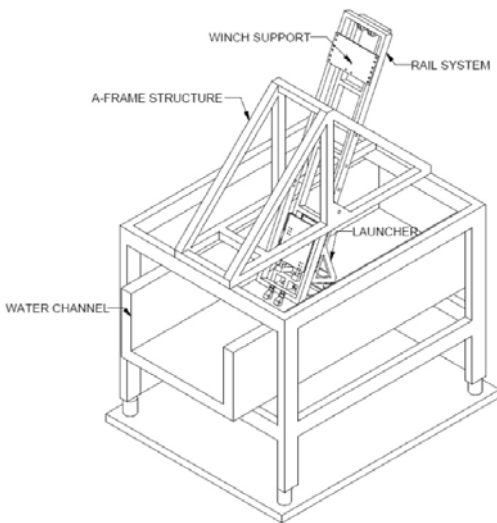


Figure 2.3.1.2 Slingshot Impact Testing System (Huera-Huarte et al., 2011)

van Nuffel et al. (2011) conducted free-drop tests to study the water entry of a rigid cylinder into calm water. Improvements were made on the accuracy and the repeatability of the pressure measurements. In their study, pressures and accelerations were recorded and further investigated. Parametric studies were carried out to examine the effects of sensor mounting, data sampling rate, temperature shock, the object surface conditions, and the water surface conditions on the measured pressure peak. Recommendations for experimental set-ups were provided. In 2012, they continued the study with the same apparatus (van Nuffel et al., 2012). Global forces were also measured in the tests. Relationships for pressure-speed and force-speed were investigated.

To investigate the slamming load distribution and its relationship with the impact velocity, Peng et al. (2011) conducted a free drop slamming test with a scaled trimaran model. Pressures were measured at the main hull, the side hull, and the cross structure of the trimaran. Comparisons were made between the experimental data and the simulation results based on the finite element method.

Stansberg et al. (2012) conducted experiments to investigate the breaking-wave induced slamming loads on vertical offshore structures. Time series of wave elevation, pressure distribution, and the integrated slamming loads were measured in the experiments. An empirical formula for slamming coefficient was also presented.

Efforts have been continuously made to address the slamming problems by Wagner's theory, potential-flow based and CFD methods. Korobkin and Khabakpasheva (2013) investigated the effect of water depth on the first peak of bending stresses during the water entry of an elastic body. Wagner's model was applied to solve the deepwater impact while the leading-order solution was presented for the shallow water impact. Two typical shapes, including a wedge with small deadrise angle and a cylindrical shell of elastic structure were considered. Computed bending stresses were compared to experimental data, and good agreement was observed.

Yan and Liu (2011) proposed a fully nonlinear numerical method based on the potential flow theory to investigate water entry of axisymmetric bodies. The method was based on an axisymmetric linear boundary element method (BEM) and a mixed Eulerian-Lagrangian (MEL) approach. A jet cutting technique, which was effective and robust, was developed. They applied the numerical method to study the effect of gravity and body geometry as well as the flow separation location on the continuous body surface. Two representative bodies, an inverted cone and a sphere, were included in the studies. They developed a formula with a single similarity parameter for evaluating the contribution of the gravity of the total impact force on the cones. For the sphere impact, it was observed the gravity effect was unimportant in the initial stage of impact, but it slightly increased the impact pressure in the later stage when Froude number is less than 2.0. The flow separation



location remained at a fixed location at the angle of 62.5 deg when the Froude number is larger than 1.0.

RANS methods along with the free surface capturing methods such as VOF and CIP have been used for slamming simulations. For example, Rahaman and Akimoto (2012) studied the slamming at the bow flare region by using a RANS-based CFD method. They investigated the pitch and heave motion as well as the pressure distribution at the bow flare region of a 3D container ship model travelling in regular head waves. Two dimensional simulations were carried out for selected bow flare sections based on the VOF method and FLUENT. Predicted slamming loads agreed reasonably well with the experimental data by Zhao et al. (1996).

Yang and Qiu (2012) continued their studies of 2D and 3D slamming problems based on a constrained interpolation profile (CIP) method. The compressible air was considered in the simulations. Validation studies of the numerical methods were carried out for 2D wedges with large and small deadrise angles, a 3D catamaran, and 3D cylinders. Numerical results were compared with solutions by other numerical methods and experimental data.

In addition, SPH has also been employed for slamming computations. For instance, Veen and Gourlay (2011) conducted parametric studies to investigate the effects of sectional shape and time-varying impact velocity on slamming loads by using the 2D SPH method. They used three section shapes, including a wedge, a bow flare and a catamaran in their studies. Veen and Gourlay (2012) further carried out numerical studies on 2D bottom slamming and bow flare slamming problems. In their work, the solid wall boundary conditions were modelled by using the ghost particle technique. The numerical method was applied to the water impact with prescribed velocity profile, and the numerical results were

compared with the experimental data (Aarsnes, 1996). Furthermore, a linear strip-theory code was combined with the SPH algorithm to compute the impact loads on hull sections. The numerical solutions were also compared to the experimental data from Ochi (1958).

In recent years, progress has also been made in addressing the structural deformation during slamming. The fluid-structure interaction (FSI) method has been employed in recent work. Jiang et al. (2012) validated two CFD methods for slamming problems by comparing the predicted impact loads with experimental data. The two CFD methods were a RANS method with STAR-CCM+ and a Lagrangian-Eulerian Fluid-Structure Interactions (FSI) method with DYSMAS. The pressure peak, the pressure time history, and the pressure-area relationship were investigated. Reasonable agreements between numerical predictions and experimental results were reported.

Vepa et al. (2011) carried out comparative studies of slamming loads on cylindrical structures with three methods: a mesh-based implicit method, a mesh-based explicit method, and the SPH method combined with the finite element (FE) model. The explicit method and the SPH-FE method were applied by using LS-DYNA while the implicit method was applied by using FLUENT-ABAQUS. Rigid and deformable cylinders were included in the computations. A significant pressure peak reduction was observed in the deformable cylinder cases. They also concluded that the SPH method had better convergence than the mesh-based methods.

Wang and Soares (2013) investigated the 2D water entry of a bow flare section and the effects of roll angle on slamming loads by applying an explicit finite element method in combination with a multi-material Eulerian formulation and a penalty coupling method. In the previous work by Wang et al. (2012), computations were carried out by using LS-

DYNA/Explicit. The predicted slamming load and pressure were compared with experimental data by Aarsnes (1996) and the numerical results by using other methods, including BEM and CIP.

Yamada et al. (2012) applied an explicit finite element code LS-DYNA to simulate the slamming loads of water-entry of a full-scale wedge. They first validated the method with a small-scale rigid wedge and an elastic cylinder. Further, the method was employed to investigate slamming of a full-scale elastic-plastic wedge. Results from numerical simulations were compared to those by the conventional Wagner method.

2.3.2 Sloshing

The problem of the sloshing of liquid cargo in tanks is especially important in the design of Liquefied Natural Gas (LNG) cargo containment systems. The liquid is stored at atmospheric pressure in insulated tanks at -161° Celsius. Due to the insulation system, tanks cannot be partitioned. As a result, liquid motions in the tanks, excited by the vessel motions, may be observed. The design of LNG ships or storage units is thus very complicated. The state-of-the-art methodology is based on the use of seakeeping computer codes to estimate ship or platform motions. Experiments on tank models and CFD simulations have been performed in order to estimate global and local fluid loadings in the tanks.

Experimental assessments of many parameters affecting the fluid motion and pressure are presented in the work of Loysel et al. (2012) and (2013). These results were acquired during two rounds of Sloshing Model Test (SMT) benchmark studies.

The first round of benchmark studies, involving nine participants, were based on a simple tank geometry (2D rectangular tank

with clear water), 14 different excitation conditions, and a measurement setup. It aimed to compare the laboratory measurements. From the comparison of experimental data, some preliminary conclusions were presented - the repeatability of single impact waves seemed to be acceptable, however notable discrepancies in event rates and probabilities of pressure exceedance were clearly observed for harmonic and irregular waves. These differences led to the next round of benchmark studies in 2012-2013.

The focus in the second round was on the accurate control of three parameters: the water filling level, the positioning of the tank and the rig motion. Many of motion rigs were hexapods (Loysel et al., 2013, Baudin et al. 2013). The results for single wave impacts with large gas pockets showed good agreement. This resulted in considering this setup as a reference configuration to validate methodologies. Differences were found when the impact location, the gas pocket location and its size were not accurately controlled. Discrepancies in the results for irregular motions still existed and they are comparable to those in the precedent benchmark studies. Temperature effects were highlighted and further investigations regarding this aspect were proposed.

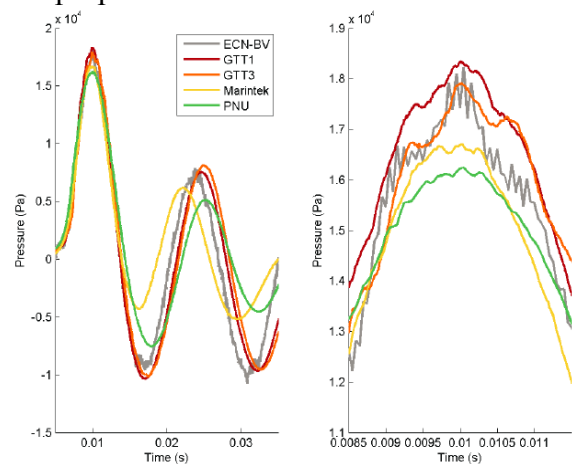


Figure 2.3.2.1: Representative Pressure Time Histories by Six Participants for A Single Impact Wave (Loysel et al., 2013)

Souto-Iglesias et al. (2011) presented a description of an experimental setup for sloshing tests involving angular harmonic motions. Details on data acquisition and synchronisation schemes were given. An uncertainty analysis was presented, focusing on the measurements of the first peak pressure.

Pistani and Thiagarajan (2012) carried out sloshing tests using a hexapod with two 2D model tanks. The maximum pressures were measured for 1-DOF motions. An analysis of the experimental setup was presented in their paper. A thermal artefact on the pressure transducers was observed when the water hit their sensitive surfaces. This effect was also reported by Loysel et al. (2012). They also checked motions of the excitation rig. The steps of data collection and analysis, as well as corrections to experimental shortcomings, were described.

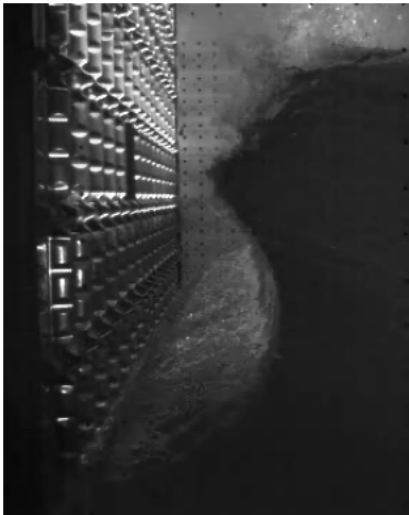


Figure 2.3.2.2 Full-Scale Air Pocket Impact on MarkIII (Kaminski and Bogaert, 2010)

Hydroelasticity in sloshing experiments was studied by Choi et al. (2012) using a hexapod and rectangular tank models. Surge motions for four different filling levels were tested using a regular rigid tank and a tank with a flexible stainless steel wall. The experiments

showed the impact pressure was higher in the case of the flexible wall.

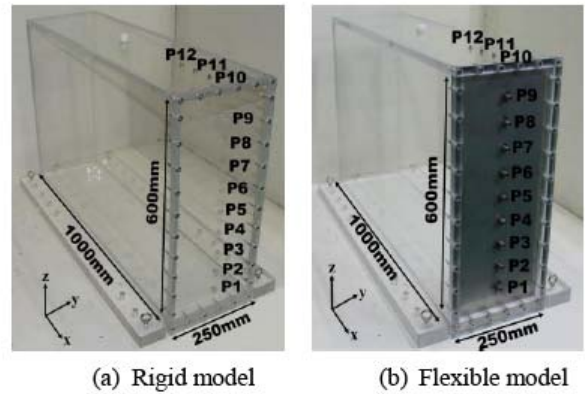


Figure 2.3.2.3 Rigid and Flexible Models and Locations of Pressure Transducers (Choi et al., 2012)

Lugni et al (2013) presented similar findings from their hydroelasticity experiments on a flexible tank wall. They also investigated the pressure effects on air cavities formed by the impact waves.

Wang et al. (2012) developed a new reliability-based methodology for the sloshing assessment of a membrane-type LNG cargo containment system (CCS) in LNGCs and FLNGs. For each individual sloshing impact event, the dependency of two parameters (the magnitude and the rising time) was taken into account in this new methodology. Based on the test data for the sloshing model, the equivalent static pressure for each individual impact event was calculated using the magnitude and the dynamic capacity factor (DCF) through the associated rising time. In the reliability analysis, the limit state function was used by applying the Load and Resistance Factor Design (LRFD) approach. Then, the sloshing load (equivalent static pressure) and structural resistance (static capacity) distributions were employed to determine the partial safety factors in the CCS design formula at a target reliability index.



Fillon et al. (2013) applied the extreme value theory to the samples of sloshing pressure in order to improve the model for predicting the maxima of sloshing pressure. Two different statistical fitting methods were used for sloshing pressure measurements in one sea state which is equivalent to a 480-hour duration sloshing test at full scale. This long duration sloshing test was in fact generated by using 96 five-hour individual experimental tests. The two methods led to a correct estimation of the maximum sloshing pressure. Graczyk et al. (2012) investigated local pressure effects based on low filling level tests of a 2D LNG tank model (scale 1:35). The tank has smooth wall surfaces and a wall with horizontal protrusions similar to Invar edges that disturb the local flows, inducing either pressure amplifications or cancellations. The authors indicated the need of advanced instrumentation in combination with high-speed cameras to explain the measurements of local pressure.

Using the same motion rig, Bouscasse et al. (2013) measured the free surface elevations in a 2D rectangular swaying tank. The experimental data were used to check the weakly-compressibility assumption in the SPH simulations.

Clauss et al. (2012) presented the comparison of model test results for a moored LNG model (scale 1:100) and numerical solutions. The study focused on the water motions within the prismatic tanks (30% filled) in beam seas.

Using a PIV system, Ji et al. (2012) measured velocities of flow in a small swaying rectangular tank excited by a crank motorised arm. The harmonic motions in non-resonant conditions were compared to the published results, and the properties of travelling waves were obtained from the velocity flow fields.

Water run-up and run-down on walls were analyzed with respect to the flow regimes.

Progress has been made to investigate the scale effect using model and full scale tests. Lafeber et al. (2012) reported the scale effect on wave impact using an instrumented wall adopted in the Sloskel JIP. The first tests were carried out using 1:6 scale in 2009 and full scale in 2010 at the same ambient conditions. The comparison of the two tests results showed the effect of the liquid properties and the air. As the compressibility of the gas was not scaled, the loading processes, 'building jets along the wall from the impact area' and 'compression of entrapped air', were not Froude-similar. The full-scale wave impact result was obtained after the loading process of 'compression of entrapped air' at scale 1:6 was corrected using the one-dimensional model of Bagnold (1939).

Pasquier and Berthon (2012) compared the sloshing impact measurements at full scale and at a model scale. The actual ship motions were used as input for the model tests (scale 1:40). A good correlation was found between the model test and full-scale results. At the small scale, the experimental simulations of LNG sloshing represented an accurate global flow inside the tanks in terms of the impact frequency. However, the authors suggested the need of studies for a wider range of conditions.

Karimi et al. (2013) also investigated the effect of scaling on the sloshing pressure. Two sets of model tests of 2D tanks at scales of 1:10 and 1:40 were carried out by GTT with a fill level of 20%. The effect of the gas-liquid density ratio and the speed of sound in the gas on measured pressures was studied.

The sloshing pressures were also measured by Kim et al. (2012) for a 1:50-scale model and a 1:70-scale model. The sloshing pressures were recorded at the same location for the



excited model tanks with irregular motions at the same Froude scale. The comparison showed the differences in the statistical results for the two models. However, when the Froude scaling was applied, a good agreement was found.

2.3.3 Wave Run-up

Research has been carried out in the past years on the study of the wave run-up on circular cylinders, monopiles, barges and columns of large semisubmersibles using CFD methods. The outcome of the studies indicates the importance of high-order nonlinearities and the need of computational efforts for accurate predictions.

Ramírez et al. (2011) presented a CFD model (NS3), which solves Navier-Stokes equations and uses the VOF method to treat the free surface. NS3 was applied to simulate the wave run-up on a vertical circular cylinder and the numerical results were compared with the experimental data from large-scale tests performed at the Large Wave Channel (GWK) in Hannover, Germany.

Cao et al. (2011) conducted simulations of wave run-up on a fixed vertical cylinder. The finite volume method was employed to solve Navier-Stokes equations based on OpenFOAM. The wave elevations were computed at several locations within a radial distance around the cylinder. The computed wave run-ups, velocities and pressures at various locations were compared with the published experimental data from MARINTEK.

Kim et al. (2011) developed a numerical wave tank model by matching the far-field wave solution based on the potential-flow theory and the CFD solution in the near field. This model was implemented in a CFD code based on the Arbitrary Lagrangian Eulerian (ALE) finite element method. The developed method was applied to a truncated vertical

cylinder exposed to nonlinear regular waves with wave lengths much greater than the diameter of the cylinder. Comparison with the theoretical and experimental data showed that the proposed method predicted wave run-ups accurately with a small computational domain confined near the cylinder.

Li et al. (2012) investigated wave run-ups on a vertical circular cylinder in an extreme wave environment. The waves were generated in a 3D wave basin using a focused wave method with different frequency and directional components. A practical method based on the velocity stagnation head theory was calibrated to calculate the wave run-up. The maximum wave kinematics at wave crest was calculated using the second-order theory. Wave run-ups on the weather side of the cylinder were computed and compared with measurements in experiments with multi-directional focused wave groups. The relations between the defined parameters and the wave parameters, such as model scale, directional spreading index and wave steepness, were discussed.

Peng et al. (2012) investigated wave run-ups on a monopile foundation in regular and irregular waves using ComFLOW. The numerical solutions are in good agreement with experimental data. It was showed that wave run-ups are dependent on the wave nonlinearity. A set of dimensionless and simple formulae have been derived to relate the non-dimensional wave run-up on the structure to the diameter of the structure and the Ursell number. The proposed formulae included the effect of the diameter of structure on wave run-ups. It led to similar results in comparison with other formulae.

Watai et al. (2011) reported some of the results from a cooperative project that investigated wave run-ups on a large moving semi-submersible platform. Wave elevations at various locations below the deck were



measured and compared with the predictions by WAMIT and by the improved ComFLOW code. Results showed that ComFLOW was able to predict the relative wave elevations at different positions below the deck.

Priyanto et al. (2012) studied wave run-ups on a large semi-submersible. Tests of a small-scale moored model in irregular waves were carried out in Marine Technology Centre (MTC)'s towing tank at Universiti Teknologi Malaysia. Significant wave run-up occurrences on the square-sectioned columns were observed.

Shan et al. (2012) presented an experimental investigation on three model configurations including a four-column array, a two-column array and a single column, aiming to understand relationships between wave run-ups and the leg spacing and between the wave interaction and the model configuration, as well as the wave run-up distributions around columns. The wave environment was restricted to monochromatic progressive waves with different wave steepness. For the three tested configurations, wave run-ups reached the maximum on the front sides of the fore columns, and decreased gradually as waves propagated. It was also found from the tests that wave run-ups decreased gradually as the leg spacing increased for the four- and the two-column arrays, which indicates the leg spacing would have important effect on the wave interaction among columns, and eventually affect wave run-ups on the columns.

2.4 VIV/VIM

2.4.1 Empirical VIV Prediction Programs

Slender structures subjected to VIV often vibrate in both in-line (IL) and cross-flow (CF) directions. The in-line motion of VIV can be a major contributor to the fatigue damage due to its higher frequencies and response modes even that the IL displacement is normally less than

the CF one. It also triggers higher-order harmonic responses in both IL and CF directions which further increase the fatigue damage. Passano et al. (2012) reported the latest development of the VIV prediction program, VIVANA, with its new IL prediction model. The modelling of risers partially covered by strakes in Shear7 was presented by Resvanis and Vandiver (2011). The hydrodynamic force model of the strake section was generalized from forced motion tests with a rigid cylinder with strakes.

Efforts have been made to develop a general methodology to calibrate Factors of Safety (FoS) for fatigue damage due to VIV. Fontaine et al. (2013) presented a reliability based method which accounts for uncertainties in S-N behaviour, metocean conditions and software predictions of VIV. Tognarelli et al. (2013) also presented similar methods, in which the uncertainties in prediction are based on the measured flow and the response data for full-scale drilling risers in the field.

2.4.2 VIV Prediction Based on CFD

Huang and Larsen (2011) presented the 2-D numerical simulation results for an elastically mounted circular cylinder subject to vortex induced vibrations. Reynolds-Averaged Navier–Stokes (RANS) equations and $k-\omega$ turbulent equations were solved by a finite volume method. The predicted response amplitudes, hydrodynamic forces and wake patterns were compared with the measured data in the equivalent experiments.

Zhao et al. (2012) simulated the one-degree-of-freedom (1-DOF) VIV of a circular cylinder in oscillatory flow. The vibration of the cylinder was confined in the cross-flow direction only. RANS equations and $k-\omega$ turbulent equations were solved by a Petrov–Galerkin finite element method. The same method was applied by Zhao et al. (2013) to study VIV responses of a cylinder in the combined steady and oscillatory flow.



Bourguet et al. (2011, 2012) performed direct numerical simulations on a tensioned beam with a length to diameter ratio of 200, subject to vortex-induced vibrations in linear varying shear flow at three different Reynolds numbers, from 110 to 1,100. The energy transfer between the structure and the fluid was studied and the presence of mono- and multi-frequency responses was investigated. Similar study was also carried out for the tensioned beam subject to the exponential flow (Bourguet et al., 2013). The mechanism of the broadband VIV responses was studied.

2.4.3 New VIV Prediction Methods

A time-domain finite element analysis method using a local hydrodynamic force model has been developed by Mainçon et al. (2011). In this model, the recent history of the velocity is used to enter a database of velocity and force measurements obtained from rigid cylinder tests, and thus to determine the force and advance the dynamic FEM analysis. Preliminary results are encouraging. The objective was to create models that can capture higher harmonics and can be used in the analysis of risers with seafloor contact or time-varying currents and waves.

Campbell et al. (2013) proposed a new random vibration method with a band-limited white-noise lift-force model to predict the VIV responses of a fully straked flexible cylinder.

Ma et al. (2012) developed a time-domain analysis tool for VIV prediction of marine risers based on a forcing algorithm and by making full use of the available high Reynolds number experimental data. In the formulation, the hydrodynamic damping is not treated as a special case but simply an extension of the experimentally derived lift curves. The forcing algorithm was integrated into a mooring analysis program based on the global-coordinate based finite element method. At

each time step, the added mass, lifting force and drag force coefficients and their corresponding loads are computed for each element. Validation studies have been carried out for a full-scale rigid riser segment and a model-scale flexible riser. The numerical results were compared with experimental data and solutions by other programs. The validation studies have shown the proposed method is promising in VIV prediction.

2.4.4 Experiments

A. 2D Tests

The semi-empirical VIV prediction programs rely on hydrodynamic force coefficients generalized from forced motion tests of rigid cylinders. In the work of Zheng et al (2011), extensive forced in-line and combined in-line and cross-flow experiments were used to provide the hydrodynamic coefficient databases, in addition to the existing CF hydrodynamic coefficients. In these tests, the IL and/or CF motions are harmonic.

It is known that the cross-flow motions of a flexible beam subjected to VIV can be far from harmonic motions. The motion amplitude can also vary in time. To investigate the VIV response subjected to the non-harmonic motions, forced motion tests for rigid risers using observed orbits extracted from flexible beam were carried out by Yin and Larsen (2011). The tests results were compared with CFD solutions. Using the same experiment technique, Yin and Larsen (2012) further compared the hydrodynamic coefficients obtained from the forced motion tests with observed motion orbits extracted from flexible beam experiments and from periodic approximations. Aglen et al. (2011) studied the added mass coefficients from forced motion tests with extracted orbits from flexible beam tests. The influence of added mass on the IL and CF interactions has been studied for tests



with mode one dominating the responses in both directions.

Raghavan and Bernitsas (2011) performed free oscillation tests of a rigid cylinder to study the Reynolds number effect within the range of 8.00×10^3 to 1.50×10^5 . The objective of their work was to design a power generation unit based on VIV that can absorb energy from the fluid. It was found that VIV is significantly different at different flow regimes. An amplitude ratio of 1.9 was achieved for a smooth cylinder in VIV even with high damping imposed.

To further investigate the effect of Reynolds number on VIV, a new innovative VIV test rig was designed and built at MARINTEK to test a rigid full-scale riser model (Lie et al., 2013). The rigid riser model was mounted vertically and can either be elastically mounted or be given a forced CF motion. The bare cylinder was tested in both sub-critical and critical Reynolds number regimes. The effect of Reynolds number on the amplitude of VIV displacement was found to be significant and further research was recommended to explore the subject.

Constantinides et al. (2013) performed the tandem riser tests at the prototype Reynolds numbers. The tests were carried out utilizing two full-scale cylinders fitted with actual VIV suppression devices and towed either in fixed or spring supported configurations. The results revealed significant differences from those by today's design practices and industry codes.

B. 3D Tests

Several VIV tests with flexible beam have been carried out during 2011-2013. Strain gauges were mostly used in these tests. Accelerometers were also used in some of the tests to provide redundancy in the measurements. All of the tests were carried out

in sub-critical Reynolds numbers due to the limitation in the test facility and the cost.

An extensive hydrodynamic test program of riser models subjected to vortex-induced vibrations was carried out in the MARINTEK Offshore Basin Laboratory on behalf of Shell Oil Company (Lie et al. 2012). Three different riser models were towed horizontally at various speeds, simulating uniform and linearly varying sheared current. The test program included approximately 400 tests with different riser configurations. VIV responses of risers with/without suppression devices as well as the effect of Reynolds number and marine growth were investigated.

Huera-Huarte et al. (2013) presented the experiment results of a long flexible cylinder with low mass ratio subject to a stepped current. The test pipe is 3m long with an external diameter of 19 mm. The effect of low mass ratio on VIV was investigated. Song et al. (2010) performed VIV tests with a long flexible riser towed horizontally in a wave basin. The riser model has an external diameter of 16 mm and a total length of 28.0 m. The asymmetrical distribution of displacement was mainly resulted from the modal composition.

Fu et al. (2013) performed VIV tests of a flexible cylinder in an oscillatory flow. A flexible cylinder was forced to harmonically oscillate at various combinations of amplitude and period. The tested cylinder is 4m long with an outer diameter of 24mm. Unique features of VIV in an oscillatory flow were presented.

Huera-Huarte and Bearman (2011) performed model tests to study the interference between two identical risers. In these tests, two flexible risers were arranged in tandem and side-by-side positions. The test pipe is 1.5m long with an outer diameter of 16mm. The dynamic responses of the two interfering risers were presented.



Efforts have also been made to further analyze the existing VIV test data. Larsen et al. (2012) applied wavelet analyses to reveal the frequency components in the measured signals, using Hanøytangen and NDP high-mode VIV test data. This study characterized the frequency components of VIV measured in flexible beams subjected to sheared current in order to establish a general model for use in the empirical VIV prediction programs.

The presence of higher-order harmonic frequency components and chaotic responses has been observed in many flexible beam tests. Price et al. (2011) studied the impact of higher-order harmonic stress components and the broad band responses on fatigue damage using NDP high-mode VIV test data. The study indicated that both factors can lead to significant fatigue damages.

Modarres-Sadeghi et al. (2011) also analyzed the NDP high-mode VIV experimental data. The stationary and chaotic VIV responses were characterized. Their influences on the fatigue damage were discussed. Vandiver (2012) proposed a dimensionless damping parameter to describe the cylinder VIV response, which overcomes the limitations in existing "mass-damping" parameters.

Swithenbank and Larsen (2012) calculated the energy in the system from measured responses of a flexible beam and the associated energy levels in the duration of the VIV with high amplitudes. Rao et al. (2013) studied the excitation competition between the bare and buoyant segments of flexible cylinders using the Shell high-mode VIV test data.

McNeill and Agarwal (2011) proposed an efficient method for modal decomposition and reconstruction of riser responses due to VIV. The travelling wave responses and the fatigue damage along the riser can be estimated accurately by this method using a limited

number of measurements. McNeill (2012) further proposed an alternative way of estimating the fatigue damage, which is based on Dirlik's method to obtain rain-flow damage for Gaussian random stress.

2.5 New Experimental Techniques

Song et al. (2013) presented a velocity measurement method derived from the PIV technique using a high speed camera, called Bubble Image Velocimetry (BIV). It directly uses air-water interfaces in the image without the use of a laser for illumination. The measurement plane is controlled by minimizing the depth of field within which objects (i.e., air bubbles and water droplets in this case) are in focus and sharp, and therefore carrying more weight (i.e., higher intensity) in the correlation process for the velocity determination.

A subsea imaging technique was described by Embry et al. (2012) for in-situ measurements, using a high resolution 3D laser imaging unit. The optical head was mounted on a 2D-scanning device. The equipment and the preliminary tests in a basin were described showing the ability of high spatial accuracy at a relatively low scanning frequency. Experimental data (clouds of points) can be processed by regular dedicated software. Shapes of objects can be measured within a large volume at a millimeter precision. The system was initially developed for surveys and maintenance purposes, and it could be used in wave tanks for underwater measurements, for example, the scours around foundations.

Chabaud et al. (2013) developed the concept of real-time hybrid testing (RTHT), defined as a hardware-in-the-loop (HiL) simulation, and applied it to scaled model testing. The authors admitted this method is not a standard and accurate method in offshore studies. In order to generalize its use, they described the global scheme and presented details on the different

stages of calculations and data processing, at least on numerical and theoretical aspects.

The modeling of fenders in experiments was presented by Cole et al. (2012). The design and development of model-scale fenders and their application in float-over topsides installation experiments were provided. Improvements were shown in term of versatility and robustness.

It should be mentioned the openings of two new facilities in UK with wave and current capacities, mainly for ocean engineering and testing of marine energy devices. The Plymouth Ocean Wave Basin, established in 2013, is 35m long and 15m wide fitted with a movable floor (0-3m depth) and multidirectional wave generator. FLOWAVE-TT, opened in 2014 and located at Edinburgh, is a 25m diameter circular tank with a rising floor. Pumps around the tank allow to generate a water current up to 1.6 m/s at any direction in the tank.

2.6 New Extrapolation Methods

During the period of 2011-2013, limited investigations have been carried out on the development of extrapolation methods. However, challenges and issues in scaling of model test results to full scale have been indicated in problems related to sloshing, dynamic positioning systems, and mooring and risers.

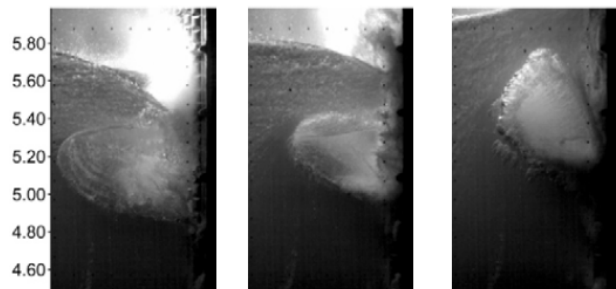
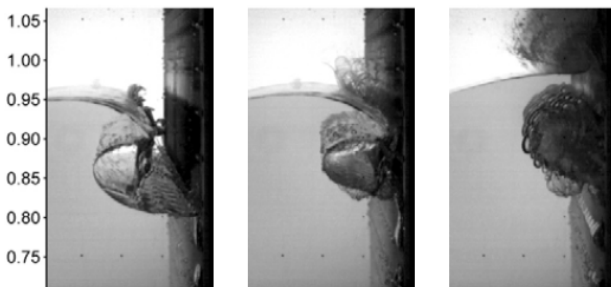


Figure 2.6.1 Air Pocket Impact on A Corrugated Wall (Upper: 1:6 Scale; Lower: Full Scale) (Bogaert et al., 2011)

For example, in the Sloskel project, Bogaert et al. (2011) discussed the uncertainties in model tests of sloshing due to scaling biases which are associated with the Froude-scaled excitations. Based on the results of experiments at 1:6 and 1:1 scales (see Figure 2.6.1), it was concluded that gas pocket pressures are greatly affected by the gas compressibility bias due to the un-scaled properties of the gas.

2.7 Practical Applications of Computational Methods to Prediction and Scaling

Koop and Bereznitski (2011) calculated current coefficients for the JBF-14000 semi-submersible using MARIN's in-house code ReFRESKO. Full-scale CFD computations were carried out to investigate possible scale effects using five subsequently refined grids for three different headings and ten different grids of different type for a scaled model. The numerical results were compared with the experimental data obtained from wind tunnel experiments and tests in the offshore basin. Approximately 15-20% lower values were found than those from the model-scale tests.

Ottens and van Dijk (2012) studied the thruster-hull interaction of a semi-submersible crane vessel in a current. CFD computations were compared with the model test data for the assessment of the thrust efficiency of the DP thrusters. From the comparison between the CFD and model test data, it was observed that



the CFD method was able to predict the relevant force components within a sufficient accuracy for engineering purposes. To assess the CFD prediction in case of full scale, numerical results were compared with the sea trial data for the vessel with different thrust combinations. The comparison suggests the improvement in CFD code.

2.8 Improving Method of Experiments, Numerical Methods and Full-Scale Measurements

Huera-Huarte (2012) used the Defocusing Digital Image Particle Velocimetry (DDPIV) method to measure vortex-induced vibrations of long flexible cylinders in wind/water tunnel. The concept of the proposed method was given by Willert and Gharib (1992). The authors suggested the method, as a better alternative to other traditional vibration response measurement techniques, could be used to study VIV in the laboratory. The good agreement of measured data with known results confirmed the effectiveness of the above technique.

The flooding process of a tank in a damaged ship was studied by Ruponen et al. (2012) at full scale. A decommissioned ship was used for the full-scale tests. Bernoulli's equation for compressible fluid was used for air flows in the time-domain flooding simulations. For numerical simulations, The NAPA flooding simulation tool was used. In general, the comparison between experimental and simulated results showed a good agreement with small inaccuracies in the calculation of transient phenomena in the beginning of the flooding process.

3. REVIEW OF THE EXISTING PROCEDURES

The Committee reviewed three existing procedures: 7.5-02-07-03.1 Floating Offshore Platform Experiments, 7.5-02-07-03.2 Analysis

Procedure for Model Tests in Regular Waves and 7.5-02-07-03.3 Model Tests on Tanker-Turret Systems.

Only very minor revisions were identified for 7.5-02-07-03.1 and 7.5-02-07-03.2. The Committee however found that there is little information in 7.5-02-07-03.3 and the limited information in 7.5-02-07-03.3 is very similar to that in 7.5-02-07-03.1. The Committee recommended to move the contents of 7.5-02-07-03.3 to 7.5-02-07-03.1.

The Committee also identified that there is no existing procedure dealing with the result analysis of model tests in irregular waves. The Committee recommended to develop a new procedure on this aspect.

4. GUIDELINES FOR VIV AND VIM TESTS

Bluff marine structural bodies such as the risers, free spanning pipelines and offshore platforms with cylindrical members (e.g., spars and semi-submersible) can undergo vortex shedding in ocean currents. The vortex shedding process and vortices induce periodic forces on the body which can cause the body to vibrate in both in-line (IL) and cross-flow (CF) directions. If the vortex induced response mainly causes elastic deformation in marine structures, such as risers, cables and free spanning pipelines, this phenomenon is known as Vortex Induced Vibrations (VIV). If the vortex induced response mainly causes rigid body motions such as a sway motion of a platform, this response often is denoted as Vortex Induced Motion (VIM).

The Committee focused on the development of guideline for VIV testing (7.5-02-07-03.10). The purpose of this guideline is to ensure that laboratory model tests of VIV responses of marine structures are adequately performed according to the best available techniques and to provide an indication of improvements that

might be made. The guideline is also to ensure that any comprises inherent in VIV tests are identified and their effects on the measured results are understood.

The Committee has also drafted the guideline for VIM testing (7.5-02-07-03.11). It is recommended to be completed by the Ocean Engineering Committee of 28th ITTC.

5. NUMERICAL BENCHMARK STUDIES OF VIV

In the previous benchmark studies organized by the 26th ITTC Ocean Engineering Committee, all participants used the two-dimensional unsteady RANS method. Various turbulence models were employed with the assumption that the flow is fully turbulent.

It was concluded from the studies that the drag crisis phenomenon on the stationary smooth cylinder was not captured by the RANS method. It is well known that the drag crisis is caused by the instability of separated shear layer in the critical Reynolds number regime ($2 \times 10^5 < Re < 5 \times 10^5$). At the critical Reynolds numbers, the transition point is located very close to the point of flow separation. As a result, the shear layer eddies cause the mixture of flow in the boundary layer so that the flow is energized and the flow separation is delayed. The delay of separation point leads to the reduction of the drag coefficient. The methodology based on two-dimensional, unsteady RANS with turbulence models is inadequate to simulate this physical phenomenon (ITTC Ocean Engineering Committee Report, 2011). It is necessary to extend the benchmark studies by including other CFD methods.

A Workshop for benchmark studies on VIV and wave run-ups was held in Nantes, France, October 17-18, 2013. Six participations presented their results of VIV studies. The benchmark studies are summarized below.

5.1 Benchmark Data

As reported in the ITTC Ocean Engineering Committee Report (2011), the benchmark data for the VIV of a circular cylinder was provided by MARIN. The rigid circular cylinder is 200mm in diameter and 3.52m in length (Figure 5.1.1). The cylinder was suspended from the carriage about 1.7m below the calm water surface. The VIV test apparatus is shown in Figure 5.1.2. The towing tank is 4m deep, 4m wide and 210m long. The cylinder was towed horizontally by the carriage at various speeds. Details of the tests can found in the work of de Wilde and Huijsmans (2001,2004) and de Wilde et al. (2003 and 2006).

For numerical computations, six (6) Reynolds numbers were selected as follows:

6.31E+04, 1.26E+05, 2.52E+05
3.15E+05, 5.06E+05, 7.57E+05

The measured drag coefficients for the smooth stationary cylinder are presented in Figure 5.1.3.



Figure 5.1.1 Smooth Cylinder

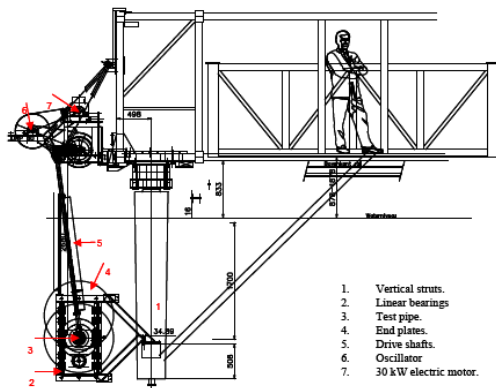


Figure 5.1.2 High Reynolds Number VIV Test Apparatus

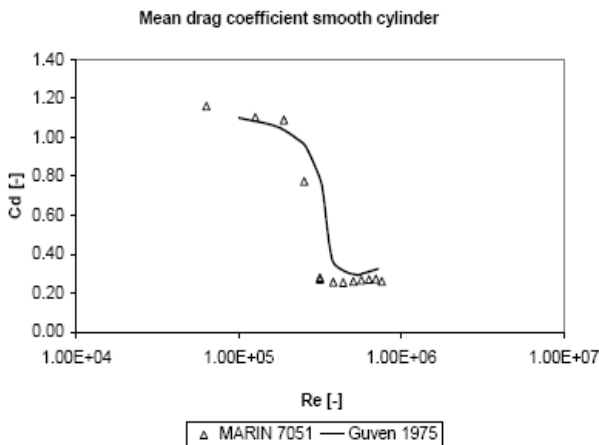


Figure 5.1.3 Drag Coefficient for the Smooth Cylinder

5.2 Participants and Numerical Methods

Various organizations and individuals have been invited to participate in the benchmark studies. A list of participants is given in Table 5.2.1. The numerical methods and computational details are summarized in Table 5.2.2.

Table 5.2.1 Participants for the VIV Benchmark Studies

| | Organization | Country |
|---|---------------------------------------|---------|
| 1 | China Ship Scientific Research Centre | China |
| 2 | Seoul National University | Korea |
| 3 | Samsung Ship Model Basin | Korea |
| 4 | Memorial University | Canada |
| 5 | Inha University | Korea |
| 6 | University of Iowa | USA |
| 7 | University of Southampton | UK |
| 8 | Shanghai Jiao Tong University | China |

Table 5.2.2 Numerical Methods Used by Participants

| | Code name | 2D/3D | Steady/Unsteady | RANS/DES/LES |
|----|--------------------------------|--------------------------|---------------------------|----------------------|
| A | FLUENT (Commercial Code) | 2D | Unsteady | RANS |
| B | SNUFOAM (In-house Code) | 2D | Unsteady | RANS |
| C | FLUENT (Commercial Code) | 2D | Unsteady | RANS |
| D | CFDSHIP-IOWA (In-house Code) | 3D | Unsteady | LES |
| E | Code-S (In-house Code) | 3D | Unsteady | LES |
| F | OpenFOAM (Open Source Code) | 3D | Unsteady | LES |
| G | Naoe-FOAM-SJTU (In-house Code) | 2D | Unsteady | RANS |
| H1 | STAR-CCM+ (Commercial Code) | 2D | Unsteady | RANS |
| H2 | STAR-CCM+ (Commercial Code) | 2D | Unsteady | RANS |
| H3 | STAR-CCM+ (Commercial Code) | 3D | Unsteady | DES |
| H4 | STAR-CCM+ (Commercial Code) | 3D | Unsteady | LES |
| | Number of Grid | Type of Grid | Convection Term | Δt |
| A | 87,223 | Structured | Upwind | 0.001/0.0005 |
| B | 32,280 | Structured | Upwind | 0.001/0.0002 /0.0001 |
| C | 43,820 | Structured | Upwind | 0.001 |
| D | 67,000,000 | Structured | QUICK/WENO | 0.00008 /0.0001 |
| E | 11,300,000 | Unstructured (Cartesian) | Upwind | (CFL=0.5) |
| F | Max 4,000,000 | Unstructured | Hybrid (Central + Upwind) | 0.005 |
| G | 100,000 | Chimera | Upwind | 0.00017 ~ 0.0015 |
| H1 | 592,478 | Hybrid | Upwind | 0.0001 |

| | | | | |
|----|------------|------------|--------|------------------|
| | | | | ~0.002 |
| H2 | 592,478 | Hybrid | Upwind | 0.0001 ~0.002 |
| H3 | 12,400,000 | Structured | Upwind | 0.002 ~0.02 |
| H4 | 12,400,000 | Structured | Upwind | 0.002 ~0.02 |

| | y^+ | Wall Function (Used/Not Used) | Turbulence Model | Transition Model (Used/ Not Used) |
|----|------------|-------------------------------|------------------|-----------------------------------|
| A | 59 | U | k-w SST | N |
| B | 2 | N | k-w SST | N |
| C | 10 | N | k-w SST | N |
| D | 0.03 ~0.15 | N | Dynamic model | N |
| E | - | N | Dynamic model | N |
| F | 1 | N | Dynamic model | N |
| G | 1~4.9 | U | k-w SST | N |
| H1 | 0.06~0.56 | N | k-w SST | N |
| H2 | 0.06~0.56 | N | k-e (Standard) | N |
| H3 | 0.06~0.56 | N | - | N |
| H4 | 0.06~0.56 | N | - | N |

5.3 Numerical Results

In the benchmark studies, unsteady RANS (URANS), detached eddy simulation (DES) and large eddy simulation (LES) methods were employed. In term of the overall trend, results by DES and LES are generally in better agreement with the experimental data than those by URANS. The steep drop of mean C_D was captured by LES. In addition, the LES results agree better with the experimental data at most points than those by URANS. Some URANS methods gave reasonably good results at high Reynolds numbers. The mean C_D , the mean C_L , the RMS of C_L , and the Strouhal number are compared with experimental data in Figures 5.3.1 to 5.3.4, respectively, and are also presented in Tables 5.3.1 to 5.3.4.

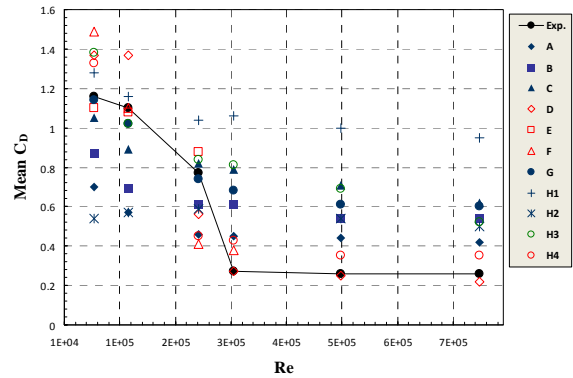


Figure 5.3.1 Mean Drag Coefficient

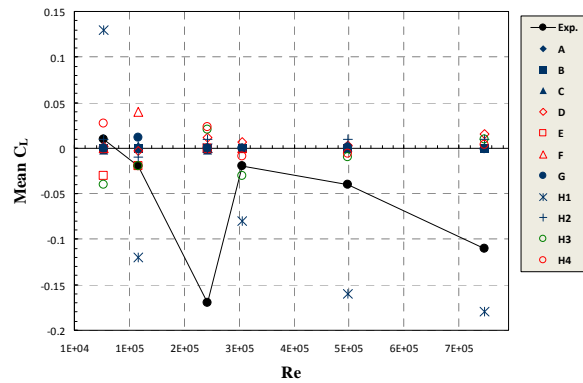


Figure 5.3.2 Mean Lift Coefficient

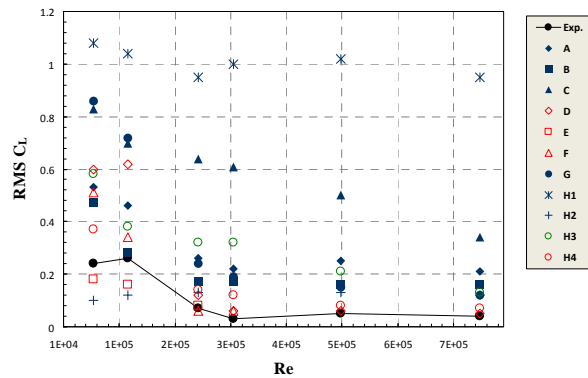


Figure 5.3.3 RMS of Lift Coefficient

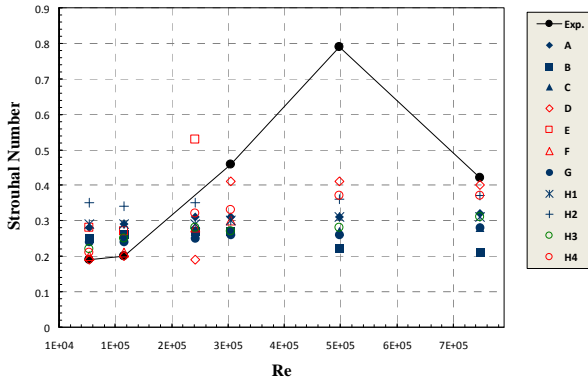


Figure 5.3.4 Strouhal Number

Table 5.3.1 Mean Drag Coefficient

| Mean C_D | Reynolds Number (E+05) | | | | | |
|------------|------------------------|------|------|------|------|------|
| | 0.631 | 1.26 | 2.52 | 3.15 | 5.06 | 7.57 |
| Exp. | 1.16 | 1.10 | 0.77 | 0.27 | 0.26 | 0.26 |
| A | 0.70 | 0.57 | 0.46 | 0.45 | 0.44 | 0.42 |
| B | 0.87 | 0.69 | 0.61 | 0.61 | 0.54 | 0.54 |
| C | 1.05 | 0.89 | 0.82 | 0.79 | 0.71 | 0.62 |
| D | 1.37 | 1.37 | 0.56 | 0.27 | 0.25 | 0.22 |
| E | 1.10 | 1.08 | 0.88 | - | - | - |
| F | 1.49 | 1.10 | 0.41 | 0.38 | - | - |
| G | 1.14 | 1.02 | 0.74 | 0.68 | 0.61 | 0.60 |
| H1 | 1.28 | 1.16 | 1.04 | 1.06 | 1.00 | 0.95 |
| H2 | 0.54 | 0.57 | 0.59 | - | 0.54 | 0.50 |
| H3 | 1.38 | 1.02 | 0.84 | 0.81 | 0.69 | 0.52 |
| H4 | 1.33 | - | 0.45 | 0.43 | 0.35 | 0.35 |

Table 5.3.2 Mean Lift Coefficient

| Mean C_L | Reynolds Number (E+05) | | | | | |
|------------|------------------------|--------|--------|--------|--------|--------|
| | 0.631 | 1.26 | 2.52 | 3.15 | 5.06 | 7.57 |
| Exp. | 0.01 | -0.02 | -0.17 | -0.02 | -0.04 | -0.11 |
| A | 0.000 | 0.000 | 0.001 | 0.000 | 0.002 | 0.000 |
| B | 0.000 | 0.000 | 0.000 | 0.000 | 0.000 | 0.000 |
| C | -0.002 | 0.003 | -0.002 | 0.000 | 0.001 | 0.001 |
| D | 0.002 | -0.003 | 0.012 | 0.007 | 0.003 | 0.015 |
| E | -0.030 | -0.020 | 0.000 | - | - | - |
| F | 0.000 | 0.040 | 0.000 | 0.000 | - | - |
| G | 0.000 | 0.012 | 0.000 | 0.000 | 0.001 | -0.001 |
| H1 | 0.130 | -0.120 | 0.000 | -0.080 | -0.160 | -0.180 |
| H2 | 0.010 | -0.010 | 0.010 | - | 0.010 | 0.010 |
| H3 | -0.040 | -0.020 | 0.020 | -0.030 | -0.010 | 0.010 |
| H4 | 0.027 | - | 0.023 | -0.009 | -0.006 | 0.004 |

Table 5.3.3 RMS of Lift Coefficient

| RMS C_L | Reynolds Number (E+05) | | | | | |
|-----------|------------------------|------|------|------|------|------|
| | 0.631 | 1.26 | 2.52 | 3.15 | 5.06 | 7.57 |
| Exp. | 0.24 | 0.26 | 0.07 | 0.03 | 0.05 | 0.04 |
| A | 0.53 | 0.46 | 0.26 | 0.22 | 0.25 | 0.21 |
| B | 0.47 | 0.28 | 0.17 | 0.17 | 0.16 | 0.16 |
| C | 0.83 | 0.70 | 0.64 | 0.61 | 0.50 | 0.34 |
| D | 0.60 | 0.62 | 0.12 | 0.06 | 0.06 | 0.05 |
| E | 0.18 | 0.16 | 0.08 | - | - | - |
| F | 0.51 | 0.34 | 0.06 | 0.06 | - | - |
| G | 0.86 | 0.72 | 0.24 | 0.19 | 0.15 | 0.12 |
| H1 | 1.08 | 1.04 | 0.95 | 1.00 | 1.02 | 0.95 |
| H2 | 0.10 | 0.12 | 0.13 | - | 0.13 | 0.12 |
| H3 | 0.58 | 0.38 | 0.32 | 0.32 | 0.21 | 0.13 |
| H4 | 0.37 | - | 0.14 | 0.12 | 0.08 | 0.07 |

Table 5.3.4 Strouhal Number

| Strouhal Number | Reynolds Number (E+05) | | | | | |
|-----------------|------------------------|------|------|------|------|------|
| | 0.631 | 1.26 | 2.52 | 3.15 | 5.06 | 7.57 |
| Exp. | 0.19 | 0.20 | N/A | 0.46 | 0.79 | 0.42 |
| A | 0.28 | 0.29 | 0.31 | 0.31 | 0.31 | 0.32 |
| B | 0.25 | 0.26 | 0.27 | 0.27 | 0.22 | 0.21 |
| C | 0.25 | 0.26 | 0.27 | 0.27 | 0.27 | 0.28 |
| D | 0.19 | 0.20 | 0.19 | 0.41 | 0.41 | 0.40 |
| E | 0.28 | 0.27 | 0.53 | - | - | - |
| F | 0.20 | 0.21 | 0.28 | 0.30 | - | - |
| G | 0.24 | 0.24 | 0.25 | 0.26 | 0.26 | 0.28 |
| H1 | 0.29 | 0.29 | 0.29 | 0.30 | 0.31 | 0.31 |
| H2 | 0.35 | 0.34 | 0.35 | - | 0.36 | 0.37 |
| H3 | 0.22 | 0.25 | 0.28 | 0.27 | 0.28 | 0.31 |
| H4 | 0.21 | - | 0.32 | 0.33 | 0.37 | 0.37 |

5.4 Summary of Presentations at the Workshop

In the Workshop, six papers were presented on VIV benchmark studies. A summary of some papers related to the benchmark studies is given below.

Yeon et al. (2013) studied drag crisis with the LES method and the computations were carried out at various Reynolds numbers. It was indicated that the solutions are strongly affected by the domain size. The mean drag coefficients were compared to experimental data by MARIN in Figure 5.4.1.

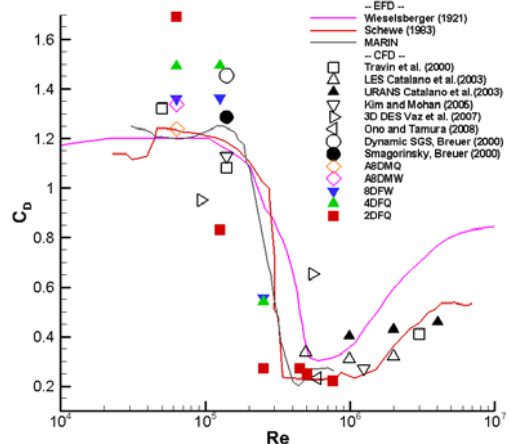


Figure 5.4.1 Drag Coefficient versus Re (Yeon et al., 2013)

Lee and Yang (2013) also employed LES for the benchmark studies and carried out

simulations at three Reynolds numbers, $Re = 6.31E+04$, $1.26E+05$, and $2.52E+05$. The 3D LES code was developed in-house based on a finite-volume method. A dynamic sub-grid scale model, in which the model coefficient is dynamically determined by the currently resolved flow field rather than by assigning a prefixed constant, was implemented for accurate turbulence modelling. Figure 5.4.2 presented time-averaged statistical data in comparison with those by MARIN. Note that Grids #1, #2 and #3 consist of 4.4, 8.7 and 11.3 millions of cells, respectively. As shown in the figure, LES captured the trends of the mean drag coefficients near the drag crisis.

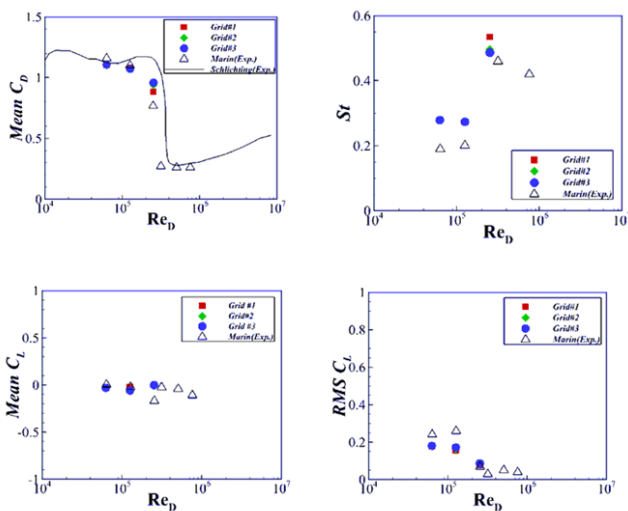
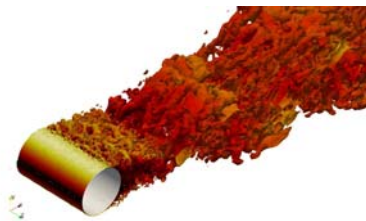


Figure 5.4.2 Simulation Results of 3D LES (Lee and Yang, 2013)

James and Lloyd (2013) studied the flow around the circular cylinder at high Reynolds numbers using LES. They found that unstructured grids provide better resolution of key flow features, when a ‘reasonable’ grid size is maintained. A blended upwind-central scheme, unique in OpenFOAM, was used, avoiding unnecessarily high numerical dissipation as well as removing artificial wiggles observed in the full central scheme. Figure 5.4.3 presents an example of vortical structures.



$$Re = 3.15 \times 10^5$$

Figure 5.4.3 Vortical Structures in terms of the Second Invariant of the Velocity Gradient Tensor (James and Lloyd, 2013)

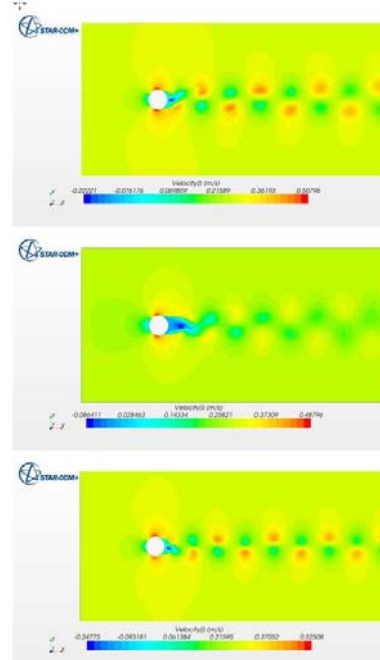
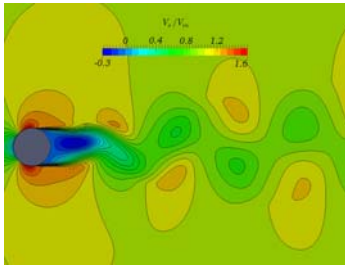


Figure 5.4.4 Horizontal Velocity Contours at $Re = 6.31E+04$ (top: SST $k-\omega$ model, middle: $k-\epsilon$ model, bottom: Reynolds stress turbulence model) (Wen and Qiu, 2013)

Wen and Qiu (2013) simulated the two-dimensional unsteady turbulence using a RANS solver, Star-CCM+, and various turbulence models. The studies showed that turbulence models have significant effects on the solutions (see Figure 5.4.4) and RANS is inadequate to address the ‘‘drag crisis’’ phenomenon.

Ye et al. (2013) used a RANS solver, pimpleFoam in OpenFOAM, coupled with an

overset grid technique. The $k-\omega$ SST turbulence model was employed. Numerical results without overset grid approach were also presented for comparison study. An example of predicted velocity contour is presented in Figure 5.4.5.



$$Re = 7.57 \times 10^5$$

Figure 5.4.5 Velocity Contour
(Ye et al., 2013)

5.5 Conclusions and Recommendations

In the benchmark studies, URANS, DES and LES were used. In terms of overall trend, numerical predictions by DES and LES are generally in better agreement with the experimental data than those by URANS. It can be concluded that the LES method captured the drag crisis phenomenon and the LES solutions agree better with experimental data at most points than those by URANS. At high Reynolds numbers, some solutions by the URANS method agree reasonably well with the experimental data.

Some of the participants are still working on completing the simulations at all the Reynolds numbers using DES and LES. More comparisons will be made in a journal paper, which is being prepared by the Committee.

The Committee recommended to continue the benchmark studies based on LES and DES.

6. BENCHMARK STUDIES OF WAVE RUN-UP

6.1 Introduction

The Committee conducted benchmark studies of wave run-ups on a single truncated cylinder and on four truncated cylinders. A Workshop was held at Nantes, France on October 17 and 18, 2013 and provided opportunities for participants to present and discuss the results of benchmark studies. Numerical solutions based on various methods were compared with experimental data. Note that six organizations of Korean Towing Tank Conference (KTTC) also carried out the comparative studies on wave run-ups using MOERI's benchmark data. A Workshop on the benchmark studies was held at Daejeon, Korea on September 12, 2013. Note that this Section focuses on the outcome of the Workshop hosted by the Committee.

6.2 Benchmark Data

The experiments for wave run-ups on a single truncated circular cylinder were carried out by both MOERI and MARINTEK. MARINTEK also conducted the model tests for wave run-ups on four truncated cylinders. The benchmark data are summarized in the following sections.

6.2.1 Single Truncated Circular Cylinder

Model tests were carried out by MOERI for the single truncated circular cylinder for six (6) wave periods and four (4) wave steepness. Table 6.2.1.1 presents the test matrix, in which the shaded cases were also tested by MARINTEK (Kristiansen et al., 2004). Note that the experimental data provided by MOERI was used in the benchmark studies. The diameter of the prototype cylinder is 16.0m and its draft is 24.0m. The model scale is 1:50.3 and the model diameter is 31.8cm. Figure 6.2.1.1 shows the locations of wave probes.



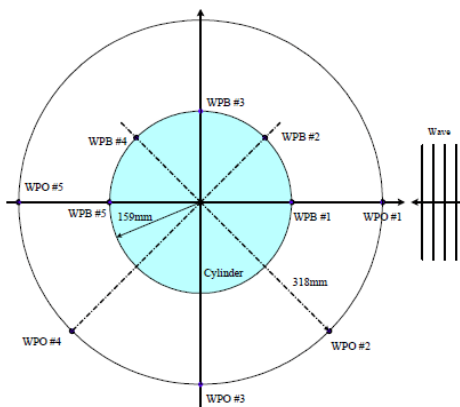
The experimental set-up used by MOERI is presented in the Figure 6.2.1.2.

In the benchmark studies, the first-order, the second-order harmonics and the mean results of following measured items were compared with numerical solutions at various wave frequencies in terms of kR (k is wave number and R is the radius of the cylinder):

- 1) Horizontal force, F_x
- 2) Vertical force, F_z
- 3) Wave elevations at 10 wave probe locations.

6.2.2 Four Truncated Cylinders

Model tests were conducted by MARNTEK for four truncated cylinders of two different cross-section geometries (circular and squared). The locations of wave probes and four truncated cylinders as well as wave headings are shown in Figure 6.2.2.1. The coordinates of wave probes are given in Table 6.2.2.1. Test conditions are summarized in Table 6.2.2.2. Note that MARINTEK has also carried out model tests for single circular and squared cylinders, as shown in Table 6.2.2.2. Only experimental data for four truncated cylinders were used in the benchmark studies.



Placement of Wave Probe on and around the Cylinder
WPB : wave probe at the cylinder surface (gap=4.1mm)
WPO : wave probe off the cylinder (gap=159.0mm)

Figure 6.2.1.1 Locations of Wave Probes (MOERI)

Table 6.2.1.1 Test Matrix for the Single Truncated Circular Cylinder

| | $T = 7s$ | $T = 8s$ | $T = 9s$ | $T = 10s$ | $T = 12s$ | $T = 15s$ |
|--------------------|----------|----------|----------|-----------|-----------|-----------|
| $H/\lambda = 1/50$ | T07S150 | T08S150 | T09S150 | T10S150 | T12S150 | T15S150 |
| $H/\lambda = 1/30$ | T07S130 | T08S130 | T09S130 | T10S130 | T12S130 | T15S130 |
| $H/\lambda = 1/16$ | T07S116 | T08S116 | T09S116 | T10S116 | T12S116 | T15S116 |
| $H/\lambda = 1/10$ | T07S110 | T08S110 | T09S110 | T10S110 | T12S110 | T15S110 |

Table 6.2.2.1 Locations of Wave Probes (in Prototype Scale)

| | Circular Cylinder | | Squared Cylinder | | |
|----------------|-------------------|---------|------------------|---------|---------|
| | X(m) | Y(m) | X(m) | Y(m) | |
| a ₁ | 34.0000 | 25.9500 | a ₁ | 34.0000 | 25.9500 |
| a ₂ | 34.0000 | 24.5300 | a ₂ | 34.0000 | 24.5300 |
| a ₃ | 34.0000 | 21.2500 | a ₃ | 34.0000 | 21.2500 |
| a ₄ | 34.0000 | 18.0000 | a ₄ | 34.0000 | 18.0000 |
| b ₁ | 28.3078 | 28.3078 | b ₁ | 27.1362 | 27.1362 |
| b ₂ | 27.3037 | 27.3037 | b ₂ | 26.1321 | 26.1321 |
| b ₃ | 24.9844 | 24.9844 | b ₃ | 23.8128 | 23.8128 |
| b ₄ | 22.6863 | 22.6863 | b ₄ | 21.5147 | 21.5147 |
| c ₁ | 25.9500 | 34.0000 | c ₁ | 25.9500 | 34.0000 |
| c ₂ | 24.5300 | 34.0000 | c ₂ | 24.5300 | 34.0000 |
| c ₃ | 21.2500 | 34.0000 | c ₃ | 21.2500 | 34.0000 |
| c ₄ | 18.0000 | 34.0000 | c ₄ | 18.0000 | 34.0000 |

Note: a₁, b₁ and c₁ are the wave probes on the cylinder surface

Table 6.2.2.2 Test Matrix

| H/λ | $k_c A$ | $T(s)$ | $k_c a$ | $\bar{A}^{(0)}$ | I | II | III | IV |
|-------------|---------|--------|---------|-----------------|------|------|------|------|
| 1/30 | 0.10 | 7 | 0.657 | 1.22 | 1100 | 2100 | 4100 | 6100 |
| | | 9 | 0.397 | 2.04 | 1110 | 2111 | 4110 | 6110 |
| | | 12 | 0.224 | 3.78 | 1120 | 2120 | 4120 | 6121 |
| | | 15 | 0.143 | 5.83 | 1130 | | 4130 | |
| 1/16 | 0.20 | 7 | 0.657 | 2.35 | 1200 | 2200 | 4200 | 6200 |
| | | 9 | 0.397 | 3.79 | 1210 | 2212 | 4210 | 6210 |
| | | 12 | 0.224 | 7.06 | 1220 | 2220 | 4220 | 6220 |
| | | 15 | 0.143 | 10.86 | 1230 | | 4230 | |
| 1/10 | 0.31 | 7 | 0.657 | 3.66 | 1300 | 2300 | 4300 | 6300 |
| | | 9 | 0.397 | 6.40 | 1310 | 2310 | 4310 | 6310 |
| | | 12 | 0.224 | 10.81 | 1320 | 2320 | 4320 | 6320 |
| | | 15 | 0.143 | 16.94 | 1330 | | 4330 | |

I) single circular column, II) single squared column
 III) four circular columns, IV) four squared columns

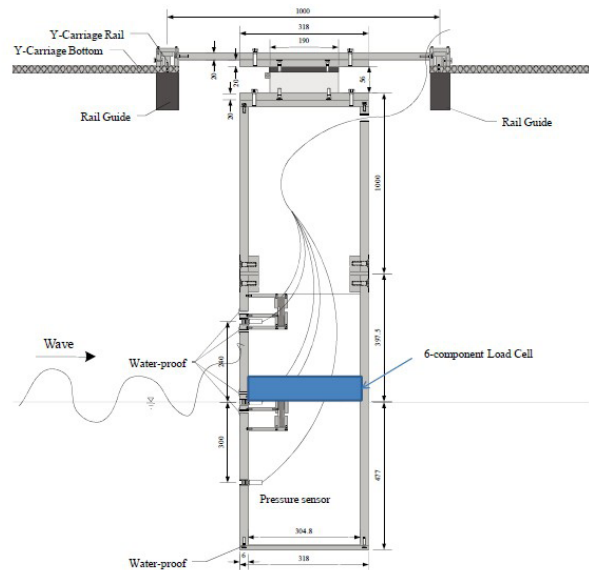


Figure 6.2.1.2 Experimental Set-up for Four Truncated Cylinders (MARINTEK)
 Figure 6.2.2.1 Experimental Set-up for Four Truncated Cylinders (MOERI)

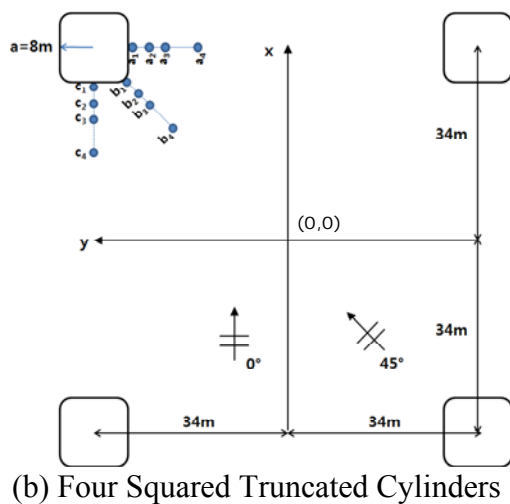
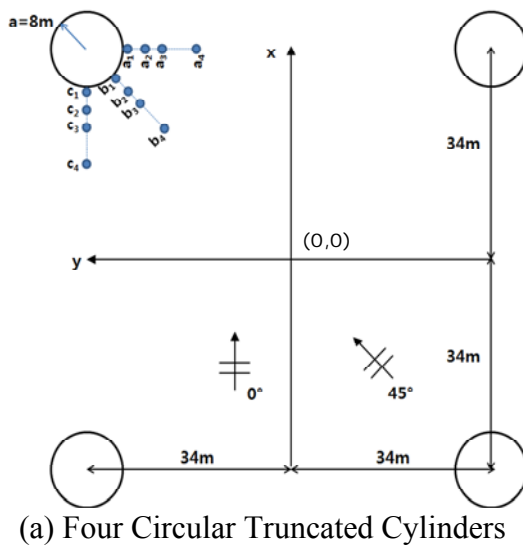


Table 6.3.1 Participants for Wave Run-up Benchmark Studies

| No. | Affiliation | Country |
|-----|---|---------|
| 1 | Ecole Centrale de Nantes (ECN) | France |
| 2 | Hyundai Heavy Industries | Korea |
| 3 | Inha University | Korea |
| 4 | University of Iowa | USA |
| 5 | MOERI(KRISO) | Korea |
| 6 | University of Bath | UK |
| 7 | MARINTEK | Norway |
| 8 | Pusan National University | Korea |
| 9 | Samsung Heavy Industries with CD-Adapco Korea | Korea |
| 10 | Seoul National University | Korea |
| 11 | Shanghai Jiao Tong University | China |

6.3 Participants

Eleven organizations participated in the benchmark studies. The list of participants is given in Table 6.3.1. Most organizations participated in the benchmark studies by carrying out numerical simulations and others



conducted model tests. Table 6.3.2 presents the cases studied by each participant.

6.4 Numerical Results

6.4.1 Grid Topology and Numerical Scheme

Nine participants employed CFD methods to simulate wave run-ups. The numerical methods, the computational domains,

boundary conditions and time steps employed by participants are summarized in Table 6.4.1.1. The grid topologies are presented in Figure 6.4.1.2.

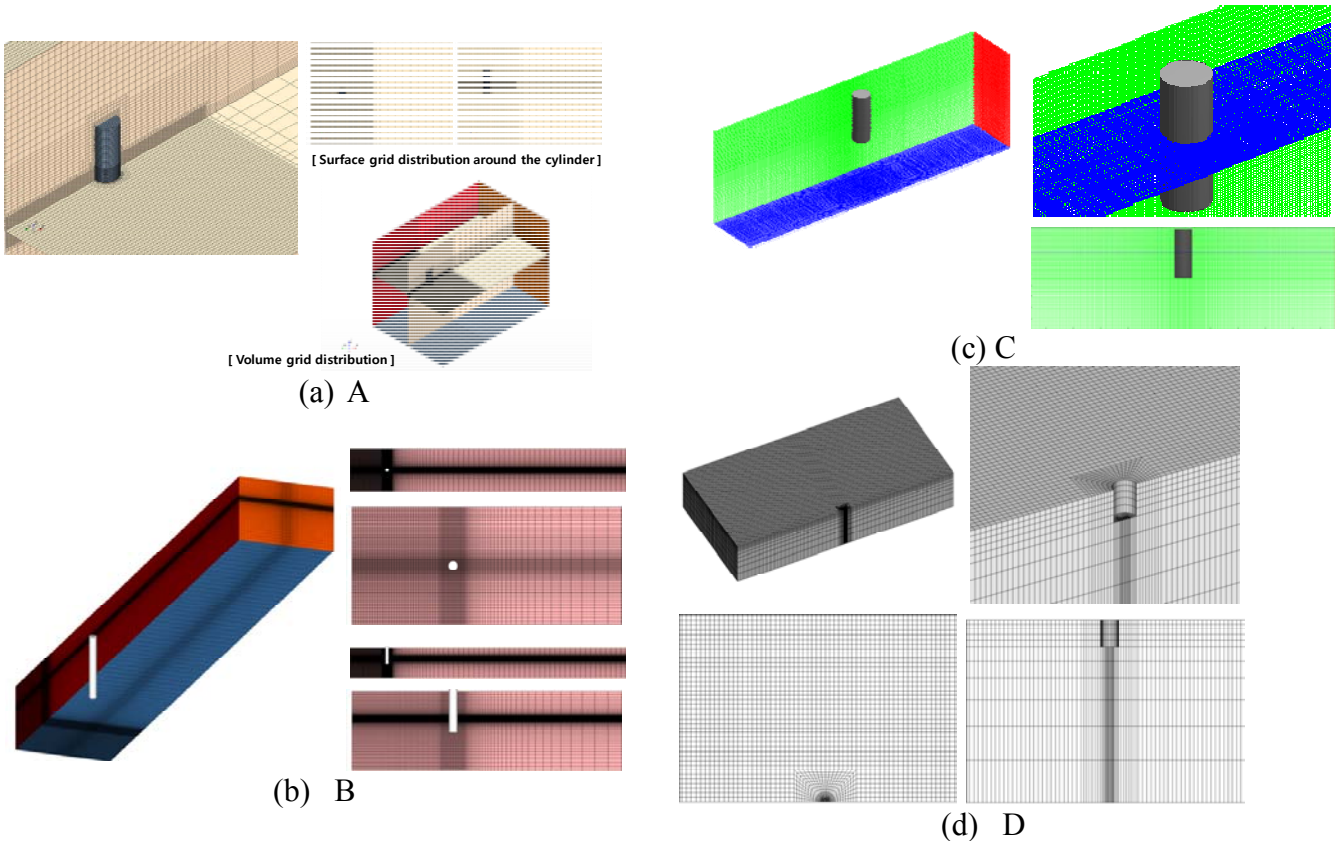
Table 6.3.2 Benchmark Studies by Participants

| Participant | Single Circular Cylinder | Single Squared Cylinder | Four Circular Cylinders | | Four Squared Cylinders | |
|---|--------------------------|-------------------------|-------------------------|--------|------------------------|--------|
| | | | 0 deg | 45 deg | 0 deg | 45 deg |
| | Wave heading: 0deg | 0 deg | 0 deg | 45 deg | 0 deg | 45 deg |
| ECN, France | O | O | | | O | O |
| Hyundai Heavy Industries | O | | | | | |
| Inha University | O | | | | | |
| University of Iowa | O | | | | | |
| MOERI | O | | | | | |
| University of Bath | O | | | | | |
| MARINTEK* | O | O | O | O | O | O |
| Pusan National University | O | | | | | |
| Samsung Heavy Industries with CD-Adapco Korea | O | | O | | O | |
| Seoul National University * | O | | | | | |
| Shanghai Jiao Tong University | O | | O | O | | |

* Note that MARINTEK and Pusan National University participated in the benchmark studies by carrying out model tests.

Table 6.4.1.1 Numerical Methods and Schemes

| Participants | | A | B | C | D | E | G-1 | G-2 | H |
|---------------------|------------|-----------------------------|-----------------------------|--------------------------------------|---|-----------------------------|----------------------------|---|-----------------------------|
| Turbulence model | | RKE | SGS | - | - | K-omega | | | SKE |
| Free-surface scheme | | VOF-Implicit | MMD-Explicit | VOF with local height function | - | - | | | VOF-Explicit |
| Wave theory | | Stoke 5 th order | Stoke 5 th order | Stoke 5 th order | Stoke 1 st & 2 nd order | Stoke 2 nd order | | Airy theory, Linear | Stoke 2 nd order |
| Boundary conditions | Inlet | Velocity | Velocity | Velocity | Damping zone w/ wall B.C | Wave pressure & Velocity | Not applicable | Patch with relaxation zone | Velocity |
| | Outlet | Pressure outlet | Pressure outlet | Pressure outlet | | Exit | Not applicable | Patch with relaxation zone | Velocity |
| | Side | Symmetry | Symmetry | Wall | | Zero gradient | Not applicable | Slip-wall | Velocity |
| | Top | Symmetry | Symmetry | - | | Far-field | Not applicable | Patch | Atmosphere |
| | Bottom | Wall | Symmetry | Wall | | Slip-wall | Not applicable | No-slip wall | Slip wall |
| Time step size | | T/250 | 1/1000s | Variable time step by courant number | 0.005 | T/250~T/100 | | Variable time step controlled by Courant number | T/200 |
| Grid size | Inlet | 1~2λ | 2λ | 1λ | ± 6λ | 2λ | | 3λ | 3D |
| | Outlet | 4λ | 15λ | 1λ | | 3λ | | 3λ | 5D |
| | Side | 8D | 12.5D | 3D | | 3λ | | 16D | 8D |
| Number of Cells | Per length | 150EA | 75EA | Min. 60EA | 20~30EA | 82EA | Not applicable | 50~70EA | 70EA |
| | Per height | 20EA | 20EA | Min. 6EA | - | At least 15 | Not applicable | 12~22EA | 10EA |
| Code | | Commercial Star-CCM+ | In-House INHAWAVE-II | Comflow ver 3.1 | In-House FEDIF | In-House CFDShip-Iowa V4.5 | In-house DIFFRACT Ver.2009 | In-house OpenFoam Ver.2.2.1 | In-house |



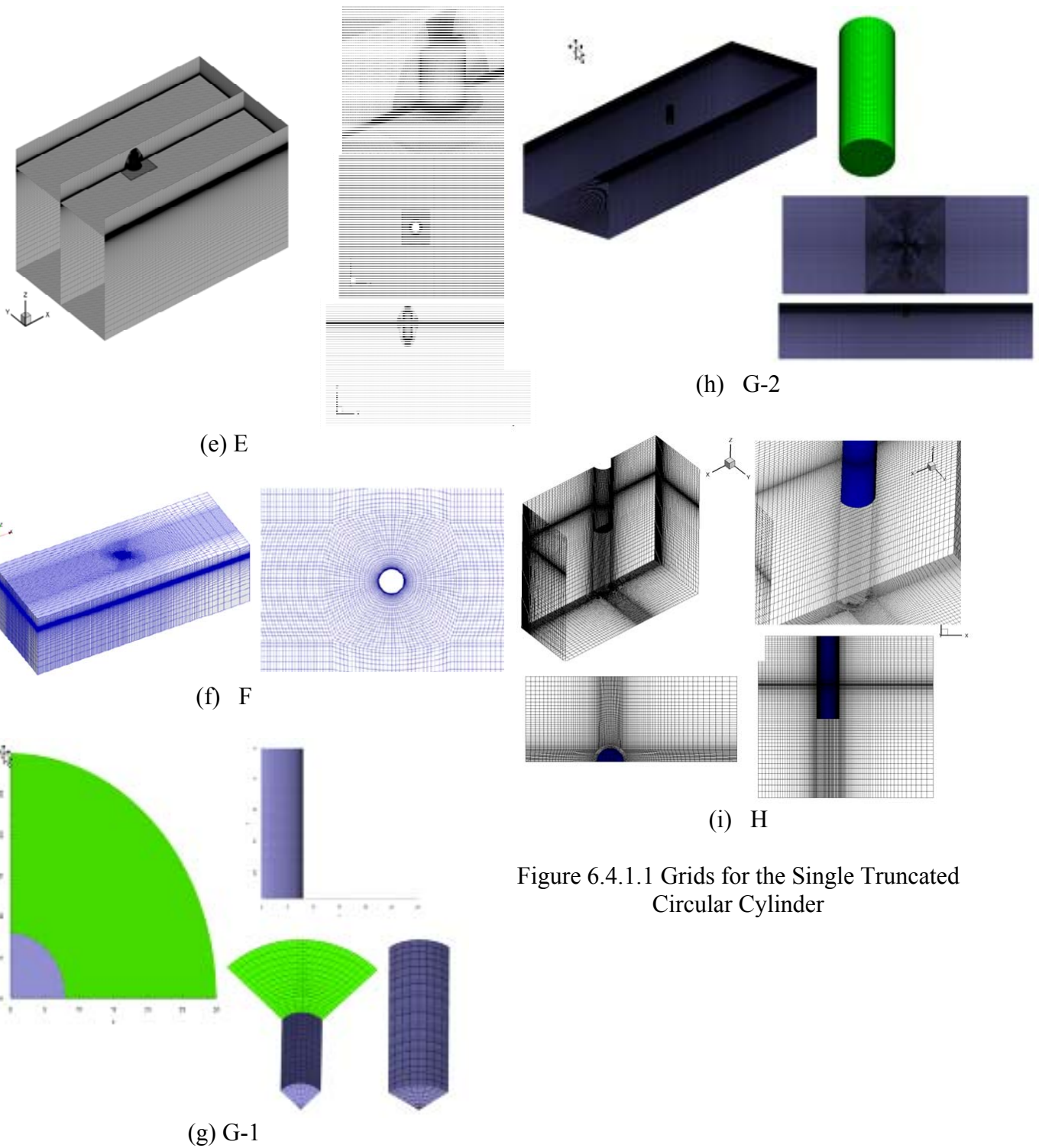
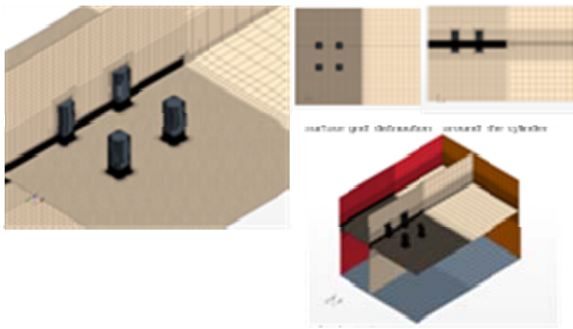
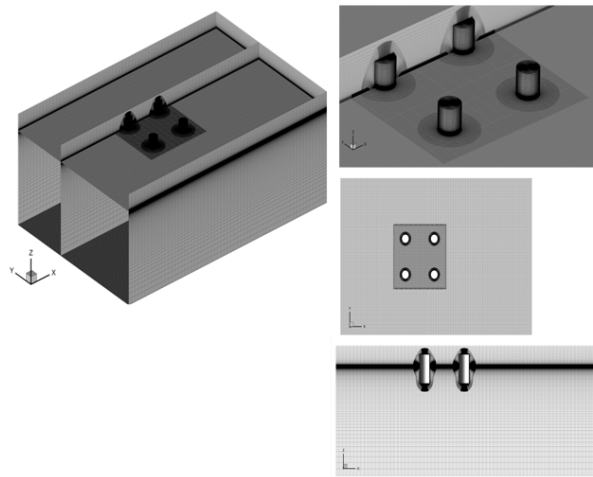


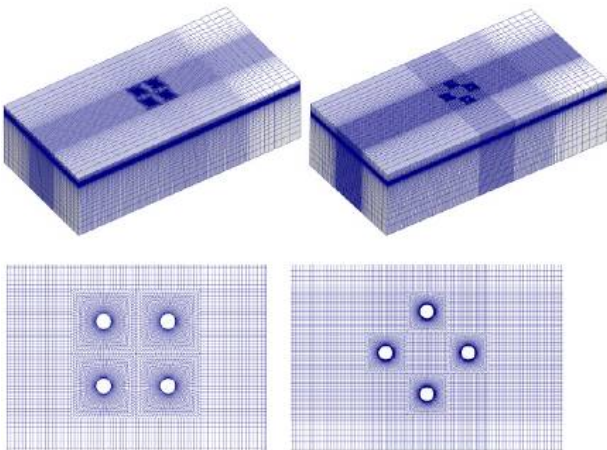
Figure 6.4.1.1 Grids for the Single Truncated Circular Cylinder



(a) A



(b) E



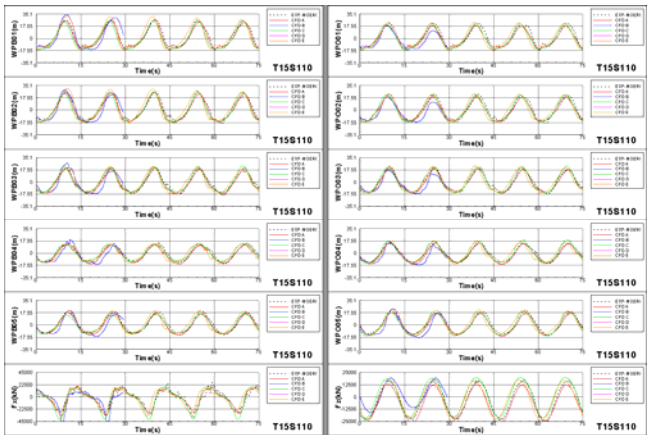
(c) F

Figure 6.4.1.2 Grids for four Truncated Circular Cylinders

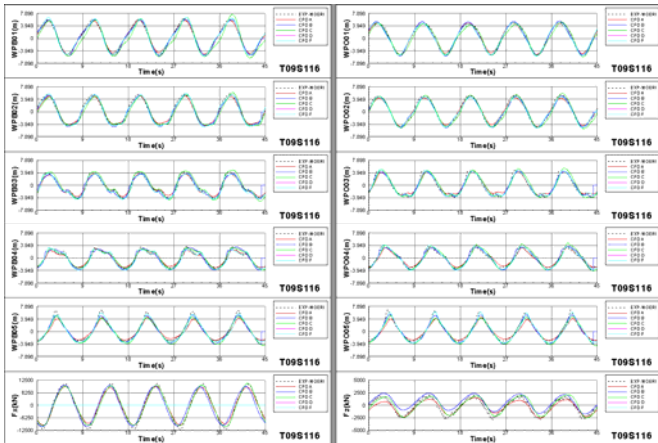
6.4.2 Single Circular Cylinder

The time series of computed wave elevations at 10 wave probe locations (WPB#01-WPB#05, WPO#01-WPO#05) and forces on the single truncated circular cylinder (F_x and F_z) are compared with the time histories of experimental data by MOERI in Figure 6.4.2.1 for two test conditions (T15S110 and T09S116). It can be observed that the predicted patterns of wave run-ups on the single truncated circular cylinder, obtained by all the participants, are very similar to those of experimental ones.

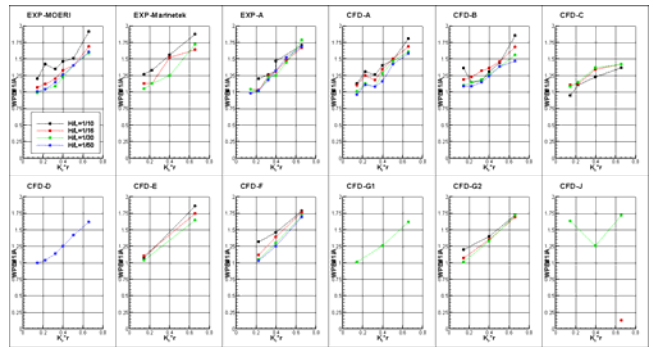
Figure 6.4.2.2(a) shows the 1st harmonic results at WPB#01. The trends of experimental results by MOERI and MARINTEK are similar at WPB#01. The trends of numerical results by participants A, B and F agree well with the experimental results by MOERI at WPB#01. Figure 6.4.2.2(b) shows the 2nd harmonic results at WPB#01. The trends of experimental results by MOERI and Pusan National University (denoted as EXP-A) are similar at WPB#01. However, the trend of those by MARINTEK is somehow different from the other two.



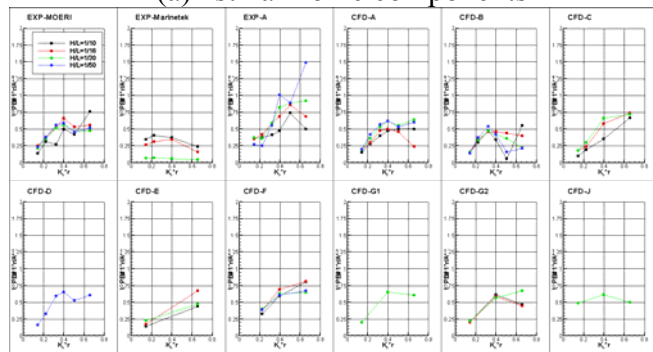
(a) T15S110



(b) T09S116



(a) 1st harmonic components



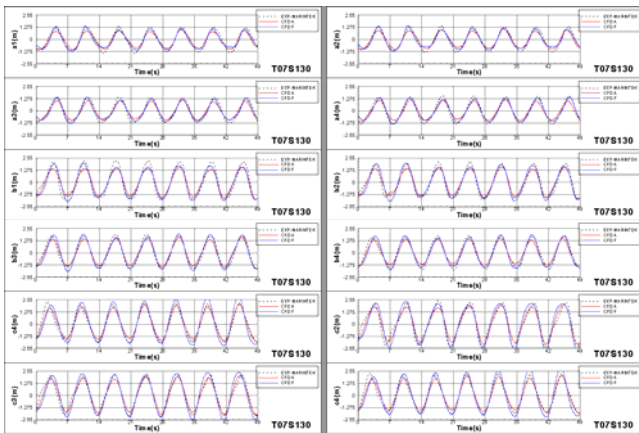
(b) 2nd harmonic components

Figure 6.4.2.2 Wave Run-ups at WPB#01 for the Single Truncated Circular Cylinder

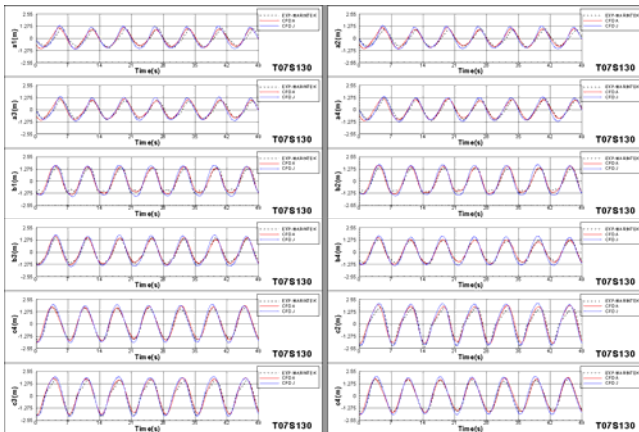
Figure 6.4.2.1 Predicted Wave Elevations and Forces with Experimental Results

6.4.3 Four Truncated Cylinders

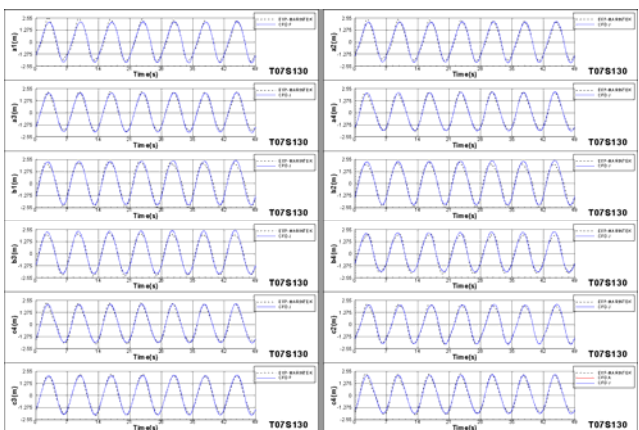
Figure 6.4.3.1 shows the time series of wave elevations at 12 locations (a1~a4, b1~b4, c1~c4) for four truncated columns. They are compared with experimental results by MARINTEK. The predicted patterns of wave run-ups on the four truncated circular and squared cylinders are similar to those of experimental data. The 1st and 2nd harmonic components of wave elevations at a1, b1 and c1 are compared with experimental data in Figure 6.4.3.2 and Figure 6.4.3.3, respectively, for the four truncated circular cylinders (wave heading of 0 degree).



(a) Four Circular Cylinders, T07S130, Wave Heading = 0 deg

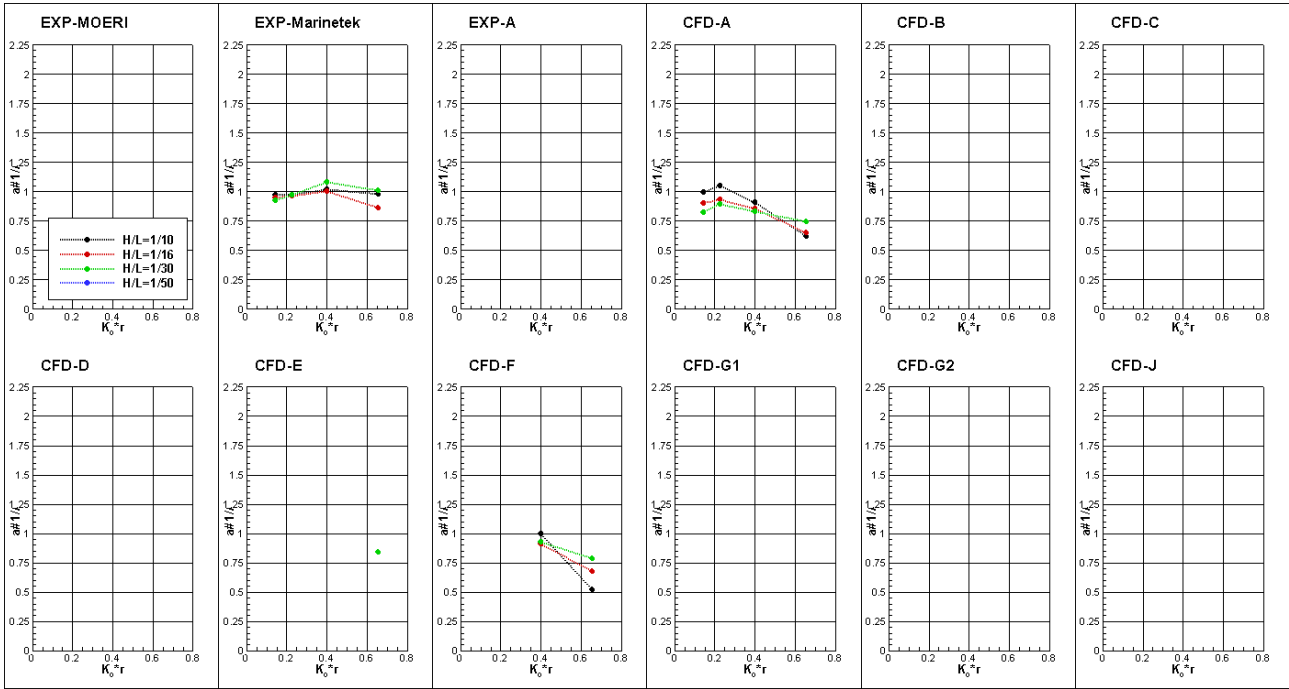


(b) Four Squared Cylinders, T07S130, Wave Heading = 0 deg

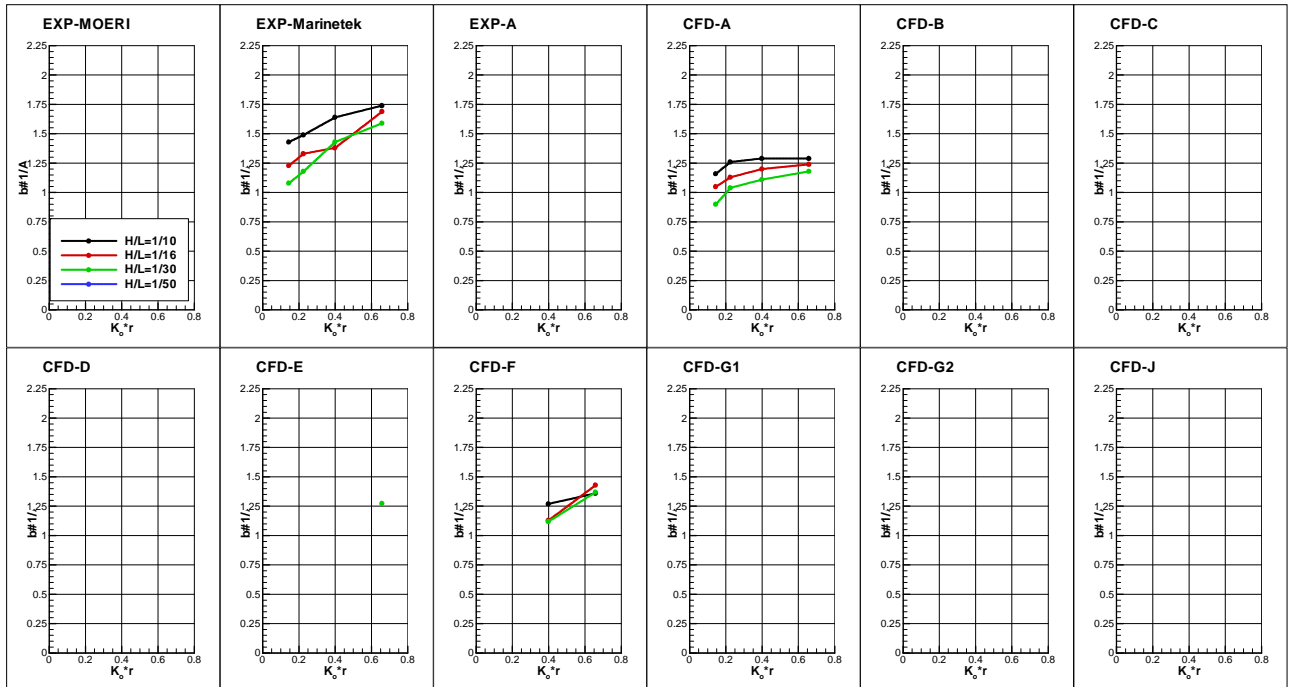


(c) Four Squared Cylinders, T07S130, Wave Heading = 45 deg

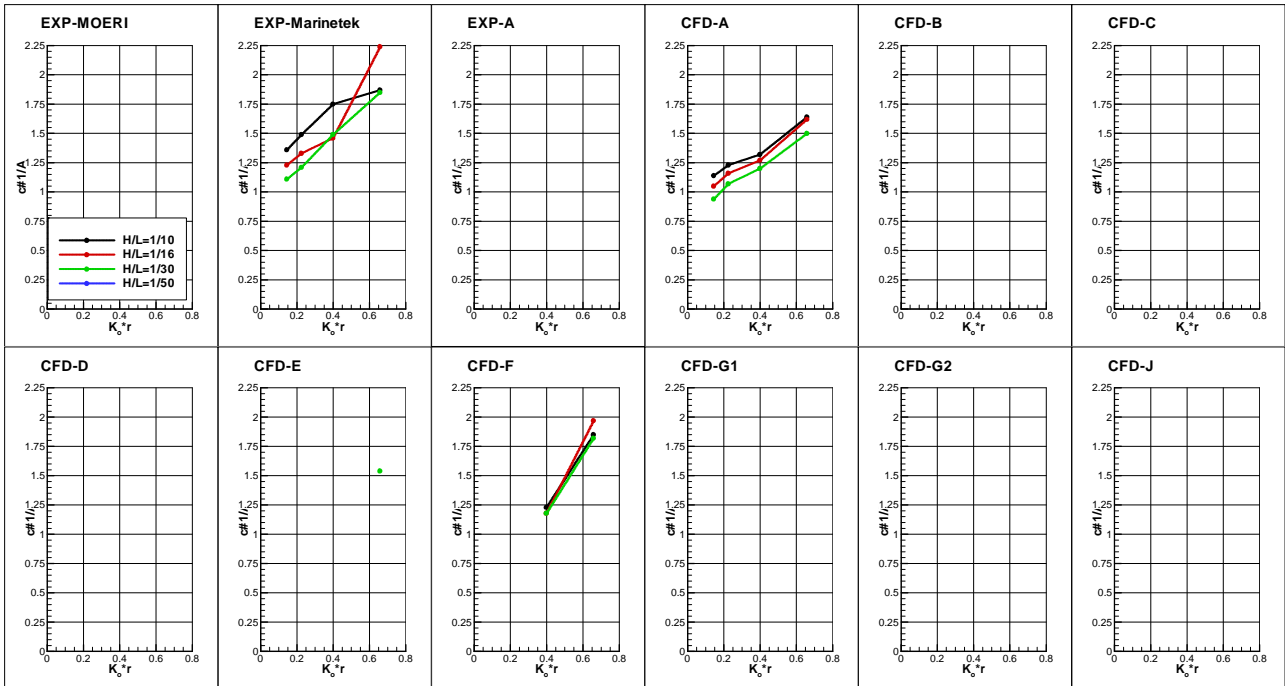
Figure 6.4.3.1 Comparison of Time Histories for Four Truncated Circular and Squared Cylinders



(a) Location - a1

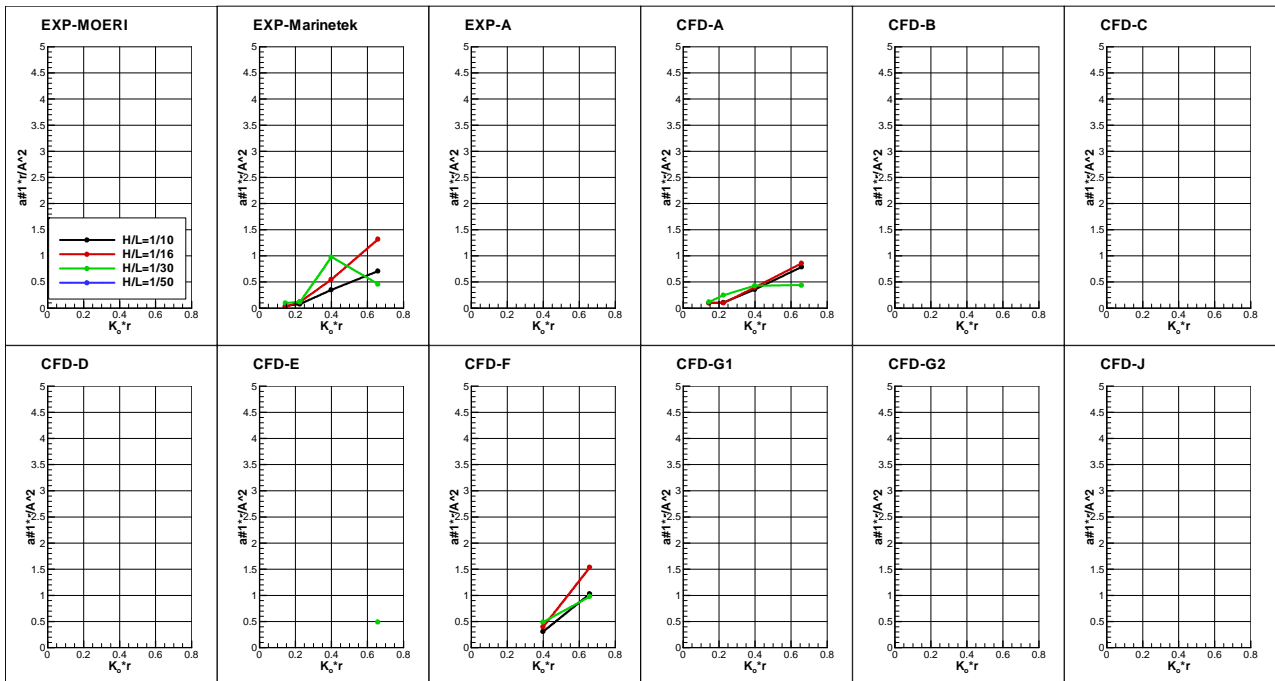


(b) Location - b1



(c) Location - c1

Figure 6.4.3.2 1st Harmonic Values for Four Truncated Circular Cylinders at Locations of Three Wave Probes (Wave Heading =0 deg)



(a) Position - a1

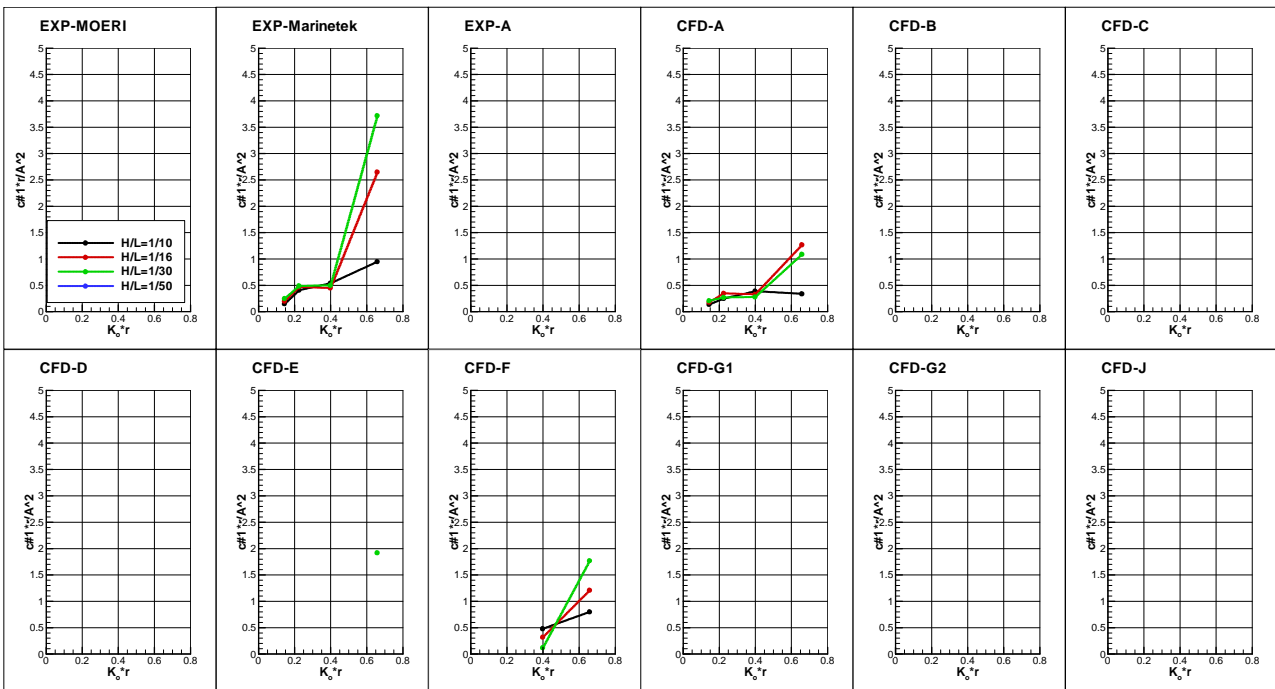
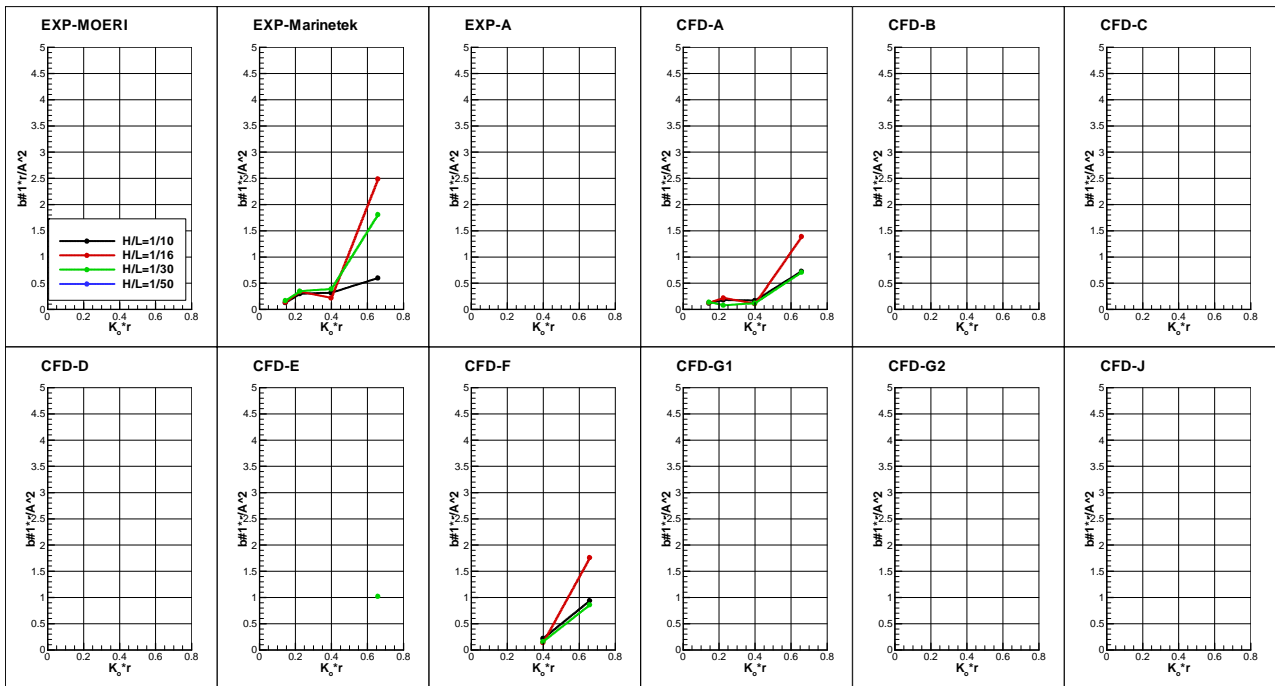


Figure 6.4.3.3 2nd Harmonic Values for Four Truncated Circular Cylinders at Locations of Three Wave Probes (Wave Heading = 0 deg)

6.5 Summary of Presentations at Workshop

In the Workshop, six papers were presented on wave run-up benchmark studies. A summary of papers related to the wave run-up benchmark studies is given below.

Yoon et al. (2013) computed wave elevations at several locations around a truncated circular cylinder using CFDShip-Iowa. Time series of wave elevations and wave forces were compared with experimental data. Figure 6.5.1 presents the comparison of predicted wave elevations with experimental ones.

Sun et al. (2013) predicted wave elevations around a single truncated circular cylinder using a potential-flow solver (DIFFRACT) and a viscous-flow solver, OpenFOAM. Results

were compared with measured time series in experiments and the solutions by WAMIT. Spectral analyses were carried out. RAOs and QTFs of wave elevations were compared with the results obtained by Kristiansen et al. (2004). Figure 6.5.2 presents an example of the first-order and second-order wave elevations.

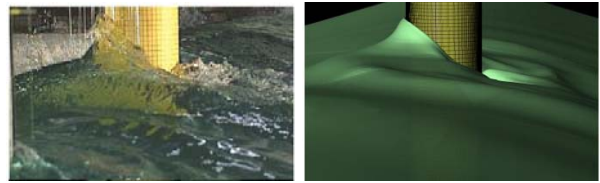


Figure 6.5.1 Experimental Wave Profiles (Stansberg and Kristiansen, 2005) and Numerical Predictions for the Case of $T=15s$, $H=35m$ (Yoon et al., 2013)

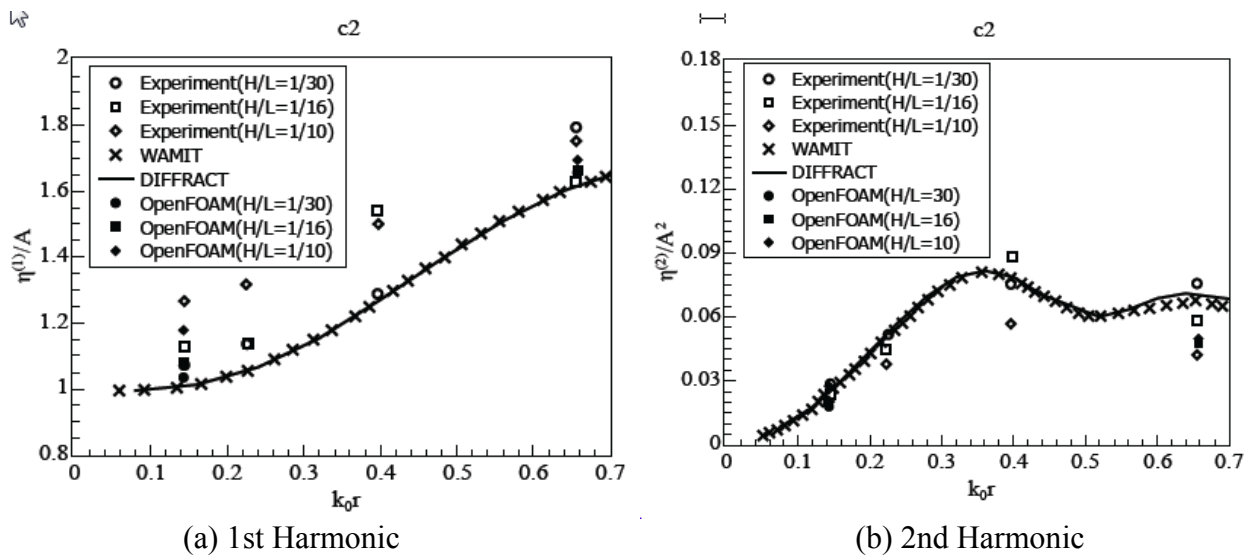
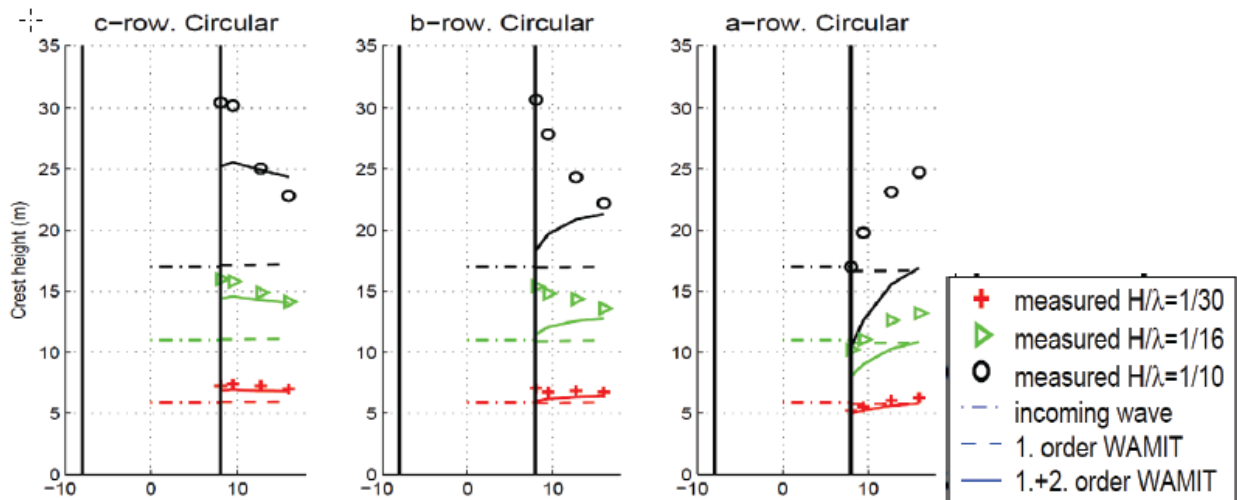


Figure 6.5.2 First and Second-order Wave Elevations (Sun et al., 2013)

Kristiansen and Stansberg (2013) studied the wave diffraction (upwelling) and run-ups on vertical columns in steep wave conditions by reviewing a data set from the scaled model tests with single and multiple fixed columns in

deep water. Measurements clearly show higher wave crests than those by the linear modelling for steep waves. The second-order modelling can be used to improve this. However, there are still deviations in steep waves, especially at

short wave periods (see Figure 6.5.3).



WAMIT vs measurements, max surface elevation. Four cylinders. $T=15$. 45 deg.

Figure 6.5.3 Wave Crest Heights for the Case of $T=15$ sec, Four Columns and Heading = 45 deg. (Kristiansen and Stansberg, 2013)

Cao et al. (2013) computed wave run-ups on a fixed single truncated circular cylinder and four circular cylinders using in-house CFD naoe-FOAM-SJTU solver. Favourable wave elevations were obtained in comparison with experimental data (see Figure 6.5.4).

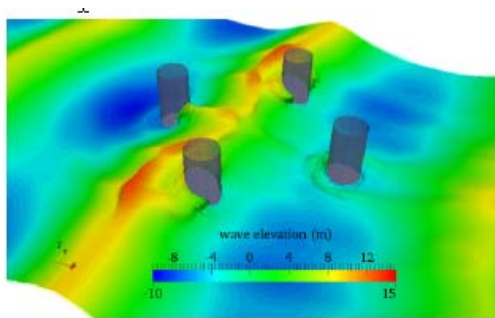


Figure 6.5.4 Wave Elevations for the Case of Four Circular Cylinders ($T = 9$ sec and Heading= 45 deg) (Cao et al., 2013)

6.6 Conclusions and Recommendations

Eleven organizations participated in the benchmark studies on the cases of the single

truncated cylinder, and four organizations participated in the benchmark studies on the cases of four truncated cylinders. Nine participants employed CFD methods in their studies. The FFT analysis was performed to predict the harmonic values, and the results of harmonic values were compared with the experimental results.

It was concluded that the values and trends of the computed wave elevations and forces by CFD methods are in good agreement with the experimental results for the cases of single and four cylinders.

Due to time constraints and limited computing resources, most of participants have focused on the single circular cylinder cases. It is recommended that more studies be extended to the four-column cases. Some of the participants are still working on completing the simulations. More comparisons will be made in a journal paper, which is being prepared by the Committee.

7. THRUSTER INTERACTION AND SCALE EFFECT IN DP TESTS

7.1 Introduction

Dynamic positioning (DP) systems and azimuthing thrusters are widely used in the offshore industry for station-keeping. The effective force generated by thrusters can be significantly smaller than those obtained from their open-water characteristics. This is a result of thruster interactions with the hull, current and the wake of neighbouring thrusters. These phenomena are often referred as thruster-thruster and thruster-hull interactions. The understanding and quantification of thruster interaction (or thrust degradation) effects is essential for the evaluation of the station-keeping capabilities of DP vessels. Figure 7.1.1 presents some typical scenarios of thruster-thruster interactions.

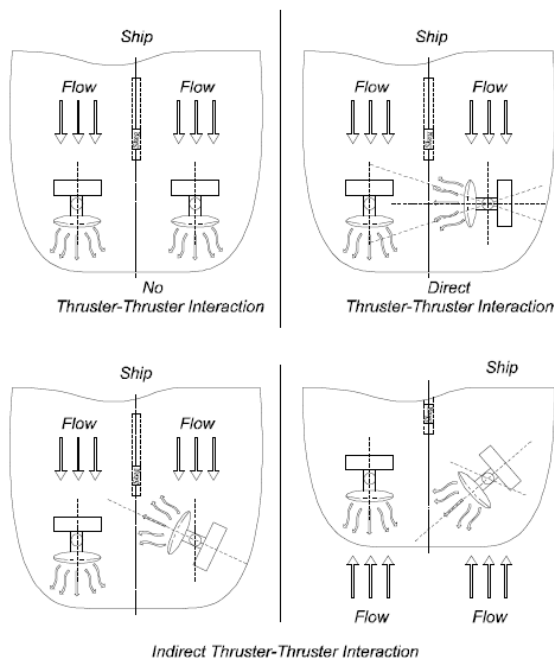


Figure 7.1.1 Scenarios for Thruster-Thruster Interactions (Tello Ruiz et al., 2012)

7.2 Literature Review

A lot of current knowledge on thruster interaction effects was due to the development

in the late 1980s and early 1990s (Nienhuis, 1992). In 1983, a semi-empirical calculation procedure was developed by MARIN to estimate the thruster-thruster interaction (Nienhuis, 1986). The underlying assumption of this method was that the propeller slipstream behaves similar to a swirling turbulent jet. The good correlation between model test results and the calculations indicated that this assumption was correct. However, this conclusion was not confirmed since the extent of the thruster-thruster interaction was largely determined by two factors: the decrease of the velocity in the slipstream and the width of the slipstream. These two factors are related by the conservation of momentum. In 1986/1987, the first detailed thruster slipstream was measured by MARIN using a 2D LDV. These measurements were carried out on a thruster mounted under a simple-shaped barge. Some of the conditions were however very similar to the open-water condition. The test results showed a jet spread and a velocity decay different from that predicted by the simple calculation procedure mentioned above.

One of the oldest data available for thruster-thruster interaction in open water were published by Lehn (1980, 1981) which are for zero-speed conditions only and cover variations in relative thruster position and thruster angle.

Nienhuis (1992) used the calculated velocity field downstream of a simplified thruster (which delivered the same thrust and the same power as Lehn's thruster) and calculated the thruster-thruster interaction. The average inflow velocity over the propeller disk of the second thruster was calculated, and the resulting advance ratio was used in conjunction with the estimated open-water diagram of the thruster used by Lehn (1980). Moreover, Nienhuis (1992) investigated the interaction of thrusters below a flat plate. By using the calculated velocity field for a simplified thruster close to a flat plate, it is possible to calculate the thruster-thruster interaction using

the same approach as for the open-water case. Both measurements and calculations showed that the interaction in open-water persists for larger distances between the thrusters. In the work of Nienhuis (1992), the thruster-hull interaction was also investigated.

API (1996) provided guidelines for the determination of available thrust, and particularly gives guidance on how the thrust varies with the inflow velocity. It indicates that the thrust reduction for dynamic positioning systems due to oblique inflow cross-coupling effects is not well researched. API states that the propeller thrust decreases with increasing inflow, which is caused by the current speed, movement of vessel or the slipstream from another thruster. A 5-15% correction factor is suggested to account for the Coanda effect. If there are support struts to the propeller in the flow, the reduction in thrust is approximately 10%.

Det Norske Veritas (DNV, 1996) outlined rules for thruster assisted (TA) mooring systems. Depending on whether manual TA or automatic control (ATA) is employed, 70% or 100% of the net thrust can be used. It is assumed that azimuthing thrusters can provide thrust in all directions, unless specific restrictions are defined.

Brandner (1998) investigated the interaction between two closely spaced ducted azimuthing thrusters through a series of experiments. Forces acting on a single thruster as well as on two thrusters were measured for a range of operating conditions and relative positions. The results showed that forces from the trailing thruster were heavily affected by interaction due to impingement of the race from the leading thruster, whereas forces from the leading thruster essentially remain unaffected despite its proximity to the trailing thruster.

van Dijk and Aalbers (2001) showed that degradation effects on a thruster in model scale

may occur due to inflow and cross flow, and due to waves if they cause ventilation effects. They stated that as the thrust is generated based on the principle of accelerating water, there is a suction flow and a jet flow. The suction flow is characterized by relatively low flow velocity over a wide area, while the jet flow is high speed and concentrated in a relatively small cross-section area. Furthermore, the jet may induce other flow patterns, depending on the local hull form and the intensity and direction of the jet. These flows, together with the current flow and waves may cause interaction effects leading to degradation of thruster performance. The following types of interaction were considered: thruster-thruster, thruster-hull (including the Coanda effect), thruster-current, and thruster-waves.

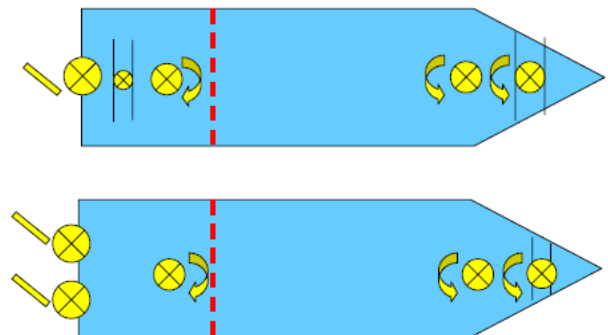


Figure 7.2.1 Thruster Configurations Reported in Nordtveit et al. (2007)

Ekstrom and Brown (2002) addressed the influence of two thrusters in close proximity. The experiments were carried out at the wave tank in the Department of Mechanical Engineering at University College London. They recognized that additional research into the thruster cross-coupling effects at a range of in-flow velocities is needed, as these effects are likely to be significant at the current speeds appropriate to manoeuvring situations using dynamic positioning systems. In their work, they drew some interesting conclusions:

- The thrust in open water tests was 8 to 15% more than that in the tests with a thruster attached to a vessel.
- Thrust losses were up to 5% for the thruster closer to the vessel.
- The loss of thrust is more likely due to the hull influence rather than the Coanda effect for thrusters placed close to the stern of the vessel.
- A reduction or an increase in thrust can occur when one thruster's slipstream is influenced by the other thruster's slipstream.
- A reduction in thrust (up to 40%) was recorded when one thruster's slipstream is pointed into the other thruster's slipstream.

Nordtveit et al. (2007) presented the results of model tests carried out in MARINTEK. The tests were to assess the thrust degradation in DP operations of an Aframax DP2 shuttle tanker, operating in rough environmental conditions in the North Sea. Investigations were conducted for tunnel thrusters, azimuth thrusters and main propellers with rudders. The results showed that thrust loss or thrust degradation effects due to thruster-thruster and thruster-hull interactions and the dynamics effects are of significant importance for the design, analysis and operation of a DP vessel. The magnitude of thrust degradation depends on the vessel type, design, operation and environmental forces. Thrust degradation coefficients are recommended for the DP capability analysis of the Aframax shuttle tanker.

Bosland et al. (2009) proposed a numerical method to predict the interaction effects. The developed propeller interaction model is based on the panel method. At the second thruster the distorted flow field due to the first thruster was modeled by means of two wake field models; a linear potential wake model and an empirical turbulent jet model. Due to the intersection of wake and the body panels at the second thruster, numerical instabilities occurred at the

collocation points. These instabilities were removed by applying a realistic vortex model instead of the analytical vortex model. It was concluded that the thruster interaction propeller model coupled with the turbulent jet wake field yielded an accurate prediction of thruster interaction. Although results based on the linear potential wake field model are promising, the prediction of the divergent and subsiding characteristics of the physical wake field needs to be improved, since the linear wake model does not correctly represent the physical properties of the wake.

Palmer et al. (2009) assessed thruster-hull and thruster-thruster interactions on for autonomous underwater vehicles (AUVs). The interactions were investigated using an experimental approach. The induced longitudinal force (thrust loss) was less than 10% of the desired thrust force and the induced lateral force was between 8% and 20% of the desired thrust.

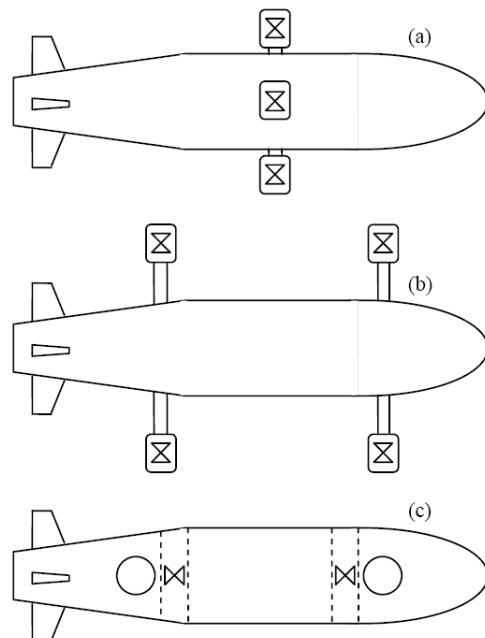


Figure 7.2.2 Possible Thruster Interactions on AUVs (Palmer et al., 2009)

de Wit (2009) and van Daalen et al. (2011) investigated the interaction effects on the optimization of DP allocation algorithms. In

their work, the effect of the thruster-thruster interaction on the reduction of delivered power was studied.

Det Norske Veritas (DNV, 2012) outlined the guidelines for the design of dynamically positioned vessels. In the design process of DP systems, the thruster interaction effect is recognized as an important issue in the determination of the desired capability. The magnitude of losses associated with the interaction effects is a function of the hull shape, the locations of thrusters, the degree of tilt of the propeller or nozzle axis. ‘Barred zones’ that prevent thrust in defined sectors can be created in the DP control system software to address issues associated with the thruster wash for azimuthing thrusters. Such barred zones may result in reduced capability. Furthermore, in order to minimize negative effects caused by thrusters interacting hydrodynamically with each other, DNV recommends that the distance between thrusters should be maximized to the feasible extent.

American Bureau of Shipping (ABS, 2013) also published a Guide for Dynamic Positioning Systems. It recommends that the thruster-thruster interaction effect should be included in the station-keeping performance assessment, and that the results from full-scale or suitable model tests for thruster-thruster interaction effects can be used whenever possible. If such results are not available, Appendix 1 of the ABS Guide provides guidelines for the assessment of the interaction effect on the available thrust.

Song et al. (2013) investigated the thrust loss by interactions between azimuth thrusters and ship hull based on the model tests and the numerical simulations. In the DP condition, two thrusts need to be considered: one is the thrust of the azimuth thrusters and the other one is the resultant thrust for the ship. The difference between these two thrusts denotes a thrust loss due to the thruster-hull interaction. In the model tests, the thrust and the torque of

an azimuth thruster were measured at 15° intervals between 0° and 360°. The resultant thrust and moment were obtained by measuring the force using the dynamometer in the towing carriage. A Wind Turbine Installation Vessel (WTIV) was used in the studies. Based on the model tests, the thrust loss due to thruster-hull interaction was up to 30% of the pure thrust. In the numerical simulations, two methodologies, MRF (Moving Reference Frame) and SM (Sliding Mesh), were applied. Although both numerical methodologies showed good agreements with experimental data, it was suggested that the MRF method is time-saving and therefore more practical to predict the thrust loss.



Figure 7.2.3 Ship Model for Thruster-Thruster/Hull Interaction Tests at Samsung Ship Model Basin (Song et al., 2013)

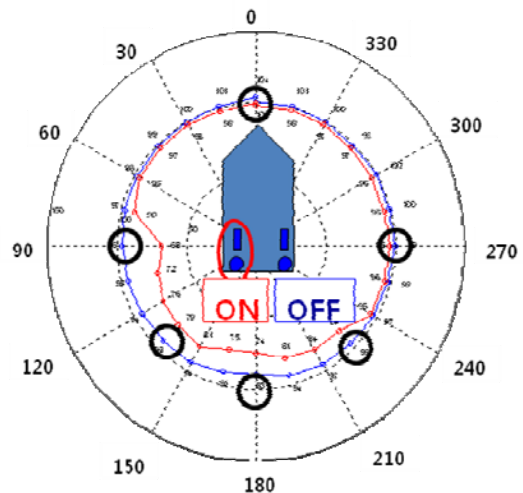


Figure 7.2.4 Polar Plot of Thrust Loss due to Thruster-Thruster Interaction (Song et al., 2013)

The work described above demonstrates progress made in the study of the effects of thruster-thruster and thrust-hull interactions on the performance of DP vessels. Thrust degradation effects can be quantified using data available from literature, or by carrying out dedicated model tests. Published data can give valuable insights, but it is often too general, or not applicable to a specific design. Model tests, on the other hand, do provide detailed results but they are relatively expensive. In addition, model test results often become available relatively late in the design process, making it difficult to incorporate the results in the design.

The CFD simulation could be an alternative method but there is little experience in the application of CFD as an engineering tool for thrust degradation effects. With the rapidly increasing capabilities of CFD models and computer hardware, the time is right for the development of new tools to analyze the thruster interactions (Cozijn, 2010).

In offshore heavy lift or pipe-laying operations, the station keeping capabilities of a DP-vessel affect the operability limits of these operations. The efficiencies of DP thrusters of these vessels have been assessed by comparing the CFD solutions with model test results (Ottens et al., 2011). Numerical studies using CFD were performed to assess thruster-hull interactions on a semi-submersible vessel. The CFD results were validated against results of a series of model tests, including an open-water thruster, the single thruster-hull interactions without current, and full thruster-hull interactions with all active thrusters and without current. The CFD results show good agreement with the model test data. The computed forces on the semi-submersible as well as on the individual floater with active thrusters are in 10% difference in comparison with the model test data. The largest discrepancies are in the bow quartering conditions where the thruster-hull interactions show the most complex flow pattern due to the

location and the shape of the stern keel. The comparisons between the CFD and the model test results demonstrate that CFD is able to predict the relevant force components well with a sufficient accuracy for engineering purposes.

7.3 Measurement of Thruster Wake

Research has been carried out to understand the thruster interaction effects by measuring the detailed wake flow using PIV systems.

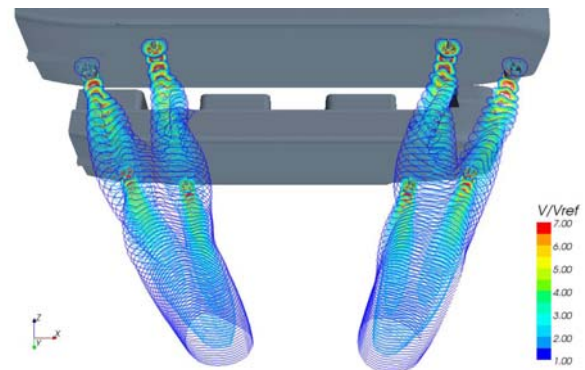


Figure 7.2.5 Downwash of Active Thrusters, Azimuth 270 deg (Ottens et al., 2011)

Cozijn et al. (2010) investigated the wake flow behind a ducted azimuthing thruster in open water and under a barge. Model tests were carried out in stationary conditions. The propeller thrust and torque were recorded and the flow velocities in a large number of cross-sections at various distances from the thruster were measured using a PIV system (see Figure 7.3.1).

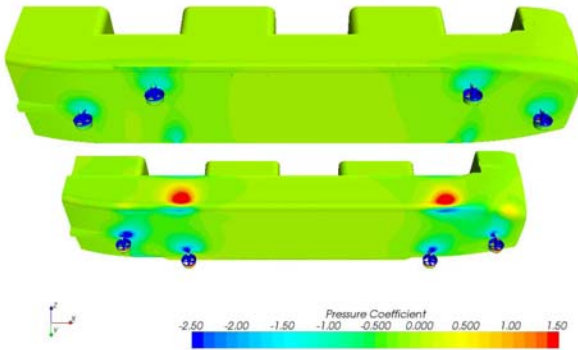


Figure 7.2.6 Visualization of the Impingement of Wakes on the Portside of the Floater, Azimuth 270 deg. (Ottens et al., 2011)

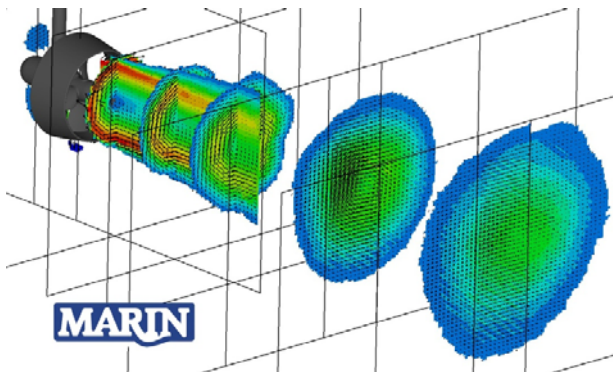


Figure 7.3.1 Measured Velocities in the Wake of an Azimuth Thruster (Cozijn et al., 2010)

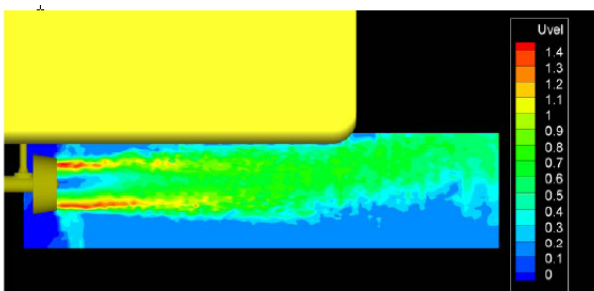


Figure 7.3.2 Flow Field of A Single Sweep Measurement with the PIV System (Cozijn et al., 2010)

In addition, velocities were measured in a longitudinal plane at the thruster centre line (see Figure 7.3.2). The PIV measurements for the thruster under a barge show the thruster wake deformed by the presence of the barge as well as by its bilge. The bottom of the barge forms a flat plate above the thruster, clearly

flattening the cross-section of the thruster wake. In addition, the wake flow along the bottom and the bilge of the barge resulted in a low pressure region, causing the wake flow to diverge up as it flows under the barge into the open water. This phenomenon is known as the Coanda effect and was clearly visible in the PIV measurements.

Cozijn and Hallmann (2013) reported on thruster-interaction model tests carried out in MARIN's Deepwater Towing Tank. The wake flow at a large number of cross-sections at different distances from the thrusters was measured with a PIV system for two different DP vessels, a semi-submersible and a drill ship. The PIV measurements provided a detailed image of the flow velocities in the thruster wake, showing the axial velocities, as well as the transverse and vertical velocity components (see Figure 7.3.3).

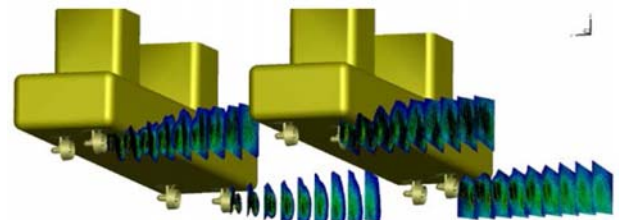


Figure 7.3.3 Measured Wake Velocity Field (Cozijn and Hallman, 2013)

7.4 Recommendations

The Joint Industry Project on the hydrodynamics of thruster interaction (TRUST JIP) was initialized to investigate the thruster interaction effects using both experimental and CFD methods. As an outcome, guidelines are also expected to be developed on how to use model tests and CFD computations in the analysis of thruster interaction effects and for the optimization of thruster configurations on DP vessels.

Although the application of CFD methods for thruster interactions is still largely



unexplored, suitable modeling methods should be investigated and developed in the near future. Thorough validation studies of CFD models against measurement results, both at model-scale and at full-scale, are required.

Research into CFD computations for thruster interactions should first focus on the computation of the velocities in the wake of a thruster in open water. The accurate computation of the velocities, especially at large distances from the thruster, is crucial for the accurate prediction of thruster interaction effects in a later stage. Different modelling options should be investigated. Subsequently, complex configurations should be considered in the computation by introducing additional physics, such as friction forces on the hull and the deflection of the thruster wake (Coanda effect).

8. MULTIPLE-BODY INTERACTION IN WAVES

8.1 Introduction

When two vessels are in a close proximity, large resonant free surface elevation occurs in the gap. Most of the linear seakeeping programs based on the potential flow theory, currently used by the industry, over-predict the free surface elevations between vessels and hence the low-frequency loadings on the hulls. This could lead to problems in the design of the fenders, hawsers and loading arms and may lead to unsafe operations.

To overcome the problems, the lid technique (Huijsmans et al., 2001), in which the free surface in the gap is replaced by a rigid lid, has been developed to suppress the unrealistic values of low-frequency forces. A linear dissipation term has also been proposed by Chen (2004) to modify the free-surface boundary condition. Newman (2003) used the generalized mode technique to model the free surface. However, artificial damping factors are

required as input in these methods. For example, Chen (2005) computed the drift forces and wave elevations in the gap for two side-by-side barges and for a barge adjacent to a Wigley hull and compared the results with experimental data. Numerical simulations showed that the wave height and the drift force in the resonance band were over-predicted using a damping coefficient $\varepsilon = 0$. A better agreement with the experimental data was achieved with $\varepsilon = 0.016$. Cheetham et al. (2007) presented numerical results by using AQWA software for side-by-side ship hydrodynamics and validation studies. A linearized damping lid boundary condition was applied in the gap region. Simulations were performed for a ship-barge case where it was determined that a value of damping factor $\alpha = 0.01$ was the most appropriate value for the boundary condition.

Since these methods are inadequate to give reasonable predictions without providing the experimental data beforehand, it may be challenging to apply them in design and analysis. It is desirable to determine the damping due to viscous effect.

8.2 State-of-the-Art Review

Many researchers have contributed to the studies of interactions of side-by-side bodies based on the potential-flow theory in the frequency domain, using lower-order and high-order panel methods. Pauw et al. (2007) carried out numerical simulations for two side-by-side LNG carriers and compared the numerical results with the experimental data. The numerical analysis was performed with a panel method code using a flexible damping lid in the gap region. A variety of gap widths were used in head seas with an attempt to obtain a rationale for predicting suitable damping factors. No unique value was found for the damping factor that could fully cover all the measured cases. It was noted that the damping factor could be tuned using the second-order



drift forces but not the first-order quantities, such as wave height. The damping factor was found to have the greatest effect on the second-order drift force.

Bunnik et al. (2009) applied the method as described in Chen (2005) to two side-by-side LNG carriers in head seas and compared the solutions with the results of model tests. The damping lid was also extended to the surface inside the vessels. The comparison with the experimental results indicated that the damping lid method worked better than the rigid lid method at frequencies of interest.

Molin et al. (2009) applied DIODORE, a potential-flow code, to two side-by-side fixed barges. A set of massless plates were used in the gap between the barges and a quadratic damping force was applied to the plates. The numerical results were compared with the model test results of two rectangular barges in irregular waves. A drag coefficient, $C_D = 0.5$, was employed to determine the quadratic damping force, which led to a good agreement with measured data. It was recommended that an investigation of freely floating ships should be performed in the future.

Kawabe et al. (2010) studied water surface responses in a moon pool of a freely floating vessel. Studies showed that a damping factor of $\alpha = 0.05$ resulted in a good agreement between the predicted and measured free surface elevations.

Zhang et al. (2013) carried out numerical studies on the hydrodynamic interactions of two bodies in arbitrary arrangements in terms of gap widths, relative sizes and relative angles. HYDROSTAR, a potential-flow program, was utilized. The numerical results showed that the resonance phenomenon became more dominant than the shielding effect as the gap width decreased. Studies also suggested that sway and heave responses were sensitive to relative angles in head seas. For parallel arrangements,

motions tended to be greater as the sizes of barges became larger.

Ten et al. (2012) used a semi-analytical method to predict the characteristics of the resonance of viscous fluid in a narrow gap. Dissipation was introduced in the form of pressure loss. This method was validated by comparing with the solution with other analytical, numerical and model test results. It was found that the conventional BEM was inapplicable to very small gap. The semi-analytical model was reported suitable for small and large ratios of gap width to the ship breadth.

Clauss et al. (2013) investigated the gap effects for side-by-side vessels with numerical methods in the frequency domain. The free surface elevation was modelled by a damping lid. WAMIT was used in their studies. The numerical and experimental investigations were conducted for a LNG carrier next to a fixed terminal. Wave propagations in terms of wave height and regions of cancellation and amplification were examined. They reported that the surface elevation in the gap was surprisingly not overestimated by WAMIT at the critical frequency around 0.81 rad/s without using any numerical damping lid.

Xu et al. (2013) computed second-order mean drift forces and moments on three side-by-side barges during the float-over operation using WAMIT. The numerical results were validated by model tests. It was reported that satisfactory numerical results could be obtained by adding viscous damping.

Kashiwagi and Shi (2010) obtained the pressure distribution for multiple bodies in a close proximity. They solved the integral equation of the diffraction potential by the Higher-order Boundary Element Method (HOBEM). It was found that when the separation distance between bodies is smaller,



there would be a larger deviation of the pressure distribution.

Hong et al. (2013) studied the gap resonance between the bodies in close proximity by two methods, in terms of a nine-node discontinuous higher order boundary element method (9dHOBEM) and a constant boundary element method based on the boundary matching formulation (BM-CBEM). The results showed that BM-CBEM combined with the free surface damping or 9dHOBEM combined with a tuned value of the wetted surface damping parameter could largely reduce the over-predicted first-order hydrodynamic coefficients, and successfully estimate the time-mean drift forces on two side-by-side floating structures.

Efforts have been made to address the interaction problem in the time domain. Xiang and Faltinsen (2011) developed a time-domain solution for linear loads and motions of two tankers paralleled in calm and deep water in lightering operation by using 3D Rankine source method. The numerical results were compared with analytical solutions, experimental data and numerical results by others. Zhu et al. (2008) computed the forces on two fixed side-by-side hull-shaped boxes with a narrow gap due to incoming and diffracted waves based on a time-domain method. The predicted resonant phenomena in the gap is in good agreement with that from the frequency-domain analysis.

Numerical methods based on nonlinear potential-flow theory, such as the finite element method, have also been developed to solve the interaction problem.

Wang et al. (2011) applied fully nonlinear potential theory to study 2D resonant waves in the gap between two floating structures. A higher-order finite element method was used to analyze the fully nonlinear resonant oscillations of the liquid in the gap. They compared the second-order time-domain results with the

corresponding fully nonlinear results and concluded that the second-order theory might overestimate the wave amplitude in the gap and the wave loads on the structures.

Ma et al. (2013) applied the fully nonlinear potential theory to study the 2D resonant waves in the gap between two floating barges by using the Quasi Arbitrary Lagrangian-Eulerian Finite Element Method (QALEFEM). Based on the computed free surface elevations and the forces acting on barges, it was recommended that nonlinear models for such cases should be used, in particular, including the 4th-order or higher-order component. These investigations provided a basis for future 3D studies.

Attempts have also been made to determine the viscous effect by solving Reynolds Averaged Navier–Stokes (RANS) equations. Lu et al. (2010a) carried out numerical studies for two identical bodies and three identical bodies at a close proximity by using the potential-flow method and the viscous-flow method without artificial damping force. The viscous flow model was based on a three-step finite element solver, and the CLEAR-VOF method was applied to capture the free surface in the gap region. Experimental results were used to assess the performance of each model. Both potential and viscous models performed well for predicting frequencies outside the resonance band, while the potential flow model over-predicts the wave height around resonant frequencies. The viscous flow model showed good agreement with measured values for all frequencies. To improve the potential flow method, Lu et al. (2010b) extended the previous work and applied artificial damping to the free surface. The results by the potential flow model with a damping coefficient $\mu = 0.4$ were in good agreement with the viscous flow results and the experimental data for the two-body cases and for both gaps in the three-body cases. In 2011, they studied on the effects of gap width, body draft, body width and number

of bodies of multi-bodies at close proximity (Lu et al., 2011).

Lu and Chen (2012) examined the energy dissipation around resonant frequencies between two bodies by CFD computations. The dissipation was found to be relatively constant over frequencies near the resonant frequency. The dissipation rate was examined over various zones. Studies showed that the over-prediction of resonant wave elevation could be reduced by using the dissipation coefficient to assimilate the friction force. An explicit formula to obtain the dissipation coefficient was recommended.

Zou and Larsson (2013) investigated the interaction of two side-by-side ships in shallow water. They completed a systematic investigation of ship-ship interactions during a lightering operation using a steady-state Reynolds Averaged Navier–Stokes (RANS) solver. The numerical results were compared with benchmark experimental data. A good agreement was found between measured and computed wave heights, indicating that the predicted pressure distribution on the free surface was appropriate.

8.3 Existing Model Tests

Many model tests of two side-by-side bodies have been identified in the review, including captive and floating tests with and without mooring lines between two bodies. Besides those listed in Section 8.2, some recent model tests on side-by-side vessels are presented below.

Kim et al. (2012) carried out a series of model tests and investigated the effect of the heading control on the offloading operability of side-by-side moored vessels, LNGC and LNG FPSO (FLNG), in multidirectional environments. The key variables affecting the offloading operability, such as hawser tensions, fender loads, and relative motions between two vessels, were measured. Several heading angles were selected to investigate the impact of the heading control on the offloading operability. The model tests indicated that the offloading operability in the multi-directional environments can be improved by heading control. In the model tests, the motion RAOs and horizontal drift forces/moments due to waves for the side-by-side moored vessels were measured.

Cho et al. (2011) carried out experimental studies of motions and drift forces of side-by-side moored FSRU and LNGC including sloshing effect. The effect of filling level on the coupling between sloshing and motions of the floating bodies was investigated in their work. The effect of gap flow was also examined.

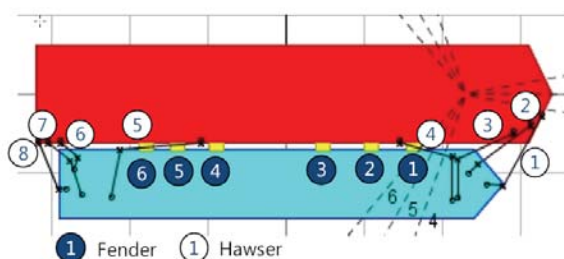


Figure 8.3.1 Side-by-Side Moored Vessels (Kim et al., 2012)

8.4 Potential Experimental Data for Benchmark Studies

To investigate the wave elevation in the gap between two side-by-side bodies and the effect of viscous effect on the prediction, it is of importance to identify benchmark data for validation studies. The Committee recommended model tests of two floating bodies without mooring lines and fenders in between. The experimental data should include at least measured wave elevations in the gap and motions of bodies and/or mean drift forces at various gaps, wave frequencies and headings. The following experimental data have been identified for potential use in the proposed benchmark studies.

Hong et al. (2005) carried out model tests of side-by-side LNG FPSO and LNGC with wired springs as mooring at the KRISO Ocean Engineering Basin. The gap was set as 4 m in full scale. Model tests were performed in both regular and irregular waves. For regular waves, the wave frequencies were from 0.25 rad/s to 1.2 rad/s in full scale and the headings were 150, 180, 240 and 270 degrees. Six DOF motions of each vessel were measured with photo sensors, relative waves at 3 locations (midship and +/- 0.3L from the midship, portside) of LNG FPSO were measured by capacitance type probes. Strain gauge type accelerometers were used for measuring horizontal and vertical accelerations. Drift forces were measured using the tension load cells at the end of spring wire moored to the ships.

The Committee have also initialized a model test program for two identical bodies with simplified geometry in regular waves (wave steepness is 1/30). The tests were carried out at Ocean Engineering Research Centre of Memorial University's 60 m towing tank. The test matrix included three gaps and three wave headings. Motions of each body and wave

elevations at three locations in the gap were measured. Figure 8.4.1 shows the simplified models in the tank. Model tests have also been carried out for the single body in regular waves. The tests are planned to be repeated in an ocean engineering basin. It is anticipated that the experimental results can be used in benchmark studies.



Figure 8.4.1 Simplified Models

8.5 Recommendations

The determination of the viscous effect on the prediction of wave elevations in the gap and the drift forces on two bodies in a close proximity remains as a challenge. As the next step, the Committee recommended to collect the experimental data available for benchmark studies. With an objective to investigate the viscous effect on the predictions by potential-flow methods, numerical tools based on the CFD methods should be included in the studies.

9. MOTIONS OF LARGE SHIPS AND FLOATING STRUCTURES IN SHALLOW WATER

The shallow water wave problem has become one of the important issues in offshore hydrodynamics as the need for floating LNG terminals increases. The amplitude of the long period resonant motion of moored structures in shallow water is greatly influenced by the low frequency part of the incident waves, which themselves are a result of interactions of the

component waves of the incident wave spectrum (ITTC Ocean Engineering Committee, 2008). The Committee was tasked to report on the motions of large ships and floating structures in shallow water. A literature review was first conducted to identify the progress made in model tests and numerical simulations of large floating structures.

In terms of the prediction of slowly varying motions and loads, Stansberg and Kristiansen (2011) conducted model tests with a large LNG carrier moored in shallow water. Quadratic Transfer Function (QTF) for slowly varying surge force was obtained using the cross-bi-spectral analysis. The off-the-diagonal QTF values have a tendency to increase significantly as the difference frequency is increased in shallow water condition, especially for smaller incident wave frequencies. In their studies, it was shown that QTF for shallow water condition was underestimated by Newman's approximation.

Pessoa et al. (2013) applied a second-order boundary element method to an axisymmetric floating body in bi-chromatic waves. The occurrence of large low-frequency motions was shown in experiments and in numerical results when the difference frequencies between bichromatic waves were close to natural frequencies of surge motion and even pitch motion.

Progress has also been made in simulations of nonlinear shallow water waves by solving Boussinesq equations. Lee et al. (2010) simulated nonlinear waves in shallow water by considering shoaling, refraction and non-linear wave interactions. By using the shallow water wave field, motion responses were further computed. The radiation and diffraction forces were predicted by a constant panel method. The wave height and velocity components, computed from the Boussinesq equations, were utilized to estimate wave forces in shallow water. The computations were applied to a

floating storage and regasification unit (FRSU) and an LNGC in shallow water waves with varied bathymetry. The numerical results were compared with those for the equivalent constant water depth condition. The comparison shows that the motion responses are in general larger than those for the cases of constant water depth. In particular, the horizontal motions are significantly large because of wave deformations due to the bottom topography and the low-frequency waves. The increased horizontal surge motion is certainly critical for the design of mooring lines in shallow water.



Figure 9.1 Tower Yoke Mooring System (Kim et al., 2011)

The motions of a LNG carrier in various bathymetric conditions were studied by Kim (2013) using a linear Rankine panel method and by solving the Boussinesq equations. The depth was assumed to be shallow (15-30m), constant or with a slope. The numerical results were compared with those with infinite depth conditions, in term of hydrodynamic coefficients and motion responses. The authors concluded that the nonlinear effects are not noticeable except for a very steep slope, and that the linear methods can be used to evaluate the hydrodynamics of floating bodies over varied bathymetry.

Model tests have also been carried out to study the responses of large floating structures such as FRSU in shallow water waves. For



example, Kim et al. (2012) carried out model tests to study the responses of a FSRU with a mooring system in shallow water. In their work, two different mooring systems, the turret catenary system and the tower yoke system, were compared.

Zeng et al. (2012) presented a shallow water mooring system for FPSO systems. Based on a turret mooring with self adjusting stiffness system (TUMSAS), the mooring systems were developed using numerical approaches and experimental validations. The design case was for a 30,000-ton FPSO in a location of 24m deep. The self adjusting stiffness was obtained by using a weight module and catenary chains. The results show a larger offset of the FPSO and a drastic reduction of the forces acting on the mooring system. Vertical motions were also reduced in comparison with a regular turret.

The shallow water wave problem and the motions of large floating structures in shallow water remain as challenging topics. The Committee recommended to identify benchmark data to validate numerical methods including those based on the potential flow theory, CFD and those based on solving the Boussinesq equations.

10. ISSC/ITTC WORKSHOPS

The first ISSC/ITTC joint workshop on uncertainty modeling for ships and offshore structures has been successfully organized by ISSC, the ITTC Ocean Engineering Committee and the ITTC Seakeeping Committee. The Committee presented the uncertainties related to predictions of loads and responses for offshore structures at the Workshop on September 8, 2012 at Rostock, Germany. The joint effort between ISSC and ITTC has led to the publication of a special issue on uncertainty modeling for ships and offshore structures in the journal of Ocean Engineering.

The second ISSC/ITTC joint workshop to be held in August 30, 2014 will focus on the wave-induced motion and structural loads on ships and offshore structures, including a computational benchmark test for a large modern ship.

11. CONCLUSIONS

11.1 State of the Art Review

Stationary Floating Structures and Ships

Experimental and numerical procedures for predicting motions of floating structures are in general well established. There is still a need of research on vortex induced motions of spars and semisubmersibles, and on the platform responses in extreme seas. Studies have been carried out on novel TLPs, spars and semisubmersible structures. Relative motions between two floating bodies remain very important research topics, especially for the safe operation of floating LNG production and storage and offloading vessels.

Highly Nonlinear Effects on Ocean Structures

Slamming, sloshing and wave run-ups, representing the highly nonlinear effects, remain as important issues for the design/operation of offshore structures in extreme sea conditions. CFD methods such as VOF, SPH and CIP, along with experiments, are the primary tools to address these highly nonlinear phenomena.

For sloshing, the state-of-the-art methodology is based on the use of seakeeping computer codes to estimate ship or platform motions. Experiments on sloshing tank models and CFD simulations have been performed in order to estimate global and local fluid loadings in the tanks. Benchmark studies of LNG sloshing have been carried out to assess the uncertainties in measurement of pressures, to investigate scale effects, and to validate the



numerical tools. Research has also been focused on hydroelasticity using experimental studies. There is still a need of research in these areas using experimental and numerical methods.

VIV and VIM

Progress has been made in the prediction of VIV and VIM using empirical prediction programs, CFD methods and experimental methods. A few new prediction programs have been developed based on the time-domain methods. Further research is required in this area.

New Experimental Techniques

A couple of new experimental techniques have been identified, including the BIV technique for velocity measurements and a subsea imaging technique with a potential to be used in a tank for underwater measurements.

New Extrapolation Methods

Limited investigations have been carried out on the development of extrapolation methods. Challenging issues in scaling of model tests results to full scale have been indicated in various applications throughout the report, particularly in sloshing tests.

11.2 Review of the Existing Procedures

The Committee reviewed three procedures. Very minor revisions were identified for 7.5-02-07-03.1 and 7.5-02-07-03.2. The Committee however found that there is little information in 7.5-02-07-03.3 and the limited information in 7.5-02-07-03.3 is very similar to that in 7.5-02-07-03.1. The Committee recommended to move the contents of 7.5-02-07-03.3 to 7.5-02-07-03.1. The Committee also identified that there is no existing procedure dealing with the result analysis of model tests in irregular

waves. The Committee recommends to develop a new procedure on this aspect.

11.3 Benchmark Studies on VIV

In this benchmark study, URANS, DES and LES were employed by six participants. In terms of overall trend, numerical predictions by DES and LES are generally in better agreement with the experimental data than those by URANS. It can be concluded that the LES method captured the drag crisis phenomenon and the LES solutions agree better with experimental data at most points than those by URANS. At high Reynolds numbers, some solutions by the URANS method agree reasonably well with the experimental data. The Committee recommended to continue the benchmark studies based on LES and DES.

11.4 Wave Run-Up Benchmark Studies

Eleven organizations participated in the benchmark studies on the cases of the single truncated cylinder and four organizations participated in the benchmark studies on the cases of four truncated cylinders. Nine participants employed CFD methods in their studies. It was concluded that the values and trends of the computed wave elevations and forces by CFD methods are in good agreement with the experimental results for the cases of single and four cylinders. Due to time constraints and limited computing resources, most of participants have focused on the single circular cylinder cases. It is recommended that more studies be extended to the four-column cases.

11.5 Thruster-Thruster Interactions

A literature review has been conducted for thruster-thruster interactions. Great progress has been made in investigating the interactions using experimental and CFD methods. Research has been carried out to understand the thruster interaction effects by measuring the



detailed wake flow using PIV systems. Although the application of CFD methods for thruster interactions is still largely unexplored, suitable modeling methods should be investigated and developed in the near future. Thorough validation studies of CFD models against measurement results, both at model-scale and at full-scale, are required.

11.6 Side-by-Side Body Interaction

A literature review has been conducted for side-by-side body interactions in waves with an emphasis on the prediction of wave elevation in the gap and the drift forces. Progress has been made in investigating the damping effect using model tests and CFD simulations. However, the determination of wave elevations and drift forces using the potential-flow based methods remains as a challenge. The Committee recommended to collect the available experimental data for benchmark studies. With an objective to investigate the viscous effect on the predictions by potential-flow methods, numerical tools based on the CFD methods should be included in the studies.

11.7 Motions of Large Ships and Floating Structures in Shallow Water

A literature review has been carried out for motions of large ships and floating structures in shallow water. The focus was on the LNG ships and terminals as well as FPSO and their mooring systems. The shallow water wave problem and motions of large floating structures in shallow water remain as challenging topics.

In shallow water, the low-frequency component induced by nonlinear wave interactions is important for the low-frequency motions of two floating bodies. The hydrodynamic effects of sloshing tank and the gap phenomena for two floating bodies in shallow water need to be studied further.

The Committee recommended to identify benchmark data to validate numerical methods including those based on the potential-flow theory, CFD and those based on solving the Boussinesq equations.

12. RECOMMENDATIONS

The Ocean Engineering Committee would like to make the following recommendation to the 27th ITTC:

- Adopt the new guideline 7.5-02-07-03.10, "Guideline for VIV Testing"

13. REFERENCES

- Aarsnes, J.V., 1996, "Drop Test with Ship Sections - Effect of Roll Angle", Report 603834.00.01, Norwegian Marine Technology Research Institute, Trondheim.
- Aglen, I.M. and Larsen, C.M., 2011, "Importance of Added Mass for the Interaction between IL and CF Vibrations of Free Spanning Pipelines", Proc. OMAE2011, Rotterdam, The Netherlands.
- Alaoui, A.E.M. and Nème, A., 2012, "Slamming Load during Vertical Water Entry at Constant Velocity", Proc. ISOPE2012, Rhodes, Greece.
- American Petroleum Institute (API), 1996, "Recommended Practice for Design and Analysis of Station-keeping Systems for Floating Structures", App. C, API, 2SK, 2nd edition.
- American Bureau of Shipping (ABS), 2013, "Guide for Dynamic Positioning Systems", Houston.
- Bachynski, E.E. and Moan, T., 2012, "Linear and Nonlinear Analysis of Tension Leg Platform Wind Turbines", Proc. ISOPE2012, Rhodes, Greece.



- Bae, Y.H. and Kim, M.H., 2013, "Rotor-floater-tether Coupled Dynamics Including Second-order Sum-frequency Wave Loads for a Mono-column-TLP-type FOWT (Floating Offshore Wind Turbine)", Ocean Eng., Vol. 61, pp.109-122.
- Bagnold, R.A., 1939, "Interim Report on Wave-Pressure Research", Report, TU Delft.
- Bai, Z., Xiao, L., Kou, Y. and Yang, L., 2013, "Research on Vortex Induced Motion of a Deep Draft Semisubmersible with Four Rectangular Columns", Proc. ISOPE2013, Anchorage, USA.
- Baudin, E, Diebold, L., Pettinotti, B, Rousset, J.M. and Weber, M., 2013, "Bureau Veritas Sloshing Model Tests & CFD Calculations within ISOPE Benchmark", Proc. ISOPE2013, Anchorage, USA.
- Bitner-Gregersen, E.M., 2011, "Reliability Assessment of TLP Air-Gap in Nonlinear Waves", Proc. OMAE2011, Rotterdam, The Netherlands.
- Bogaert, H., Kaminski, M.L.M. and Brosset, L., 2011, "Full and Large Scale Wave Impact Tests for a Better Understanding of Sloshing: Results of the Sloskel Project", Proc. OMAE2011, Rotterdam, The Netherlands.
- Bosland, R., Dijk, J.M. and Huijsmans, R.H.M., 2009, "Numerical Prediction of Thruster-Thruster Interaction", Proc. OMAE2009, Honolulu, USA.
- Bourguet, R., Karniadakis, G.E. and Triantafyllou, M.S., 2013, "Multi-Frequency Vortex-Induced Vibrations of a Long Tensioned Beam in Linear and Exponential Shear Flows", J. Fluid and Structures, Vol. 41, pp.33-42.
- Bourguet, R., Triantafyllou, M.S., Tognarelli, M. and Beynet, P., 2011, "Fluid-Structure Energy Transfer of a Tensioned Beam Subject to Vortex-Induced Vibrations in Shear Flow", Proc. OMAE2011, Rotterdam, The Netherlands.
- Bourguet, R., Triantafyllou, M.S., Tognarelli, M. and Beynet, P., 2012, "Distributed Wake-Body Resonance of a Long Flexible Cylinder in Shear Flow", Proc. OMAE2012, Rio de Janeiro, Brazil.
- Bouscasse, B., Colagrossi, A., Antuono, M. and Lugni, C., 2013, "A Classification of Shallow Water Resonant Sloshing in a Rectangular Tank", Proc. OMAE2013, Nantes, France.
- Brandner, P.A., 1998, "An Experimental Investigation into the Interaction between Two Closely Spaced Azimuthing Thrusters", Report AME CRC C 98/4, Australian Maritime Engineering CRC Limited.
- Bunnik, T., Pauw, W. and Voogt, A., 2009, "Hydrodynamic Analysis for Side-by-Side Offloading", Proc. ISOPE2009, Osaka, Japan.
- Campbell, B. and Slocum, S., 2013, "Prediction of VIV for Risers with Effective Strakes", Proc. OMAE2013, Nantes, France.
- Cao, H., Liu, Y. and Wan, D. 2013, "Benchmark Computations of Wave Run-Up on Single Cylinder and Four Cylinders by naoe-FOAM-SJTU Solver", Proc. ITTC Workshop on Wave Run-up and Vortex Shedding, Nantes, France,
- Cao, H., Zha, J. and Wan, D., 2011, "Numerical Simulation of Wave Run-up Around a Vertical Cylinder", Proc. ISOPE2011, Maui, USA.
- Chabaud, V., Steen, S. and Skjetne, R., 2013, "Real-Time Hybrid Testing for Marine Structures: Challenges and Strategies", Proc. OMAE2013, Nantes, France.
- Chandrasekaran, S., Sundaravadivelu, R., Pannerselvam, R., Madhuri, S. and Varthini, D.S., 2011, "Experimental Investigations of Offshore Triceratops under Regular Waves", Proc. OMAE2011, Rotterdam, The Netherlands.
- Cheetham, P., Du, S., May, R. and Smith, S., 2007, "Hydrodynamic Analysis of Ships Side By Side in Waves", Proc. International Aerospace CFD Conference, Paris, France.



- Chen, X.B., 2004, "Hydrodynamics in Offshore and Naval Applications - Part I", Keynote lecture of 6th Intl. Conf. Hydrodynamics, Perth (Australia).
- Chen, X.B., 2005, "Hydrodynamic Analysis for Offshore LNG Terminals", Proc. International Workshop on Applied Offshore Hydrodynamics, Rio de Janeiro, Brazil.
- Cho, S., Sung, H., Hong, S., Hong, S., Ha, M., Choi, Y., Yu, B., Jang, R. and H. Choi, 2011, "Experimental Study on the Effect of Sloshing on Side-by-Side moored FSRU and LNGC", Proc. ISOPE2011, Maui, USA.
- Choi, H.I., Park, J.H., Kwon, S.H., Lee, K.H., Lee, S.B. and Yang, Y.J., 2012, "An Experimental Study on Hydro-Elasticity in Sloshing", Proc. OMAE2012, Rio de Janeiro, Brazil.
- Clauss G.F., Dudek M. and Testa D., 2013, "Gap Effects at Side-by-Side LNG-Transfer Operations", Proc. OMAE2013, Nantes, France.
- Clauss, G.F., Sprenger, F., Dudek, M. and Testa, D., 2012, "Sloshing: From Theory to Offshore Operations", Proc. OMAE2012, Rio de Janeiro, Brazil.
- Cole, J.C., Islam, M., Garvin, M. and Herrington, P., 2012, "Modelling Details of Fenders in Float-Over Installation Experiments", Proc. OMAE2012, Rio de Janeiro, Brazil.
- Constantinescu, A., Alaoui, A.E.M., Nême, A. and Jacques, N. and Rigo, P., 2011, "Numerical and Experimental Studies of Simple Geometries in Slamming", Inter. J. Offshore and Polar Eng., Vol. 21, pp.216-224.
- Constantinides, Y. and Oakley, O.H., 2013, "Prediction and Screening of Truss Spar VIM with CFD", Proc. OMAE2013, Nantes, France.
- Constantinides, Y., Raghavan, K., Karayaka, M. and Spencer, D., 2013, "Tandem, Riser Hydrodynamic Tests at Prototype Reynolds Number", Proc. OMAE2013, Nantes, France.
- Copple, R.W. and Capanoglu, C., 2012, "Tension Leg Wind Turbine (TLWT) Conceptual Design Suitable For a Wide Range of Water Depths", Proc. ISOPE2012, Rhodes, Greece.
- Cozijn, H., 2010, "New Initiatives Probe: Thruster Interaction Effects", Maritime Report, Num. 99, pp.10-12.
- Cozijn, J.L. and Hallmann, R., 2013, "Thruster-Interaction Effects on a DP Semi-Submersible and a Drill Ship: Measurement and Analysis of the Thruster Wake Flow", Proc. OMAE2013, Nantes, France.
- Cozijn, J.L., Hallmann, R. and Koop, A.H., 2010, "Analysis of the Velocities in the wake of an Azimuthing Thruster Using PIV Measurements and CFD Calculations", Proc. Dynamic Positioning Conference, Houston, USA.
- Cruz, R.E., Neves, M.A.S., Rivera, L.A. and Esperança, P.T.T., 2012, "An Investigation on the Excitation of Yaw Parametric Resonance of a Tension Leg Platform", Proc. OMAE2012, Rio de Janeiro, Brazil.
- van Daalen, E.F.G., Cozijn, J.L., Loussouarn, C. and Hemker, P.W., 2011, "A Generic Optimization Algorithm for the Allocation of DP Actuators", Proc. OMAE2011, Rotterdam, The Netherlands.
- Damblans, G., Berhault, C., Marcer, R., Cinello, A. and Pétrié, F., 2012, "CFD and Experimental Investigations of Slamming Load Prediction on Subsea Structures in Splash Zone", Proc. ISOPE2012, Rhodes, Greece.
- DaSilva, O. and Knecht, H., 2011, "Airgap on Semi Submersibles, A Practical Guide on the Implementation of a Stochastic Approach", Proc. OMAE2011, Rotterdam, The Netherlands.
- Det Norske Veritas (DNV), 1996, "Rules for Classification of Mobile Offshore Units, Position Mooring", Part 6 Ch. 2.



- Det Norske Veritas (DNV), 2012, "Dynamic Positioning Vessel Design Philosophy Guidelines", Recommended Practice DNV-RP-E306.
- van Dijk, R.R.T. and Aalbers, A.B., 2001, "What Happens in Water: The use of Hydrodynamics to Improve DP", Dynamic Positioning Conference, Houston, USA.
- Ekstrom, L. and Brown, D.T., 2002, "Interaction Between Thrusters Attached to a Vessel Hull", Proc. OMAE2002, Oslo, Norway.
- Embry, C., Hardy, M., Nickerson, B., Manning, N., Goodyear, D., Richardson D. and Pappas, J.M., 2012, "SS MTS: Subsea Monitoring – High Resolution 3D Laser Imaging for inspection, Maintenance, Repair and Operations", Proc. OTC2012, Houston, USA
- Fillon, B., Henry, J., Diebold, L. and Derbanne, Q., 2013, "Extreme Values Theory Applied to Sloshing Pressure Peaks", Proc. ISOPE2013, Anchorage, USA.
- Fontaine, E.R., Rosen, J., Marcollo, H., Vandiver, J.K., Triantafyllou, M., Resvanis, T.L., Larsen, C.M., Tognarelli, M.A., Oakley, O.H., Constantinides, Y. and Johnstone, D.R., 2013, "Using Model Test Data to Assess VIV Factor of Safety for SCR and TTR in GOM", Proc. OMAE2013, Nantes, France.
- Forrstal, G.Z. and Aubault, A., 2013, "Improving Offshore Platforms Wave Measurements", Proc. OMAE2013, Nantes, France.
- Forrstal, G.Z., 2011, "Maximum Crest Heights under a Model TLP Deck", Proc. OMAE2011, Rotterdam, The Netherlands.
- Fu, S., Wang, J., Baarholm, R., Wu, J. and Larsen, C.M., 2013, "VIV of Flexible Cylinder in Oscillatory Flow", Proc. OMAE2013, Nantes, France.
- Gaidai, O., Naess, A. and Stansberg, C., T., 2012, "Airgap Statistics for a Tension Leg Platform", Proc. OMAE2012, Rio de Janeiro, Brazil.
- Gonçalves, R.T., Franzini, G.R., Rosetti, G.F., Fajarra, A.L.C. and Nishimoto, K., 2012, "Analysis Methodology for Vortex-Induced Motion (VIM) of a Monocolumn Platform Applying the Hilbert–Huang Transform Method", J. Offshore Mech. and Arctic Eng., Vol. 134.
- Gonçalves, R.T., Rosetti, G.F., Fajarra, A.L.C. and Nishimoto, K., 2012a, "An Overview of Relevant Aspects on VIM of Spar and Monocolumn Platforms", J. Offshore Mech. and Arctic Eng., Vol. 134.
- Gonçalves, R.T., Rosetti, G.F., Fajarra, A.L.C., Nishimoto, K. and Oliveira, A.C., 2012, "Wave Effects on Vortex-Induced Motion (VIM) of a Large-Volume Semi-Submersible Platform", Proc. OMAE2012, Rio de Janeiro, Brazil.
- Gonçalves, R.T., Rosetti, G.F., Fajarra, A.L.C., Nishimoto, K. and Oliveira, A.C., 2012, "Vortex-Induced Yaw Motion (VIY) of a Large-Volume Semi-Submersible Platform", Proc. ISOPE2012, Rhodes, Greece.
- Graczyk, M., Berget, K. and Allers, J., 2012, "Experimental Investigation of Invar Edge Effect in Membrane LNG Tanks", J. Offshore Mech. and Arctic Eng., Vol. 134.
- Hagen, Ø., 2011, "Reliability Assessment for TLP Tether Overload in Nonlinear Waves", Proc. OMAE2011, Rotterdam, The Netherlands.
- Hennig, J., Scharnke, J., Buchner B. and van den Berg, J., 2011, "Extreme Load-Response Mechanisms of a Tension Leg Platform due to Larger Wave Crests – Some Results of the 'Crest' JIP", Proc. OMAE2011, Rotterdam, The Netherlands.
- Hong, D.C., Hong, S.Y., Nam, B.W. and Hong, S.W., 2013, "Comparative Numerical Study of Repulsive Drift Forces and Gap Resonances between Two Vessels Floating Side-By-Side in Proximity in Head Seas Using A Discontinuous HOBEM and A Constant BEM with Boundary Matching Formulation", Ocean Eng., Vol. 72.



- Hong, S.Y., Kim, J.H., Cho, S.K., Choi, Y.R. and Kim, Y.S., 2005, "Numerical and Experimental Study on Hydrodynamic Interaction of Side-by-Side Moored Multiple Vessels", Ocean Eng., Vol. 32.
- Hong S., Lee, I., Park, S.H., Lee, C. and Chun, H., 2013, "Scale Model Experiments of the SPAR-Type Floating Offshore Platform", Proc. ISOPE2013, Anchorage, USA.
- Huang, Z. and Larsen, C.M., 2011, "Numerical Simulation on Vortex-Induced Vibration of an Elastically Mounted Circular Cylinder with Two Degrees-of-Freedom", Proc. OMAE2011, Rotterdam, The Netherlands.
- Huera-Huarte, F. J., 2012, "An Optical Tool for Measuring Vortex-Induced Vibrations of Long Flexible Cylinders", Proc. OMAE2012, Rio de Janeiro, Brazil.
- Huera-Huarte, F.J. and Gharib, M., 2011, "Vortex and Wake-Induced Vibrations of a Tandem Arrangement of Two Flexible Circular Cylinders with Far Wake Interference", J. Fluid and Structures, Vol. 27, pp.824-828.
- Huera-Huarte, F.J. and Gharib, M., 2011, "Flow-Induced Vibrations of a Side-by-Side Arrangement of Two Flexible Cylinders", J. Fluid and Structures, Vol. 27, pp.354-366.
- Huera-Huarte, F.J., Jeon, D. and Gharib, M., 2011, "Experimental Investigation of Water Slamming Loads on Panels", Ocean Eng., Vol. 38, pp.1347-1355.
- Huijsmans, R.H.M., Pinkster, J.A. and de Wilde, J.J., 2001, "Diffraction and Radiation of Waves Around Side by Side Moored Vessels", Proc. ISOPE2001, Oslo, Norway.
- James, M. and Lloyd, T., 2013, "Large Eddy Simulations of Circular Cylinders at a Range of Reynolds Numbers", Proc. ITTC Workshop on Wave Run-up and Vortex Shedding, Nantes, France.
- Ji, Y.M., Shin, Y.S., Park, J.S., and Hyun, J.M., 2012, "Experiments on Non-Resonant Sloshing in a Rectangular Tank with Large Amplitude Lateral Oscillation", Ocean Eng., Vol. 50, pp.10-22.
- Jiang, M., Lien, V., Lesar, D., Engle, A. and Lewis, R., 2012, "A Validation of Various Codes Using Hydrodynamic Wedge Impact Data", Proc. OMAE2012, Rio de Janeiro, Brazil.
- Johannessen, T.B., 2011, "High Frequency Loading and Response of Offshore Structures in Steep Waves", Proc. OMAE2011, Rotterdam, The Netherlands.
- Kaminski, M.L. and Bogaert, H., 2010, "Full Scale Sloshing Impact Tests – Part 2", Proc. ISOPE2010, Beijing, China.
- Karimi M.R., Kosinski, C. and Brosset, L., 2013, "Comparison of Sloshing Model Test Results at Scales 1:10 and 1:40", Proc. ISOPE2013, Anchorage, USA.
- Kashiwagi, M. and Shi, Q., 2010, "Pressure Distribution Computed by Wave-Interaction Theory for Adjacent Multiple Bodies", J. Hydrodynamics, Vol. 22(5), pp.526-531.
- Kawabe, H., Kwak, H. U., Park, J. and Ha, M., 2010, "The Numerical and Experimental Study on Moonpool Water Surface Response of a Ship in Wave Condition", Proc. ISOPE2010, Beijing, China.
- Kim, J., Jaiman, R., Cosgrove, S. and O'Sullivan, J., 2011, "Numerical Wave Tank Analysis of Wave Run-Up on a Truncated Vertical Cylinder", Proc. OMAE2011, Rotterdam, The Netherlands.
- Kim, M.S., Jeong, H.S., Kwak, H.W., Kim, B.W. and Eom, J.K., 2012, "Improvement Method on Offloading Operability of Side-by-side Moored FLNG", Proc. ISOPE2012, Rhodes, Greece.
- Kim, T. and Kim, Y., 2013, "Numerical Analysis on Floating-Body Motion Responses in Arbitrary Bathymetry", Ocean Eng., Vol. 62, pp. 123-139.
- Kim, H.J., Kwak, H.U., Lee, J.H., Kim, S.E. and Seo, J.S. 2012, "Offloading Operability with Heading Control of Side-by-Side Moored FLNG and LNGC", Proc. OMAE2012, Rio de Janeiro, Brazil.



- Kim, S., Kim, K. and Kim, Y., 2012, "Comparative Study on Model-Scale Sloshing Tests", J. of Marine Sci. and Tec., Vol. 17, pp. 47–58.
- Kim, H.T., Lee, D.Y. and Kwon, J.W., 2013, "Numerical Simulations of Wave Run-Up on Single cylinder and Four Cylinders Using CFD Tools", Proc. KTTC Daejeon Workshop on Wave Run-up.
- Kim, Y.S., Sung, H.G., Kim, J.H, Hong, S.Y. and Hong, J.P. 2012, "An Experimental Study on the Response of FSRU in Shallow Water in Comparison of Mooring Systems", Proc. ISPOE 2012, Rhodes, Greece.
- Koop, A. and Berezniński, A., 2011, "Model-Scale and Full-Scale CFD Calculations for Current Loads on Semi-Submersible", Proc. OMAE2011, Rotterdam, The Netherlands.
- Korobkin, A.A. and Khabakhpasheva, T.I., 2013, "Impact of Elastic Body on the Deep and Shallow Water", Proc. OMAE2013, Nantes, France.
- Kristiansen, T., Barrholm, R. and Stansberg, C.T., 2004, "Validation of Second-order Analysis in Predicting Diffracted Wave Elevation around a Vertical Circular Cylinder", Proc. ISOPE2004, Toulon, France.
- Kristiansen, T. and Stansberg, C.T., 2013, "Empirical Prediction of Nonlinear Wave Diffraction and Run-Up on Vertical Columns", Proc. ITTC Nantes Workshop on Wave Run-up and Vortex Shedding, Nantes, France.
- Kurian, V.J., Ng, C.Y. and Liew, M.S., 2013, "Effect of Short-crested Waves on the Dynamic Responses of Truss SPAR Platforms", Proc. ISOPE2013, Anchorage, USA.
- Kyoung, J. and Yang, C.K., O'Sullivan, J. and Miliante, T., 2013, "Validation of the HVS Semisubmersible Global Performance by Model Tests", Proc. OMAE2013, Nantes, France.
- Kurian, V.J., Yassir, M.A. and Harahap, I.S.H., 2012, "Dynamic Response of Semisubmersibles with Damaged Mooring Lines", Proc. ISOPE2012, Rhodes, Greece.
- Lafeber, W., Bogaert, H. and Brosset, L., 2012, "Comparison of Wave Impact Tests at Large and Full Scale: Results from the Sloskel Project", Proc. ISOPE2012, Rhodes, Greece.
- Larsen, C.M., Zhao, Z.G. and Lie, H., 2012, "Frequency Components of Vortex Induced Vibrations in Sheared Current", Proc. OMAE2012, Rio de Janeiro, Brazil.
- Lee, H.W., Lee, D.Y., Kim, B.K., Shin Y. S. and Choi, H.S., 2010, "A Motion Analysis of Two Floaters in Shallow Water using Boussinesq Equations", Proc. ISPOE 2010, Beijing, China.
- Lee, K. and Yang, K.S., 2013, "Large Eddy Simulation of Turbulent Flow Past a Circular Cylinder", Proc. ITTC Nantes Workshop on Wave Run-up and Vortex Shedding, Nantes, France.
- Lefevre, C., Constantinides, Y., Kim, J.W., Henneke, M., Gordon, R., Jang, H. and Wu, G., 2013, "Guidelines for CFD Simulations of Spar VIM", Proc. OMAE2013, Nantes, France.
- Lehn, E., 1980, "Thruster Interaction Effects", NSFI, Marintek, R102-80, Trondheim, Norway.
- Lehn, E., 1981, "Thruster-hull Interaction Effects", NSFI, Marintek, R119-81, Trondheim, Norway.
- Li, G., Kipp, R. and Leverette, S., 2012, "Horizontal Installation of TLP Tendons", Proc. OMAE2012, Rio de Janeiro, Brazil.
- Li, J., Wang, Z. and Liu, S., 2012, "Calculations of Wave Run-up on Cylinder in Multi-Directional Focused Waves", Proc. ISOPE2012, Rhodes, Greece.



- Lie, H., Braaten, H., Jhingran, V.G., Sequeiros, O.E. and Vandiver, K., 2012, "Comprehensive Riser VIV Model Tests in Uniform and Sheared Flow", Proc. OMAE2012, Rio de Janeiro, Brazil.
- Lie, H., Braaten, H., Szwalek, J., Russo, M. and Baarholm, R., 2013, "Drilling Riser VIV Tests with Prototype Reynolds Numbers", Proc. OMAE2013, Nantes, France.
- Loyse, T., Chollet, S., Gervaise, E., Brosset, L. and De Seze, P.E., 2012, "Results of the First Sloshing Model Test Benchmark", Proc. ISOPE2012, Rhodes, Greece.
- Loyse, T., Gervaise, E., Morean, S. and Brosset, L., 2013, "Results of the 2012 – 2013 Sloshing Model Test Benchmark", Proc. ISOPE2013, Anchorage, USA.
- Lu, L. and Chen, X., 2012, "Dissipation in the Gap Resonance between Two Bodies", Proc. IWWF2012, Copenhagen, Denmark.
- Lu, L., Cheng, L., Teng, B. and Sun, L., 2010a, "Comparison of Potential Flow and Viscous Fluid Models in Gap Resonance", Proc. IWWF2010, Harbin, China.
- Lu, L., Cheng, L., Teng, B. and Sun, L., 2010b, "Numerical Simulation and Comparison of Potential Flow and Viscous Fluid Models in Near Trapping of Narrow Gaps", J. Hydrodynamics, Vol. 22, pp.120–125.
- Lu, L., Teng, B., Cheng, L., Sun, L. and Chen, X., 2011, "Modelling of Multi-Bodies in Close Proximity under Water Waves - Fluid Resonance in Narrow Gaps", Science China Physics, Mechanics & Astronomy, Vol. 54, pp.16–25.
- Lugni, C., Bardazzi, A., Faltinsen, O. and Graziani, G., 2013, "Hydroelastic Challenges for Wave-Impact Phenomena in Sloshing Flow", Proc. OMAE2013, Nantes, France.
- Ma, P., Qiu, W. and Spencer, D., 2012, "Time-Domain VIV Prediction of Marine Risers", Proc. OMAE2012, Rio de Janeiro, Brazil.
- Ma, Q., Yan, S. and Zhou, J., 2013, "Fully Nonlinear Simulation of Resonant Wave Motion in Gap between Two Structures", Proc. ISOPE2013, Anchorage, USA.
- Mainçon, P. and Larsen, C.M., 2011, "Towards a Time-Domain Finite Element Analysis of Vortex Induced Vibrations", Proc. OMAE2011, Rotterdam, The Netherlands.
- Mansour, A.M., Gordon, B.J., Ling, Q. and Shen, Q., 2013, "TLP Survivability against Progressive Failure of Tendon and Foundation Systems in Offshore Western Australian Harsh Environment", Proc. OMAE2013, Nantes, France.
- Mansour, A.M. and Kumar, D., 2013, "High Performance Semisubmersible Design for Dry Tree Applications in Harsh Environment", Proc. OMAE 2013, Nantes, France.
- McNeill, S.I., 2012, "Spectral Formulations for Vortex-Induced Vibration Modal Decomposition and Reconstruction", J. Offshore Mech. and Arctic Eng., Vol. 134.
- McNeill, S.I. and Agarwal, P., 2011, "Efficient Modal Decomposition and Reconstruction of Riser Response due to VIV", Proc. OMAE2011, Rotterdam, The Netherlands.
- Minnebo, J., Izadparast, A.H., Duggal, A. and Huijsmans, R.H.M., 2012, "Response-Based Analysis of FPSO Systems for Squall Loadings", Proc. OMAE2012, Rio de Janeiro, Brazil.
- Modarres-Sadeghi, Y., Chasparis, F., Triantafyllou, M.S., Tognarelli, M. and Beynet, P., 2011, "Chaotic Response is Generic Feature of Vortex-Induced Vibrations of Flexible Risers", J. Sound and Vibration, Vol. 330, pp.2565-2579.
- Molin, B., Remy, F., Camhi, A. and Ledoux, A., 2009, "Experimental and Numerical Study of the Gap Resonances in-between Two Rectangular Barges", Proc. IMAM2009, Istanbul, Turkey.



- Muehlner, E., Banumurthy, S. and Murray, J., 2012a, "Effect of High-Frequency Response on TLP Tendon Fatigue", Proc. OMAE2012, Rio de Janeiro, Brazil.
- Muehlner, E., Murray, J., Banumurthy, S. and Lakhotia, C., 2012b, "Comparison Between Numerical Prediction and Model Tests Measurements on the Centerwell Tank of a Radial Wellbay Spar", Proc. OMAE 2012, Rio de Janeiro, Brazil.
- Murray, J., Muehlner, E., Banumurthy, S. and Choi, G., 2012, "Model Tests on a Radial Wellbay Spar in Gulf of Mexico, Norwegian Sea and Offshore Brazil Environments", Proc. OMAE 2012, Rio de Janeiro, Brazil.
- Myhr, A. and Nygaard, T.A., 2012, "Load Reductions and Optimizations on Tension-Leg-Buoy Offshore Wind Turbine Platforms", Proc. ISOPE2012, Rhodes, Greece.
- Newman, J.N., 2003, "Application of Generalized Modes for the Simulation of Free Surface Patches in Multi Body Hydrodynamics", WAMIT Consortium Report.
- Nienhuis, U., 1986, "Simulations of Low Frequency Motions of Dynamically Positioned Offshore Structures", RINA Spring Meeting, London.
- Nienhuis, U., 1992, "Analysis of Thruster Effectivity for Dynamic Positioning and Low Speed Manoeuvring", Ph.D. Thesis, Delft University of Technology.
- Nordtveit, R., Nygård, B. and Jullumstrø, E., 2007, "Thrust Degradation in DP Operations: DP Model Test of an Aframaz Shuttle Tanker - Methods, Results, Operations", Dynamic Positioning Conference.
- van Nuffel, D., Vepa, S., de Baere, I., Degrieck, J., de Rouck, J. and van Paepegem, W., 2011, "Pressure Measurement on the Surface of a Rigid Cylindrical Body during Slamming Wave Impact", Proc. OMAE2011, Rotterdam, The Netherlands.
- van Nuffel, D.V., Vepa, S., Baere, I., Degrieck, J., Rouch, J. and Paepegem, W.V., 2012, "Experimental Study on the Impact Loads Acting on a Horizontal Rigid Cylinder during Vertical Water Entry", Proc. OMAE2012, Rio de Janeiro, Brazil.
- Ochi, M.K., 1958, "Model Experiments on Ship Strength and Slamming in Regular Waves", Trans. Royal Society of Naval Architects and Marine Engineers, Vol. 66, pp. 345-383.
- Oliveira, M.C., 2012, "Selecting the Best Heading for FPSOs in Santos Basin Considering the Wave Induced Motions", Proc. OMAE2012, Rio de Janeiro, Brazil.
- Ottens, H. and van Dijk, R., 2012, "Benchmark Study on Thruster-Hull Interaction in Current on a Semi-Submersible Crane Vessel", Proc. OMAE2012, Rio de Janeiro, Brazil.
- Ottens, H., van Dijk, R. and Meskers, G., 2011, "Benchmark Study on the Thruster-Hull Interaction on a Semi-Submersible Crane Vessel", Proc. OMAE2011, Rotterdam, The Netherlands.
- Palmer, A.R., Hearn, G.E. and Stevenson P., 2009, "Thruster Interactions on Autonomous Underwater Vehicles", Proc. OMAE2009, Honolulu, USA.
- Pasquier, R. and Berthon, C., 2012, "Model Scale Test Vs. Full Scale Measurement: Findings from the Full Scale Measurement of Sloshing Project", Proc. ISOPE2012, Rhodes, Greece.
- Passano, E., Larsen, C.M. and Lie, H., 2012, "Comparison of Calculated In-Line Vortex Induced Vibrations Response to Model Tests", Proc. OMAE2012, Rio de Janeiro, Brazil.
- Pauw, W. H., Huijsmans, R. H.M. and Voogt, A., 2007, "Advances in the Hydrodynamics of Side-By-Side Moored Vessels", Proc. OMAE2007, San Diego, USA.
- Peng, S., Sun, H., Pan, J. Xia, Z. and Wu, W., 2011, "Experimental Study and Numerical Simulation on Slamming of Trimaran", Proc. ISOPE2011, Hawaii, USA.



- Peng, Z., Wellens, P. and Raaijmakers, T., 2012, "3-D Numerical Modeling of Wave Run-Up on Monopiles", Proc. OMAE2012, Rio de Janeiro, Brazil.
- Pessoa, J, Fonseca, N. and Soares, C.G., 2013, "Analysis of the First Order and Slowly Varying Motions of an Axisymmetric Floating Body in Bichromatic Waves", J. Offshore Mechanics and Arctic Eng., Vol.135.
- Pistani, F. and Thiagarajan, K., 2012," Experimental Measurements and Data Analysis of the Impact Pressures in a Sloshing Experiment", Ocean Eng., Vol. 52, pp. 60-74.
- Piterbarg, V.I., 1996, "Asymptotic Methods in the Theory of Gaussian Processes and Fields", AMS Trans. of Math. Monographs, Vol. 148, Providence, R.I.
- Price, R., Zheng, H., Modarres-Sadeghi, Y. and Triantafyllou, M.S., 2011, "Effect of Higher Stress Harmonics and Spectral Width on Fatigue Damage of Marine Risers", Proc. OMAE2011, Rotterdam, The Netherlands.
- Priyanto, A., Maimun, A., Ghani, M.P.A., Nasrudin, N. and Kader, A.S.A., 2012, "Recurrence Wave Run Up on a Large Volume Semisubmersible", Proc. ISOPE2012, Rhodes, Greece.
- Raghavan, K. and Bernitsas, M. M., 2011, "Experimental Investigation of Reynolds Number Effect on Vortex Induced Vibration of Rigid Cylinder on Elastic Supports," Ocean Eng. Vol. 38, pp.719-731.
- Rahaman, M.M. and Akimoto, H., 2012, "Analysis of the Mechanism of Slamming on the Bow Flare Region of a Container Ship Using RaNS CFD Method", Proc. ISOPE2012, Rhodes, Greece.
- Ramirez, J., Frigaard, P., Andersen, T.L. and Christensen, E.D., 2011, "Numerical Modelling of Wave Run-up: Regular Waves", Proc. ISOPE2011, Hawaii, USA.
- Rao, D.S.B., Selvam, R.P. and Srinivasan, N., 2012, "Hydrodynamic Analysis of Tension Based Tension Leg Platform", Proc. OMAE2012, Rio de Janeiro, Brazil.
- Rao, Z., Vandiver, J.K. and Jhingran, V., 2013, "VIV Excitation Competition between Bare and Buoyant Segments of Flexible Cylinders", Proc. OMAE2013, Nantes, France.
- Ren, N., Li, Y. and Ou, J., 2012, "The Wind-wave Tunnel Test of a New Offshore Floating Wind Turbine with Combined Tension Leg-mooring Line System", Proc. ISOPE2012, Rhodes, Greece.
- Resvanis, T.L. and Vandiver, J.K., "Modelling Risers with Partial Strake Coverage", Proc. OMAE2011, Rotterdam, The Netherlands.
- Rijken, O., 2013, "Installation Methodologies for a Tension Leg Platform under Ocean Swell Conditions", Proc. OMAE2013, Nantes, France.
- Rodriguez, C.A. and Neves, M.A.S., 2012, "Nonlinear Instabilities of Spar Platforms in Waves", Proc. OMAE2012, Rio de Janeiro, Brazil.
- Rudman, M. and Cleary, P.W., 2013, "Rogue Wave Impact on a Tension Leg Platform: The Effect of Wave Incidence Angle and Mooring Line Tension", Ocean Eng., Vol. 61.
- Ruponen, P., Kurvinen, P., Saisto, I. and Harras, J., 2012, "Air Compression in a Flooded Tank of a Damaged Ship", Ocean Eng., Vol. 57, pp.64-71.
- Shan, T., Li, X., Chen, G., Xiao, L., Lu, H. and Li, J., 2012, "Leg Spacing Effect on Wave Run-up and Non-linear Wave Disturbance along Semi-Submersible Columns", Proc. ISOPE2012, Rhodes, Greece.
- Smit, M.R., Tjallema, A.R. and Huijsmans, R.H.M., 2011, "Current Feed Forward Control in Dynamic Positioning", Proc. OMAE2011, Rotterdam, The Netherlands.



- Song, Y.K., Chang, K.A., Ryu, Y. and Kwon, S.H., 2013, "Flow Velocity and Impact Pressure in Liquid Sloshing", Proc. OMAE2013, Nantes, France.
- Song, J.S., Kim, H.J., Park, H.G. and Seo, J.S., 2013, "The Investigation for Interaction Phenomenon of Azimuth Thruster of Ship", Proc. PRADS 2013, Changwan City, Korea.
- Song, J., Teng, B., Tang G., Wu, H., Park, H., Lu, L. and Zhang, J., 2010, "Experimental Investigation on VIV Responses of a Long Flexible Riser Towed Horizontally in a Wave Basin", Proc. ISOPE2010, Beijing, China.
- Souto-Iglesias, A., Botia-Vera, E., Martin, A. and Pérez-Arribas, F., 2011, "A Set of Canonical Problems in Sloshing. Part 0: Experimental Setup and Data Processing", Ocean Eng., Vol. 38, pp.1823–1830.
- Srinath, V. and Chandrasekaran, S., 2013, "Experimental Investigation of Dynamic Response of Tension Leg Platform with Perforated Members", Proc. OMAE2013, Nantes, France.
- Stansberg, C.T., Berget, K., Graczyk, M., Muthanna, C. and Pakozdi, C., 2012, "Breaking Wave Kinematics and Resulting Slamming Pressures on a Vertical Column", Proc. OMAE2012, Rio de Janeiro, Brazil.
- Stansberg, C.T. and Kristiansen, T., 2011, "Experimental Study of Slow-drift Ship Motions in Shallow Water Random Waves", Proc. OMAE2011, Rotterdam, The Netherlands
- Stewart, G., Lackner, M., Robertson, A., Jonkman, J. and Goupee, A., 2012, "Calibration and Validation of a FAST Floating Wind Turbine Model of the DeepCwind Scaled Tension-leg Platform", Proc. ISOPE2012, Rhodes, Greece.
- Sun, L., Chen, L., Zang, J., Taylor, R.E. and Taylor, P.H., 2013, "Nonlinear Interactions of Regular Wave with Truncated Circular Column", Proc. ITTC Nantes Workshop on Wave Run-up and Vortex Shedding, Nantes, France.
- Sun, M. and Huang, W., 2012, "A New Concept of Spar in Deep Water and Its Hydrodynamic Performance under Internal Wave", Proc. ISOPE 2012, Rhodes, Greece.
- Swithenbank, S.B. and Larsen, C.M., 2012, "Occurrence of High Amplitude VIV With Time Sharing", Proc. OMAE2012, Rio de Janeiro, Brazil.
- Tannuri, E.A., Simos, A.N., Sparano, J.V. and Matos, V.L.F., 2012, "Motion-Based Wave Estimation: Small-Scale Tests with a Crane-Barge Model", Marine Structures, Vol. 28.
- Tello Ruiz, M., Delefortrie, G., Vantorre, M. and Geerts, S., 2012, "Propulsion and Steering Behaviour of a Ship Equipped with Two Contra-Rotating Z-drives", Proceedings of X International Conference on Hydrodynamics, ICHD-2012.
- Ten, I., Lu, L. and Chen, X., 2012, "A Semi-Analytical Method with Dissipation for Fluid Resonances", Proc. OMAE2012, Rio de Janeiro, Brazil.
- Tognarelli, M.A., Panicker, N., Campbell, M. and Winterstein, S.R., 2013, "VIV Safety Factors for Drilling Risers: Propagating Model Uncertainty in a Long-Term Reliability Analysis", Proc. OMAE2013, Nantes, France.
- Vandiver, J.K., 2012, "A Damping Parameter for Flow Induced Vibration", J. of Fluids and Structures, Vol. 35, pp.105-119.
- Veen, D.J. and Gourlay, T.P., 2011, "A 2D Smoothed Particle Hydrodynamics Theory for Calculating Slamming Loads on Ship Hull Sections", Proc. High Speed Marine Vessels Conference, Fremantle.
- Veen, D.J. and Gourlay T.P., 2012, "A Combined Strip Theory and Smoothed Particle Hydrodynamics Approach for Estimating Slamming Loads on a Ship in Head Seas", Ocean Eng., Vol. 43, pp.64-71.
- van't Veer, R., Pistidda, A. and Koop, A., 2012, "Forces on Bilge Keels in Regular and Irregular Oscillating Flow", Proc. ISOPE2012, Rhodes, Greece.



- Vepa, K.S., van Nuffel, D.V., Paepegem, W.V., Degroote, J. and Vierendeels, J., 2011, "Comparative Study of Slamming Loads on Cylindrical Structures", Proc. OMAE2011, Rotterdam, The Netherlands.
- Wang, S., Luo, H. and Soares, C.G., 2012, "Explicit FE Simulation of Slamming Load on Rigid Wedge with Various Deadrise Angles during Water Entry", Maritime Tech. and Eng., pp. 399-406.
- Wang, B., Shin, Y. and Wang, X., 2012, "Reliability-based Sloshing Assessment of Containment Systems in LNGCs and FLNGs", Proc. ISOPE2012, Rhodes, Greece.
- Wang, S. and Soares, C.G., 2013, "Slam Induced Loads on Bow-flared Sections with Various Roll Angles", Ocean Eng., Vol. 67, pp. 45-57.
- Wang, C., Wu, G. and Khoo, B.C., 2011, "Fully Nonlinear Simulation of Resonant Motion of Liquid Confined Between Floating Structures", J. Computers & Fluids, Vol. 44(1), pp. 89-101.
- Watai, R.A., Matsumoto, F.T., Sparano, J.V., Simos, A.N. and Ferreira, M.D.A.S., 2011, "Wave Run-up Simulations with a Moving Large Volume Semi-submersible Platform", Proc. OMAE2011, Rotterdam, The Netherlands.
- Wen, P. and Qiu, W., 2013, "Numerical Studies of VIV of a Smooth Cylinder", Proc. ITTC Nantes Workshop on Wave Run-up and Vortex Shedding, Nantes, France.
- de Wilde, J.J. and Huijsmans, R.H.M., 2001, "Experiments for High Reynolds Numbers VIV on Risers", Proc. ISOPE2001, Stavanger, Norway.
- de Wilde, J.J. and Huijsmans, R.H.M., 2004, "Laboratory Investigation of Long Riser VIV Response", Proc. ISOPE2004, Toulon.
- de Wilde, J.J., Huijsmans, R.H.M. and Triantafyllou, M.S., 2003, "Experimental Investigation of the Sensitivity to In-line on Vortex-induced Vibrations", Proc. ISOPE2003, Hawaii, USA.
- de Wilde, J.J., Huijsmans, R.H.M. and Tukker, J., 2006, "Experimental Investigation into the Vortex Formation in the Wake of an Oscillating Cylinder Using Particle Image Velocimetry", Proc. ISOPE2006, San Francisco, USA.
- Willert, C. and Gharib, M., 1992, "Three-Dimensional Partical Imaging with a Single Camera", Experiments In Fluids, Vol. 12(6), pp. 353-358.
- de Wit, C., 2009, "Optimal Thrust Allocation Methods for Dynamic Positioning of Ships", M.Sc. Thesis, Delft Univ. of Technology.
- Xiang, X. and Faltinsen, O. M., 2011, "Time Domain Simulation of Two Interacting Ships Advancing Parallel in Waves", Proc. OMAE2011, Rotterdam, Netherlands.
- Xu, Q., 2011, "A New Semisubmersible Design for Improved Heave Motion, Vortex-induced Motion and Quayside Stability", Proc. OMAE2011, Rotterdam, The Netherlands.
- Xu, Q., Kim, J., Bhaumik, T., O'Sullivan, J. and Ermon, J., 2012, "Validation of HVS Semisubmersible VIM Performance by Model Test and CFD", Proc. OMAE2012, Rio de Janeiro, Brazil.
- Xu, S., Wang, X., Wang, L. and Li, J., 2013, "Dynamic Positioning with Roll-pitch Motion Control for a Semi-Submersible", Proc. ISOPE2013, Anchorage, USA.
- Xu, X., Yang, J., Li, X. and Lu, H., 2013, "Wave Drift Forces on Three Barges Arranged Side by Side in Floatover Installation", Proc. OMAE2013, Nantes, France.
- Yamada, Y., Takami, T. and Oka, M., 2012, "Numerical Study on the Slamming Impact of Wedge Shaped Obstacles Considering Fluid-structure Interaction (FSI)", Proc. ISOPE2012, Rhodes, Greece.
- Yan, H. and Liu, Y., 2011, "Nonlinear Computation of Water Impact of Axisymmetric Bodies", J. Ship Research, Vol. 55, No. 1, pp. 29-44.



- Yang, Q. and Qiu, W., 2012, "Numerical Simulation of Water Impact for 2D and 3D Bodies", Ocean Eng., Vol. 43, pp. 82-89.
- Ye, H., Zhong, Q. and Wan, D., 2013, "Benchmark Computations of Flows around a Stationary Cylinder with High Reynolds Number by RANS- Overset Grid Approach", Proc. ITTC Nantes Workshop on Wave Run-up and Vortex Shedding, Nantes, France.
- Yeon, S.M., Yang, J. and Stern, F., 2013, "Large Eddy Simulation of Drag Crisis in Turbulent Flow Past a Circular Cylinder", Proc. ITTC Nantes Workshop on Wave Run-up and Vortex Shedding, Nantes, France.
- Yin, D. and Larsen, C.M., 2011, "Experimental and Numerical Analysis of Forced Motion of a Circular Cylinder", Proc. OMAE2011, Rotterdam, The Netherlands.
- Yin, D. and Larsen, C.M., 2012, "Forced Motion Experiments with Measured Motions from Flexible Beam Tests under Uniform and Sheared Flows", Proc. OMAE2012, Rio de Janeiro, Brazil.
- Yoon, S.H., Kim, D.H., Sadat-Hosseini, H., Yang, J. and Stern, F., 2013, "High Fidelity CFD Simulation of Wave Run-up around Vertical Cylinders in Monochromatic Waves", Proc. ITTC Nantes Workshop on Wave Run-up and Vortex Shedding, Nantes, France.
- Zeng, H., Li, X., Chen, J., Chen, M., Tan, J., Jing, Y., Shi, S., Li, Z. and Li, X., 2012, "TUMSAS: a New Solution for Shallow Water FPSO Mooring", Proc. OTC2012, Houston, USA
- Zhang, Z., Kim, M.H., Kang, H.Y., Zong, Y. and Wu, J.F., 2012, "A Study on SPM Mooring System for Side-by-side Two Vessels", Proc. ISOPE2012, Rhodes, Greece.
- Zhang, Z., Sun L., Ma, Q.W. and Xu, G., 2013, "A Numerical Investigation on Hydrodynamics of Two Floating Bodies of Arbitrary Arrangements in Regular Waves", Proc. ISOPE2013, Anchorage, USA.
- Zhang, H., Yang, J., Peng, T. and Lu, H., 2012, "Experimental Investigation on Added Mass Coefficient of a Truss Spar Subjected to Vortex-Induced Motions", Proc. OMAE2012, Rio de Janeiro, Brazil.
- Zhao, M., Cheng, L. and An, H., 2012, "Numerical Investigation of Vortex-Induced Vibration of a Circular Cylinder in Transverse Direction in Oscillatory Flow", Ocean Eng., Vol. 41, pp. 39-52.
- Zhao, R., Faltinsen, O.M. and Aarsnes, J.V., 1996, "Water Entry of Arbitrary Two-Dimensional Sections With and Without Flow Separation", Proc. 21st Sym. on Nav. Hydro., pp. 408-423
- Zhao, M., Kaja, K., Xiang, Y. and Yan, G. 2013, "Vortex-Induced Vibration (VIV) of a Circular Cylinder in Combined Steady and Oscillatory Flow", Ocean Eng., Vol. 73, pp. 83-95.
- Zheng, H., Price, R., Modarres-Sadeghi, R., Triantafyllou, G. and Triantafyllou, M., 2011, "Vortex-Induced Vibration Analysis (VIVA) Based on Hydrodynamic Databases", Proc. OMAE2011, Rotterdam, The Netherlands.
- Zhu, H., Zhu, R. and Miao, G., 2008, "A Time Domain Investigation on the Hydrodynamic Resonance Phenomena of 3-D Multiple Floating Structures", J. Hydrodynamics, Vol. 20, pp. 611-616.
- Zou, L. and Larsson, L., 2013, "Numerical Predictions of Ship-to-Ship Interaction in Shallow Water", Ocean Eng., Vol. 72, pp. 386-402.